U.PORTO

MESTRADO

QUÍMICA FARMACÊUTICA

Development of new chiral stationary phases for liquid chromatography based on small molecules and polymeric materials

João Luís Pinto Ribeiro

M

2017

U.PORTO

João Luís Pinto Ribeiro. Development of new chiral stationary phases for liquid chromatography based on small molecules and polymeric materials

M.FFUP 2017

Development of new chiral stationary phases for liquid chromatography based on small molecules and polymeric materials

João Luís Pinto Ribeiro

FACULDADE DE FARMÁCIA

João Luís Pinto Ribeiro

Development of new chiral stationary phases for liquid chromatography based on small molecules and polymeric materials

Dissertation presented to the Faculdade de Farmácia da Universidade do Porto, to obtain the degree of Master in Pharmaceutical Chemistry.

Work developed under the scientific supervision of
Professor Carla Sofia Garcia Fernandes and Professor Maria Elizabeth Tiritan.

November 2017

Advisor

(Prof. Dr.ª. Carla Sofia Garcia Fernandes)

Co-advisor

(Prof. Dr.ª. Maria Elizabeth Tiritan)

Masters Director

(Prof. Dr.ª. Madalena Maria de Magalhães Pinto)

This work was developed in Laboratório de Química Orgânica e Farmacêutica, Departamento de Ciências Químicas, Faculdade de Farmácia da Universidade do Porto. This work was partially supported through national funds provided by FCT/MCTES - Foundation for Science and Technology from the Minister of Science, Technology and Higher Education (PIDDAC) and European Regional Development Fund (ERDF) through the COMPETE – Programa Operacional Factores de Competitividade (POFC) programme, under the Strategic Funding UID/Multi/04423/2013, the project PTDC/MAR-BIO/4694/2014 (reference POCI-01-0145-FEDER-016790; Project 3599 – Promover a Produção Científica e Desenvolvimento Tecnológico e a Constituição de Redes Temáticas (3599-PPCDT)) in the framework of the programme PT2020 as well as by the project INNOVMAR - Innovation and Sustainability in the Management and Exploitation of Marine Resources (reference NORTE-01-0145-FEDER-000035, within Research Line NOVELMAR), supported by North Portugal Regional Operational Programme (NORTE 2020), under the PORTUGAL 2020 Partnership Agreement, through the European Regional Development Fund (ERDF), and Chiral_Drugs_CESPU_2017.

Some results presented in this dissertation are part of the following scientific communications:

- **Published review article**

João Ribeiro; Maria Elizabeth Tiritan; Madalena M.M. Pinto; Carla Fernandes; "Chiral stationary phases for liquid chromatography based on chitin- and chitosan-derived marine polysaccharides", Symmetry, **2017**, 9, 190, 1-28.

- **Poster communications**

J. Ribeiro*; Y.Z. Phyo; C. Leite; C. Fernandes; M.E. Tiritan; A. Kijjoa; M.M.M. Pinto; "Carboxyxanthone derivatives: synthesis and structure elucidation"; Escola de Inverno de Farmácia, 2nd ed, Porto, Portugal, 19-27 January 2017.

J. Ribeiro*; C. Fernandes; M.E. Tiritan; M.M.M. Pinto. "Synthesis and structure elucidation of one carboxyxanthone derivative", 10th Meeting of Young Researchers of University of Porto (IJUP17), Porto, Portugal, 8-10 February 2017, P. 26.

* Presenting author

Acknowledgements

À Professora Doutora Carla Fernandes, minha orientadora, pela oportunidade de realizar este trabalho, pelo conhecimento científico transmitido, espirito crítico, disponibilidade, apoio, paciência e preocupação demonstrados ao longo deste ano. Muito obrigado pelos ensinamentos, pelo incentivo constante, amabilidade e simpatia demonstradas e, principalmente, por ter acreditado em mim e no meu trabalho desde o início.

À Professora Doutora Maria Elizabeth Tiritan, minha coorientadora, pelo apoio demonstrado, pelos conhecimentos científicos transmitidos e por toda a colaboração no decorrer do meu trabalho. Muito obrigado pela simpatia e pelos votos de confiança demonstrados ao longo deste ano.

À Professora Doutora Madalena Pinto, responsável pelo Laboratório de Química Orgânica e Farmacêutica, por toda a disponibilidade, pelo conhecimento científico transmitido e principalmente pela oportunidade de integrar o grupo de investigação neste ano.

À Dr.ª Sara Cravo, pelo apoio científico, pelos conhecimentos transmitidos e pela disponibilidade demonstrada ao longo de todo o projeto. Também agradeço a amizade e preocupação demonstradas ao longo deste ano.

À Gisela e à Liliana pelo apoio técnico, pela simpatia e principalmente pela amizade criada.

Aos meus colegas e amigos do laboratório, pela amizade, pelo companheirismo e apoio demonstrado, obrigado.

Aos meus amigos, em especial à Bárbara Claro e à Bárbara Abreu pela amizade de 7 anos, pelo apoio demonstrado e por sempre estarem presentes, Muito obrigado!

Às minhas avós por todo o carinho e apoio incondicional, a vossa presença foi essencial para a conclusão deste ciclo, muito obrigado.

À minha madrinha pelo carinho demonstrado e pelo apoio incondicional, em particular nos últimos 7 anos, muito obrigado.

À restante família que sempre me apoiou e me ajudou a singrar.

Aos meus pais, pela constante motivação, pela preocupação, carinho e amor incondicionais, pela compreensão e cuidado constantes. Muito obrigado por tudo, sem vocês, nada disto seria possível!

Abstract

The development of chiral stationary phases (CSPs) for liquid chromatography (LC) revolutionized the enantioseparation processes and, nowadays, several types of CSPs are available for the resolution of racemates.

Pirkle-type CSPs, based on small molecules as chiral selectors, can enantioresolve a large spectrum of chiral analytes. Among them, CSPs based on chiral derivatives of xanthones (CDXs) were recently developed and demonstrated promising results of enantioresolution.

Polysaccharide-based CSPs are one of the most versatile and widely used, both for analytical and preparative applications, especially the phenylcarbamates of amylose- and cellulose-derived CSPs. They proved to have excellent chiral recognition abilities being able to resolve several classes of racemates. Polysaccharide-based CSPs comprising other natural polymers such as marine derived chitin and chitosan are also described, revealing high chiral recognition performance.

This dissertation describes the preparation of four CSPs for LC. **CSP-1** is new and comprises a CDX as small molecule chiral selector. The CDX was synthesized by coupling the suitable functionalized xanthone derivative (XD) 5,7-dimethyl-9-oxo-9*H*-xanthene-2-carboxilic acid (XD-1) with the enantiomerically pure building block (*R*)-(-)-phenylglycinol. The obtained CDX was further covalently bonded to silica gel through previous synthesis of a silylated derivative.

CSPs-2 and **CSP-3** comprise polysaccharide derivatives as chiral selectors and were prepared through the synthesis of 3,5-dimethylphenylcarbamates of amylose and cellulose, respectively, and further coating onto aminopropylsilica (APS).

CSP-4 is new and comprises a xanthone-polysaccharide derivative as chiral selector. It was successfully prepared by the reaction of chitosan with 2-((9-oxo-9*H*-xanthene-3-yl)oxo)acetic acid (XD-2) through the corresponding acyl chloride that was, then, derivatized with 3,5-dimethylphenylisocianate to afford the chiral selector chitosan 3,6-*bis*(3,5-dimethylphenylcarbamate)-2-((9-oxo-9*H*-xanthene-3-yl)oxo)acetamide). Finally, the obtained chiral selector was coated onto APS to give the CSP.

Herein, it was the first time that this type of approach to obtain new and different selectors was described, by synthesis of a derivative comprising simultaneously a polysaccharide derivative with xanthonic moieties. Other several attempts of binding XDs to cellulose, amylose, chitin and chitosan are reported, however being unsuccessful.

The total synthesis of XD-1 and XD-2 was also described by a multi-step synthetic pathway, *via* diaryl ether or benzophenone intermediates, respectively.

All prepared CSPs were packed in chromatographic columns and their LC enantioselective capability was evaluated using different commercial chiral standard

analytes for CSP evaluation and several enantiomeric mixtures of CDXs synthesized *in house*.

Keywords: Chiral Stationary Phases, Chiral Derivatives of Xanthones, Amylose, Cellulose Chitin, Chitosan.

Resumo

O desenvolvimento de fases estacionárias quirais (FEQs) para cromatografia líquida revolucionou os processos enantioseparativos e, nos dias de hoje, vários tipos de FEQs estão disponíveis para a resolução de racematos.

As FEQs do tipo Pirkle, baseadas em pequenas moléculas como seletores quirais, são capazes de resolver um grande número de analitos quirais. As FEQs baseadas em derivados xantónicos quirais (DXQs), desenvolvidas recentemente, demonstraram resultados promissores de enantioresolução.

As FEQs baseadas em polissacarídeos são das fases mais usadas e mais versáteis, quer para aplicações analíticas ou preparativas, particularmente os fenilcarbamatos de amilose e celulose. Estes provaram ter excelentes capacidades de reconhecimento quiral sendo capazes de resolver diversas classes de racematos. As FEQs baseadas em outros polissacarídeos naturais de origem marinha, tais como a quitina e o quitosano, foram também descritas e revelaram alta capacidade de resolução quiral.

Nesta dissertação é descrita a preparação de quatro FEQs. A **FEQ-1**, descrita aqui pela primeira vez, e é constituída por um DXQ como seletor quiral. O DXQ foi sintetizado através do acoplamento de um derivado xantónico (DX) adequadamente funcionalizado, ácido 5,7-dimetil-9-oxo-9*H*-xanthene-2-carboxilico (DX-1), com o bloco quiral enantiomericamente puro, (*R*)-(-)-fenilglicinol. O DXQ obtido foi posteriormente ligado covalentemente à sílica através da síntese prévia do respetivo derivado sililado.

A **FEQ-2** e a **FEQ-3** são baseadas em derivados de polissacarídeos e foram preparadas através da síntese de 3,5-dimetilfenilcarbamatos de amilose e celulose, respetivamente, e posterior adsorção em aminopropilsílica (APS).

A **FEQ-4**, descrita aqui pela primeira vez, é constituída por um derivado polissacarídeo-xantona como seletor quiral. Esta foi preparada com sucesso através da reação do quitosano com o cloreto de ácido do ácido 2-((9-oxo-9*H*-xanthene-3-yl)oxo)acético (DX-2) e posterior derivatização com 3,5-dimetilfenilisocianato de modo a obter o seletor quiral quitosano 3,6-*bis*(3,5-dimetilfenilcarbamato)-2-((9-oxo-9*H*-xanthene-3-yl)oxo)acetamida). Por fim, o seletor quiral obtido foi adsorvido em APS para a obtenção da FEQ.

Esta abordagem para a obtenção de novos seletores quirais através da síntese de um derivado constituído simultaneamente por um polissacarídeo com porções de natureza xantónica, é nova. Várias tentativas de ligação dos DXs aos polissacarídeos celulose, amilose, quitina e quitosano são descritas, no entanto, estas não foram bem-sucedidas.

A síntese total do DX-1 e do DX-2 é também descrita envolvendo vários passos reacionais, através da síntese de intermediários éter bifenílico e benzofenona, respetivamente.

Todas as FEQs preparadas foram empacotadas em colunas cromatográficas e as suas capacidades enantioseletivas foram avaliadas usando diferentes padrões quirais comerciais, assim como diversas misturas enantioméricas de DXQ sintetizados pelo grupo de investigação.

Palavras-chave: Fases Estacionárias Quirais, Derivados Xantónicos Quirais, Amilose, Celulose, Quitina, Quitosano.

Index

Figures Index

Schemes Index

Table Index

ABBREVIATIONS AND SYMBOLS

^{13}C NMR	Carbon Nuclear Magnetic Resonance
^{1}H NMR	Proton Nuclear Magnetic Resonance
Å	Angström
ADMPC	3,5-Dimethylphenylcarbamate of amylose
br	Broad
CDMPC	3,5-Dimethylphenylcarbamate of cellulose
CDX	Chiral Derivative of Xanthone
CIIMAR	Centro Interdisciplinar de Investigação Marinha e Ambiental
CLEC	Chiral Ligand-Exchange Chromatography
COMU	(1-Cyano-2-ethoxy-2-oxoethylidenaminooxy)dimethylamino-morpholino-carbenium hexafluorophosphate
CSP	Chiral Stationary Phase
d	doublet
DCC	Dicyclohexylcarboxamide
dd	double doublet
ddd	double double doublet
DHU	Dicyclohexylurea
DMA	Dimethylacetamide
DMF	Dimethylformamide
DMPC	3,5-Dimethylphenylcarbamate
DMSO	Dimethylsulfoxide
HMBC	Heteronuclear Multiple-Bond Correlation Spectroscopy
HPLC	High Performance Liquid Chromatography
HSQC	Heteronuclear Single-Quantum Correlation Spectroscopy
IR	Fourier Transform Infrared Spectroscopy
k	Retention Factor
LC	Liquid Chromatography
LQOF	Laboratory of Organic and Pharmaceutical Chemistry
m	multiplet
MDPV	3,4-Methylenedioxypyrovalerone
NHS	*N*-Hydroxysuccinimide
Rs	Resolution
s	singlet
SylCDX	Silylated Chiral Derivative of Xanthone

TBTU	*O*-(Benzotriazol-1-yl)-*N,N,N′,N′*-tetramethyluronium tetrafluoroborate
TEA	Triethylamine
THF	Tetrahydrofuran
TLC	Thin Layer Chromatography
XD	Xanthone Derivative
XD-1	5,7-Dimethyl-9-oxo-9*H*-xanthene-2-carboxilic acid
XD-2	2-((9-oxo-9*H*-Xanthen-3-yl)oxy)acetic acid
α	Separation Factor
δ	Chemical Shift
υ	Wavenumber

Outline of the Dissertation

This dissertation is divided into seven chapters:

I. Introduction

The first chapter starts with a brief description of some key concepts regarding chirality. The chiral stationary phases (CSPs) frequently used for enantioresolution are introduced, with focus on Pirkle-type and polysaccharide-based CSPs. Among the polysaccharide-based CSPs, especial emphasis is given to chitin and chitosan marine derived polysaccharides. Finally, a brief description of the importance and the most common synthetic pathways for the synthesis of xanthone derivatives are highlighted.

II. Aims

The aims of the work that lead to this dissertation are presented in this chapter.

III. Results and Discussion

This chapter is divided in two main sections: A - Synthesis and structure elucidation and B – Evaluation of enantioresolution by liquid chromatography (LC).

In section A, the results from the original research concerning the synthesis and structure elucidation of final products and their intermediates to obtain CSPs are described. In section B, the results of the LC evaluation of the enantioresolution performance of the prepared CSPs are presented and discussed.

IV. Experimental

In this chapter the reagents, experimental conditions and procedures for the synthesis performed, as well as for the liquid chromatography evaluations, are described.

V. Conclusions

In this chapter the general conclusions of the developed work are described, based on the proposal aims.

VI. References

All the references used as support in this dissertation are listed in this chapter. The databases used are also presented.

VII. Appendixes

Appendix A. Abstract and poster of Escola de Inverno de Farmácia, 2nd ed, 19-27 January 2017.

Appendix B. Abstract and poster of 10th Meeting of Young Researchers of University of Porto (IJUP17), Porto, Portugal, 8-10 February 2017, P. 26.

Appendix C. Table 1 comprising the chemical structures of chitin-based CSPs and separated analytes.

Appendix D. Table 2 comprising the chemical structures of chitosan *tris*-carbamate CSPs and separated analytes.

Appendix E. Table 3 comprising the chemical structures of chitosan *bis*-carbamate CSP with the amine group of the chitosan modified by *N*-nicotinoyl-L-phenylalanine and separated analytes.

Appendix F. Table 4 comprising the chemical structures of chitosan *bis*-carbamate CSPs with the amine group of the chitosan replaced by an imide moiety and separated analytes.

Appendix G. Table 5 comprises the chemical structures of chitosan *bis*-carbamate CSPs with the amine moiety of chitosan modified by an alkylamide moiety and separated analytes.

Appendix H. Table 6 comprising the chemical structures of chitosan *bis*-carbamate CSPs with the amine moiety of chitosan modified by an *N*-alkyl urea and separated analytes.

I. Introduction

1. Chirality

The term chirality comes from the Greek "cheir" that means hand. It is a geometric property of a given object or molecule and is based on the asymmetry of three-dimensional structures [1]. Molecules that exist as non-superimposable structures and being mirror image-like are designated enantiomers. They present identical physical and chemical properties, when they are in an achiral environment, being distinguished by their optical activity: one enantiomer rotates the plane-polarized light to clockwise (dextrorotatory) and the other to counter clockwise (levorotatory), referred by the symbols (+) and (-), respectively [1].

Chirality is often associated with sp^3 (tetrahedral) carbon atoms with four different substituents within a molecule, called stereogenic centres (or stereocenters); being the most common type of chirality [1-2]. Other atoms like sulphur, phosphorus and nitrogen can also be considered as stereogenic centres [2]. In addition to central chirality, other types of chirality are described including planar, axial and helical [3]. The spatial arrangement of the substituents around the stereogenic centre is termed configuration. Cahn, Ingold and Prelog nomenclature are frequently used to assign the configuration and is based on a set of priority rules considering the substituents around the stereogenic centre. The configurations are expressed as (*R*) and (*S*), from the Latin words *rectus* and *sinister* which signify right and left, respectively (**Figure 1**) [1].

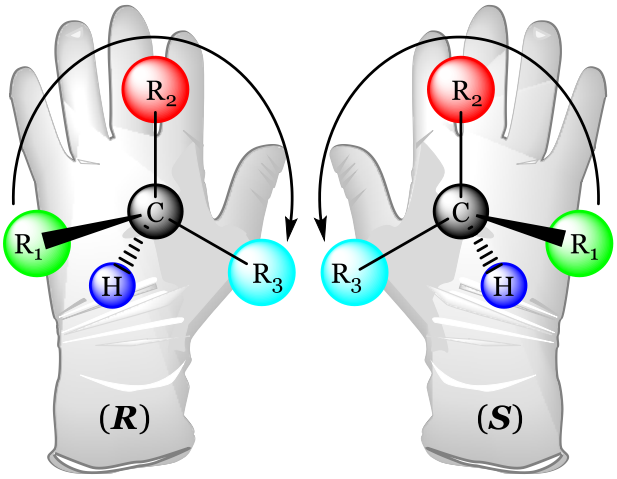

***Figure 1**. Example of the (R)/(S) configurations.*

The understanding of chirality has become of great importance in the study of biological systems, organic chemistry and especially in pharmaceutical sciences. By the early 20th century, several progresses had already been achieved within those fields, which included studies on biological enantioselectivity [4]. These studies triggered a vast academic interest by biochemists, medicinal chemists and pharmacologists that saw the potential of these phenomena in the therapeutics. Taking into account that single enantiomers of a drug may exhibit different effects, whether in terms of pharmacokinetics [5-6], pharmacodynamics

[7-8] or toxicity [9], the interest and study of chirality/enantioselectivity in pharmaceutical industry has greatly increased in recent years, leading to the development of new enantiomerically pure drug entities [3].

This trend in the development of enantiomerically pure drugs led to the development of new methodologies of synthesizing and/or separating enantiomers [10]. Considering enantioseparation, several methodologies can be used such as liquid chromatography (LC) [11-12]. Moreover, the resolution of enantiomers can be achieved by two distinct methods: direct and indirect [13].

The indirect method is based on the synthesis of a pair of diastereoisomers from the reaction of the racemate with an enantiomerically pure reagent, and further separation of the obtained diastereoisomers by conventional procedures [14]. Then, the enantiomers can be recovered by overturn the derivatization procedure [3]. The direct method uses a chiral environment to perform the separation of both enantiomers, and is based on the distinct interactions of the enantiomers with a chiral selector, frequently by LC. The chiral selector may be an additive in the mobile phase or, alternatively, as component of the stationary phase detained in a chromatographic support, chiral stationary phase (CSP) [15].

2. Chiral Stationary Phases

For the last 30-40 years, there has been an increasingly interest in enantioseparation methods using CSPs, for both analytical and preparative applications [16]. In fact, intensive studies performed by Pirkle[17-18], Okamoto [4, 19-20], Cass [21-24], Armstrong [25-26], among many other research groups [27-29] were described.

Nowadays, there are several types of CSPs including, Pirkle-type, ligand-exchange-type, crown ether-based, cyclodextrin-based, macrocyclic antibiotics-based, ion-exchange-type, polysaccharide-based, molecular imprinted, synthetic polymer-based, protein-based, among others [13, 30].

Pirkle-type and polysaccharide-based CSPs are pointed out as one of the most useful and widely applied [4, 31]. In this work, these two types of CSPs were chosen to obtain new CSPs.

2.1. Pirkle-type CSPs

Pirkle-type CSPs, also called brush-type or donor-acceptor CSPs, were first introduced by Pirkle *et col.* in 1979 [17], and are based on chiral selectors with low molecular weight [13]. The resolution of enantiomers using this type of CSPs is achieved mostly by π-π interactions between the chiral selector and the analyte. H-bond, dipole-dipole interactions and steric hindrance also may contribute to the chiral distinction between enantiomers [13]. These CSPs preferably operated under normal phase elution conditions [30, 32] even though, it

is possible to work, for example, under reversed phase elution conditions [33-34]. Whelk-O1 (**Figure 2**) is the most widely used Pirkle-type CSP being able to enantioseparate a broad spectrum of classes of analytes [32] mainly, compounds that contain an aromatic moiety near to the stereogenic centre [28].

The evolution of several and successive generations of CSPs developed by Pirkle *et col.* [18, 35] was an inspiration to other research groups to develop new CSPs based on small molecules as chiral selectors [36-37].

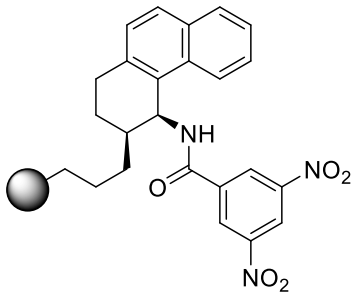

***Figure 2**. Structure of Whelk-O1 CSP.*

2.2. Polysaccharide-based CSPs

Polysaccharides are polymers comprising several units of monosaccharides linked to each other by a glycosidic bond [2]. There are several types of polysaccharides, and some of them have been studied as possible chiral selectors for LC (**Figure 3**).

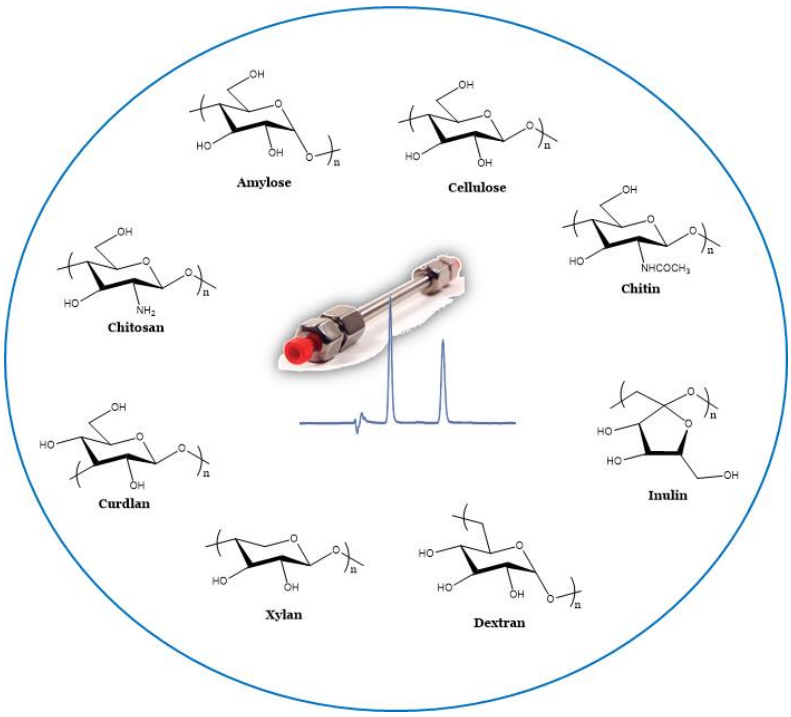

***Figure 3**. Structures of different types of polysaccharides studied as selectors for LC.*

The first study reporting the use of polysaccharide derivatives as a practical chiral packing material for LC columns was described by Hesse and Hagel in 1973 [38]. Therefore, several polysaccharides were derivatized, and coated on macroporous aminopropyl silica. Cellulose and amylose-based CSPs showed the best chiral recognition for all the tested analytes [39]. Phenylcarbamates, esters, alkylcarbamates and benzylcarbamates derivatives of cellulose and amylose derivatives were developed as selectors for CSPs. Since then, other research groups demonstrated interest on the development of amylose [40-47] and cellulose [42, 46, 48-53] derivatives as CSPs, including coating onto microporous silica [22, 24, 41, 54]. Several reviews focusing the preparation and evaluation of this type of CSPs can be found [4, 16, 19, 29, 55-61]. Phenylcarbamates are the derivatives most studied, due to their high chiral ability recognition and the possibility to explore different aryl substituents [62-68]. The *tris*-phenylcarbamate CSPs generally have high enantioseparation abilities however, the chiral recognition is greatly influenced by the substituents present on the phenyl moiety of the phenylcarbamates [20, 39-41, 45]. Among the developed amylose and cellulose *tris*-phenylcarbamates, the 3,5-dimethylphenyl derivatives proved to have the best enantiorecognition performance [40-41, 69-70] being, nowadays, the most widely used CSPs (**Figure 4**).

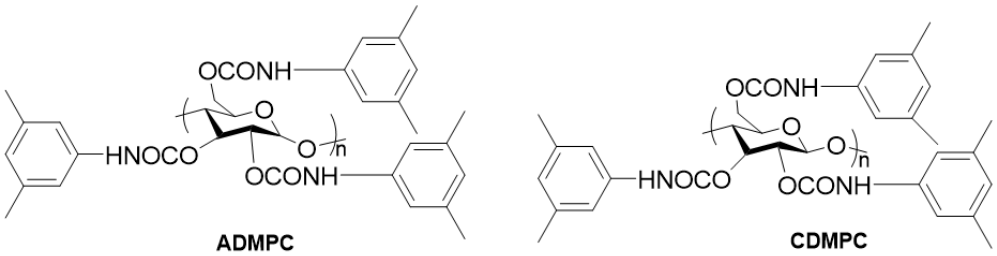

***Figure 4**. Structures of amylose 3,5-dimethylphenylcarbamate (ADMPC) and cellulose 3,5-dimethylphenylcarbamate (CDMPC).*

The carbamate derivatives of amylose and cellulose can be synthesized by reaction of the polysaccharide with the corresponding isocyanate comprising the moiety of the desired derivative for the CSP [39-40, 69]. The phenylcarbamates of amylose and cellulose can be coated [39-40, 43] or be immobilized [19, 55-56, 71] on a chromatographic support, mainly aminopropyl silica.

These CSPs are recognized as being one of the most powerful in terms of enantioresolution both for analytical [22-23, 54, 72-79] and preparative scale [24, 80-85]. In our group, this type of CSPs has demonstrated to be effective for analytical [86-87] as well as preparative resolution [88] of chiral derivatives of xanthones (CDXs). For the same library of CDXs and comparing to other types of CSPs [89-90], polysaccharide-based proved to be the most suitable to separate this group of compounds [86, 91].

Recently, we also described the analytical enantioresolution of several cathinone derivatives present in "legal highs" using polysaccharide-based CSPs [92]. Additionally, the analytical enantioresolution of 3,4-methylenedioxypyrovalerone (MDPV) was efficiently scaled up to multimilligram using a semipreparative column [92].

Although the coated CSPs showing high chiral recognition abilities for a wide variety of racemates, the range of mobile phases that can be used is very limited. Mobile phases containing organic solvents such as tetrahydrofuran, dichloromethane or ethyl acetate, among others, are not suitable for the coated CSPs. The immobilization of phenylcarbamates of amylose and cellulose was carried out to solve this problem [59-60]. However, the immobilized CSPs have also some drawbacks. Their lower chiral recognition ability is the main disadvantage, which can be explained by the fact that the immobilization of the polysaccharide derivative on the chromatographic support is done through the hydroxyl groups, causing a disturbance in the high-ordered structures of the polysaccharide [56].

2.2.1. Marine polysaccharide-based CSPs

Marine-derived polysaccharides have also been exploited as chiral selectors (**Figure 5**), and some of them proved to be good alternatives to amylose and cellulose derivatives.

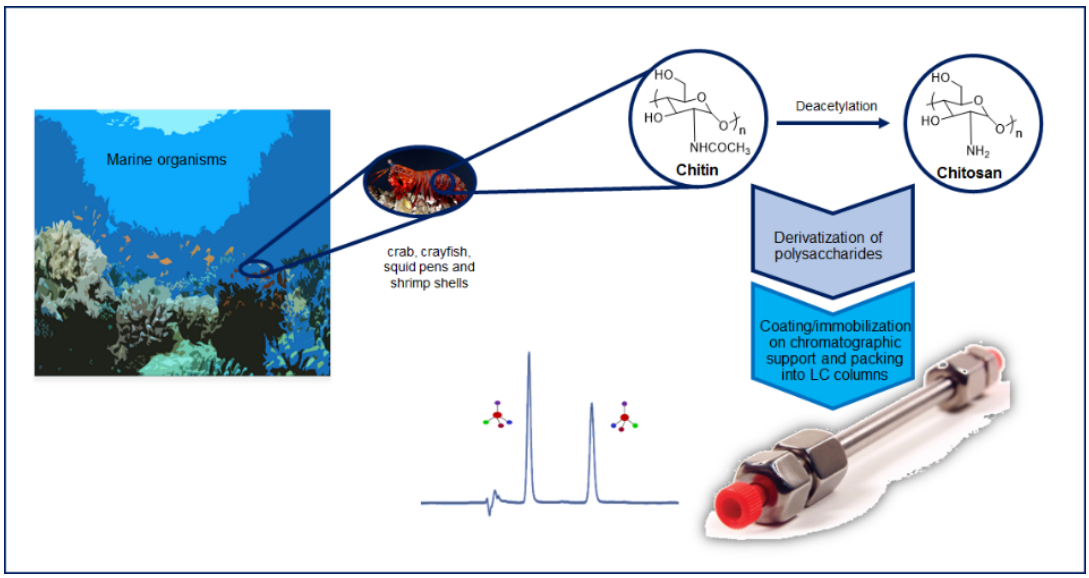

Figure 5. *General strategy for development of chitin and chitosan marine-derived CSPs.*

Braconnot discovered chitin, a marine polysaccharide obtained by isolation from shells of crustaceans and molluscs, in the early 19th century [93]. Chitin is one of the most abundant polysaccharides comprising *N*-acetyl-D-glucosamine units linked by β-(1,4).

Chitosan is a 2-deoxy-2-glucosamine polysaccharide, discovered in 1859 by Rouget after deacetylation of chitin by boiling in concentrated potassium hydroxide solution [94]. Both marine-derived polysaccharides have diverse applications whether in medicine as wound healing agents [95], as drug carriers [96-97], in bone tissue regeneration [98] as well as in the food industry as clarification agents [99], among others. Other important application is their use as suitable chiral selectors for LC [19]. In fact, they have been used as CSPs, since Okamoto *et al.* in 1984, introduced the first phenylcarbamate of chitosan. Considering chitin, the first reported study was published by Cass *et al.* in 1996, describing the chiral discrimination ability of two arylcarbamates of chitin [100]. A literature survey covering the report on chitin and chitosan based CSPs is presented. Different CSPs were developed allowing the enantioresolution of several different analytes (α> 1.00) (**Tables 1-5**, **Appendix C-G**).

2.2.1.1. Chitin-based CSPs

The *bis*-phenylcarbamate (**1**) and *bis*-3,5-dimethylphenylcarbamate (**2**) (**Table 1**, **Appendix C**), coated on microporous aminopropyl silica, were the first described chitin-based CSPs [100]. Two distinct sources of chitin (commercial and non-commercial) were used for the preparation of both polysaccharide derivatives. Interestingly, the results obtained demonstrated that the chiral discrimination of both aryl carbamate derivatives was significantly affected by the source of chitin used. For example, from the series of racemates tested, only (*E*)-1-chloro-1,2-diphenylethene oxide was resolved on the CSPs prepared using a commercial chitin. The similar *bis*-aryl carbamate derivatives of a non-commercial chitin presented higher resolution power compared with commercial chitin. These results are due to the differences related to the resource and method used for isolation and purification of chitin, which can influence its quality and, consequently, the length of its molecular chain, number of acetyl groups as well as the 3D structure [100].

Yamamoto *et al.* developed a chiral selector from chitin, the *bis*-3,5-dichlorophenylcarbamate (**3**) (**Table 1**, **Appendix C**) as well as both derivatives previously described (**1** and **2**) to study the influence of the aryl groups as substituents on chiral discrimination performance [101]. Among the three, the *bis*-3,5-dimethylphenylcarbamate (**2**) and *bis*-3,5-dichlorophenylcarbamate (**3**) exhibited, in general, higher chiral recognition than *bis*-phenylcarbamate (**1**). Moreover, some chiral 2-arylpropionic acids such as ketoprofen and ibuprofen were efficiently resolved on *bis*-3,5-dichlorophenylcarbamate (**3**) with α values of 1.72 and 1.39, respectively [101].

In a continuous interest in developing new chitin-based CSPs, the same group developed 3,5-disubstituted (**2-5**) and several 4-substituted phenylcarbamate (**6-13**) chitin derivatives in an extensive study that also included both configurations of one optically active arylalkylcarbamate (**14**) and three cycloalkylcarbamates (**15-17**) (**Table 1**,

Appendix C) [102]. All CSPs were obtained by coating the chitin derivatives on macroporous silica gel. The nature of the substituents as well as their position on the phenyl moiety of the carbamate demonstrated to have a significant role on chiral recognition. It was proposed that the polar carbamates and acetamide residues of the chitin phenylcarbamates were the most important interaction sites for chiral recognition, with the substituents of the phenyl group having influence on the polarities of these sites [102]. Regarding the chitin 3,5-disubstituted phenylcarbamates, the 3,5-dimethylphenylcarbamate (**2**) showed the highest chiral recognition although the remaining three 3,5-disubstituted phenylcarbamates (**3**-**5**) also presented good chromatographic results. Additionally, the 3,5-dimethyl- (**2**) and 3,5-dichlorophenylcarbamates (**3**) demonstrated some complementary in terms of enantiorecognition. Considering the 4-substituted phenylcarbamates of chitin (**6**-**13**), some interesting results were obtained. The 4-methylphenyl- (**8**), 4-trifluoromethylphenyl- (**9**) and 4-chlorophenyl- (**11**) carbamates showed the highest enantiorecognition while 4-*tert*-butyl- (**6**) and 4-isopropylphenyl- (**7**) carbamates presented lower retention and enantioselectivity for the tested racemates. For both enantiomers of chitin 1-phenylethylcarbamate (**14**), low chiral recognition ability was observed which was depended on their configuration. For example, (*S*)-1-phenylethylcarbamate of chitin showed enantioselectivity for benzoin, 2-phenylcyclohexanone and 1-(9-anthry1)-2,2,2-trifluoroethanol, whereas no separation was observed for these analytes with its antipode CSP, which separated other racemates (**Table 1**, **Appendix C**). The CSPs comprising the cycloalkylcarbamates **15** and **16** revealed relatively low enantiorecognition, both resolving only two of the ten analysed racemates [102].

Considering that the chitin derivatives have a very low solubility, the possibility to perform enantioseparations under reversed phase as well as using different solvents in normal phase, such as chloroform and ethyl acetate, was also studied (**Table 1**, **Appendix C**). Both chromatographic elution conditions were tested for 3,5-dimethyl- (**2**) and 3,5-dichlorophenylcarbamates (**3**) and, in some cases, the racemates were more efficiently resolved under reversed phase mode [102].

Following the same strategy, and aiming the enantioseparation of tadalafil and its intermediates, *Zhang et al*. synthesized new chitin bis-arylcarbamates, specifically chitin 4-trifluoromethoxy- (**18**), 3-chloro-4-methyl- (**19**) and 4-chloro-3-trifluoromethyl- (**20**) phenylcarbamates (**Table 1**, **Appendix C**) [103]. The three chitin derivatives were coated on macroporous 3-aminopropyl silica and the obtained CSPs were successful in the enantioresolution of all tested analytes [103].

Recently, the same group developed a new strategy to enhance the chromatographic performance of chitin-based CSPs [104-105]. The aim was combining amylose or cellulose with chitin derivatives and coated on silica gel to improve the chiral recognition as well as their

stability and solvent resistance. The first report of this type of biselector as CSPs comprised amylose *tris*-3,5-dimethylphenylcarbamate and chitin *bis*-3-chloro-4-methylphenlcarbamate (**19**) blended at different molar ratios [104]. Although the chiral recognition of the blended CSPs did not improve significantly, comparing to the single selector CSPs, there was a vast improvement in the solvent tolerance and stability. Interestingly, the biselector CSPs prepared by blending chitin *bis*-3,5-dimethylphenylcarbamate (**3**) with cellulose *bis*-4-methylbenzoate and cellulose *bis*-3,5-dimethylphenylcarbamate sowed better chiral recognition capabilities compared to the corresponding single selectors [105]. They can also work in a wider range of mobile phases.

All the described chitin-based CSPs were prepared by coating method and, to the best of our knowledge, there is no studies reporting immobilized chitin derivatives as well as commercially available chitin-based CSPs.

2.2.1.2. Chitosan-based CSPs

Several studies regarding chitosan-based CSPs are found in literature. The first studies were focused mainly on *tris*-phenylcarbamates of chitosan. In the last decades, an increasingly number of *bis*-phenylcarbamates of chitosan have been described. Furthermore, besides the traditional coating method, same chitosan-based CSPs were prepared by immobilization of the chitosan-derivatives on the chromatographic support.

2.2.1.2.1. Chitosan *tris*-carbamate CSPs

As previously mentioned, the first study of a chitosan derivative as a CSP was published by Okamoto *et al.* in 1984 [39]. In this study, they compared the chiral discrimination ability of various polysaccharide phenylcarbamates as CSPs. Chitosan *tris*-phenylcarbamate derivative (**21**) coated on macroporous aminopropyl silica was found to resolve the enantiomers of 1-(9-anthryl)-2,2,2-trifluoroethanol with a α value of 2.25 (**Table 2**, **Appendix D**) [39].

In 1998, the same group compared the chiral recognition performance of 3,5-dichloro- and 3,5-dimethylphenylcarbamate derivatives of several polysaccharides, including chitosan (**22**, **23**) (**Table 2**, **Appendix D**) [106]. These two chitosan derivatives presented a relatively high chiral recognition for the tested racemates, setting their potential use as CSPs [106]. In the same year, Franco *et al.* described another strategy to obtain new chitosan-based CSPs by bonding the chitin-carbamate derivatives on chromatographic support [70]. The obtained bonded CSPs allowed the use of a larger panel of solvents in the mobile phases compared to coated ones. Accordingly, the 3,5-dimethylphenylcarbamate derivative of chitosan (**23i**) was mixed with 10-undecenoyl and covalently immobilized on allyl silica gel, which demonstrate to be very useful in the separation of several racemates

(**Table 2**, **Appendix D**). The mobile phases comprising either different proportions of heptane/2-propanol and heptane/chloroform mixtures allowed the best enantioresolutions [70].

Other mixed 10-undecenoyl/phenylcarbamate (**22i**) or benzoyl derivatives of chitosan (**24i**-**25i**), comprising different substituents in the aromatic ring, were prepared and immobilized on allyl silica gel (**Table 2**, **Appendix D**) [107]. Among the chitosan derivatives, the 3,5-dichlorophenylcarbamate derivative (**22i**) was found to have the most significant chiral discrimination ability.

In another study, the synthesis and chromatographic evaluation of the chitosan derivatives **22** and **23** as well as four new chitosan derivatives (**25-28**) were described (**Table 2**, **Appendix D**)[108]. All derivatives were coated on macroporous silica gel and evaluated as CSPs. Among them, the 3,5-dichloro- (**22**), 3,5-dimethyl- (**23**), and 3,4-dichlorophenylcarbamate (**27**) derivatives showed the best enantioseparation results for the tested racemates. The chiral recognition of the CSP based on the latter chitosan derivative (**27**) was investigated using chloroform as a component of the mobile phase, and some racemates were better resolved.

Another group described a study focused on the enantioresolution ability of the *tris*-3-chlorophenylcarbamate of chitosan (**26**) using various mobile phases [109]. They demonstrated that, in general, the alcohol used as organic modifier in the mobile phase greatly influenced the enantioseparation performance of the CSP. Baseline separations or near-baseline separations were achieved for benzoin, penconazole, hexaconazole and epoxiconazole, whereas the other racemates were partially separated (**Table 2**, **Appendix D**) [109].

Zhang *et al.*, also evaluated the enantioresolution of fourteen derivatives (**21-26**, **28-35**) (**Table 2**, **Appendix D**) and concluded that like chitin phenylcarbamates [102], the nature of substituents and their position in the phenyl moiety, played a great role in the enantiorecognition of the derivative [110]. In fact, the 3,5-disubstituted phenylcarbamates of chitosan (**22-23**) CSPs have the highest chiral recognition abilities while 2-substituted phenylcarbamate (**24-26**, **28-35**) CSPs showed the lowest enantiorecognition. Additionally, mobile phases containing ethyl acetate and chloroform were studied and, once again, revealed to improve the enantiorecognition performance of the CSPs [110].

To our knowledge, the most recent study with chitosan *tris*-phenylcarbamates was published by Guntari *et. al.* in 2014 [111]. In this study they developed and evaluated a new way of immobilization of chitosan *tris*-3,5-dimethylphenylcarbamate (**23**) using continuous assembly of polymers techniques. These techniques employed a catalyst immobilized on silica particles to produce stable CSPs suitable to be used in a wide range of

mobile phases. The obtained CSP proved to be effective in separating the enantiomers of Trögers base and *trans*-stilbene oxide [111].

2.2.1.2.2. Chitosan *bis*-carbamate CSPs

The first study related to *bis*-carbamate derivatives as chiral selectors for LC was described by Son *et al.* in 2006, which reported the development of a CSP based on chitosan *bis*-3,5-dimethylphenylcarbamate in which the amine group of the chitosan was modified with *N*-nicotinoyl-L-phenylalanine (**36**) (**Table 3**, **Appendix E**) [112]. The *bis*-phenylcarbamate derivative **36** demonstrated a high solubility in several organic solvents and, consequently, was easy to coat on aminopropyl silica. The LC performance of the obtained CSP was evaluated using different mobile phases and all the tested racemates were enantioseparated. The best chromatographic result was achieved for flavanone with α and Rs values of 4.70 and 4.33, respectively, using a mixture of hexane/2-propanol 80:20 as mobile phase [112].

In 2008, Yamamoto *et al.*, prepared several *bis*-carbamate derivatives with the amino group of chitosan replaced by an imide moiety (**37-45**) (**Table 4**, **Appendix F**) [108]. This study showed interesting results of enantioresolution for all the CSPs based on imide-chitosan derivatives.

In recent studies (2016), Tang *et al.* prepared several *bis*-phenylcarbamate derivatives in which the amine moiety of chitosan was modified by an isobutyrylamide moiety (**46-57**) [113-114]. The synthesized chitosan derivatives were coated on aminopropyl silica resulting in a series of new CSPs for LC. Considering their poor solubility, they were able to withstand operations with other mobile phases than the typical hexane/2-propanol (**Table 5**, **Appendix G**). They demonstrated high solvent tolerance and could still work after being flushed with chloroform (100%), ethyl acetate (100%) or tetrahydrofuran/*n*-hexane (70:30 *v/v*) without significant loss of enantioseparation. Furthermore, the CSPs presented excellent chiral recognition performance for some of the tested racemates (**Table 5**, **Appendix G**) [113-114].

In the same year, some *bis*-phenylcarbamate derivatives with different substituents in both phenylcarbamate and amine moieties (**58-61**) were obtained by the same group (**Table 5**, **Appendix G**) [115]. The synthesized chitosan derivatives were coated on aminopropyl silica, and showed excellent chiral recognition for the majority of the tested racemates. These new CSPs also proved to be stable when used with other mobile phases than the typical hexane/2-propanol [115].

Other CSPs based on the substitution of the amine of chitosan with an alkyl moiety, prior to the derivatization of the hydroxyl groups with different isocyanates were described [116-117]. Actually, Feng *et. al.* prepared several *bis*-4-methylphenylcarbamates with different

alkyl moieties linked in the amine group of chitosan (**62-64**) (**Table 5**, **Appendix G**) [116]. These derivatives were coated on aminopropyl silica and showed good chiral recognition abilities, being equivalent to the CSP comprising 3,5-dimethylphenylcarbamate of amylose.

Furthermore, Zhang *et. al.* developed several CSPs based on *N*-cyclobutylformilated chitosan derivatives (**65-71**) (**Table 5**, **Appendix G**) [117]. These CSPs showed good chiral recognition abilities, specially the CSPs comprising the chitosan-derivatives **66, 67** and **68**, being able to recognize most of the tested racemates. Additional analysis were performed to evaluate the tolerability to other organic solvents, which showed no significant changes in the enantiorecognition abilities of the tested CSPs after being flushed with ethyl acetate (100%), chloroform (100%) and hexane/tetrahydrofuran (50/50, 40/60, 30/70 *v/v*)[117].

Recently, Feng *et. al.* developed several new CSPs containing a *n*-pentyl-amide moiety (**72-76b**) (**Table 5**, **Appendix G**)[118]. The LC performance of these CSPs was evaluated, and proved to have excellent chiral recognition abilities. The influence of the molecular weight of the chitosan on the chiral recognition capability of the developed CSPs (**76a** and **76b**) was also evaluated, showing that a lower molecular weight allowed better chiral recognition abilities. Once again, this type of CSPs (chitosan-based) showed high tolerability for other organic solvents than the typically used for coated-type CSPs.

Wang *et. al.* developed several new chitosan *bis*-phenylcarbamates with the amine moiety being derivatized with a *N*-octyl urea (**77-82**) (**Table 6**, **Appendix H**)[119]. The obtained CSPs showed good chiral recognition abilities, being equivalent to those comprising 3,5-dimethylphenylcarbamates of amylose and cellulose.

Other chitosan *bis*-3,5-dimethylphenylcarbamates with different moieties linked to the chitosan amine group (**83-87**) were developed by Wang *et al.* (**Table 6**, **Appendix H**) [120]. The obtained CSPs showed excellent chiral recognition abilities, specially the CSP comprising the chitosan-derivative **87**, being able to recognize all the tested racemates.

To our knowledge, the most recent study on chitosan *bis*-phenylcarbamate derivatives was published by Liang *et.al.*[121]. In this study, several CSPs based on chitosan *N*-isobutylurea (**88a-91b**) were prepared (**Table 6**, **Appendix H**). Two types of chitosan with different molecular weights were used. In this study, the CSPs developed with higher molecular weight chitosan (**88a, 89a, 91a**) showed lower chiral recognition ability than their low molecular weight chitosan counterparts (**88b, 89b, 91b**), with the exception of derivative **90a** that showed higher chiral recognition ability than derivative **90b**. These CSPs were also able to withstand organic solvents such as ethyl acetate (100%) and chloroform (100%) [121].

2.2.1.2.3. Chitosan amine-derived CSP

Liu *et al.,* in 2006, postulated that the development of a chitosan CSP would be an excellent tool to be used in chiral ligand-exchange chromatography (CLEC), considering the high binding capacity of chitosan to heavy metals [122]. Consequently, they described the immobilization of chitosan into silica gel and the application of the obtained CSP (**Figure 6**) in CLEC to achieve enantioresolution of a variety of α-hydroxycarboxylic acids and α-aminoacids using $CuSO_4$ 100% or $CuSO_4$/MeOH (80:20 *v/v*) as mobile phases [122]. To the best of our knowledge, this is the only report related to the application of chitosan-derived CSPs for this type of study.

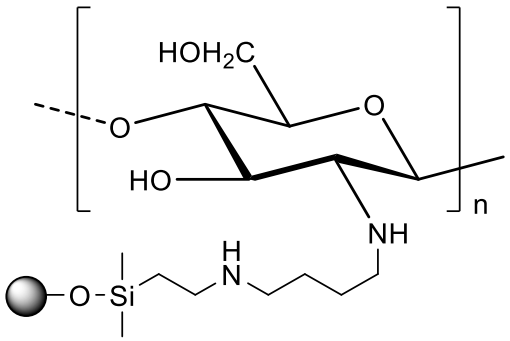

***Figure 6**. Structure of chitosan amine-derived CSP.*

3. Xanthone derivatives

Xanthones (9*H*-xanthen-9-ones) are oxygenated heterocyclic compounds with a dibenzo-γ-pirone scaffold (**Figure 7**), well known for their role in Medicinal Chemistry [123]. In fact, this class of compounds proved to have several biological and pharmacological activities, such as anticonvulsant [124], antitumor [125-127], anticoagulant [128], antifungal [129], among others [123, 130-131], depending on the nature and positions of the substituents in the xanthone scaffold, being considered as privileged structures [132-134].

Xanthones are frequently found in nature in plants, fungi, lichens, bacteria [130, 135], as well as in many marine sources [136] as secondary metabolites. Although natural xanthone have proved to be very interesting bioactive compounds, molecular modifications using their structures as models or total synthesis of new xanthonic compounds have been of great interest and will contribute to expand the spectrum of new bioactive compounds. Therefore, it is crucial to understand the methods used for synthesis of xanthone derivatives (XDs).

For the last several years, the synthesis of bioactive XDs using different synthetic methodologies has been extensively studied by the research Group of Medicinal Chemistry of Laboratory of Organic and Pharmaceutical Chemistry (LQOF) of the Faculty of Pharmacy of the University of Porto/CIIMAR [126, 137].

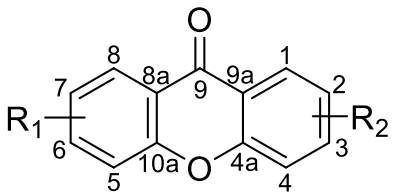

Figure 7. *General structure of a xanthone derivative.*

3.1. Synthetic routes of xanthone derivatives

XDs can be synthesized through different methodologies as represented in **Scheme 1** [134, 138], including *via* benzophenone intermediate, *via* diaryl ether intermediate, and *via* one-step synthesis.

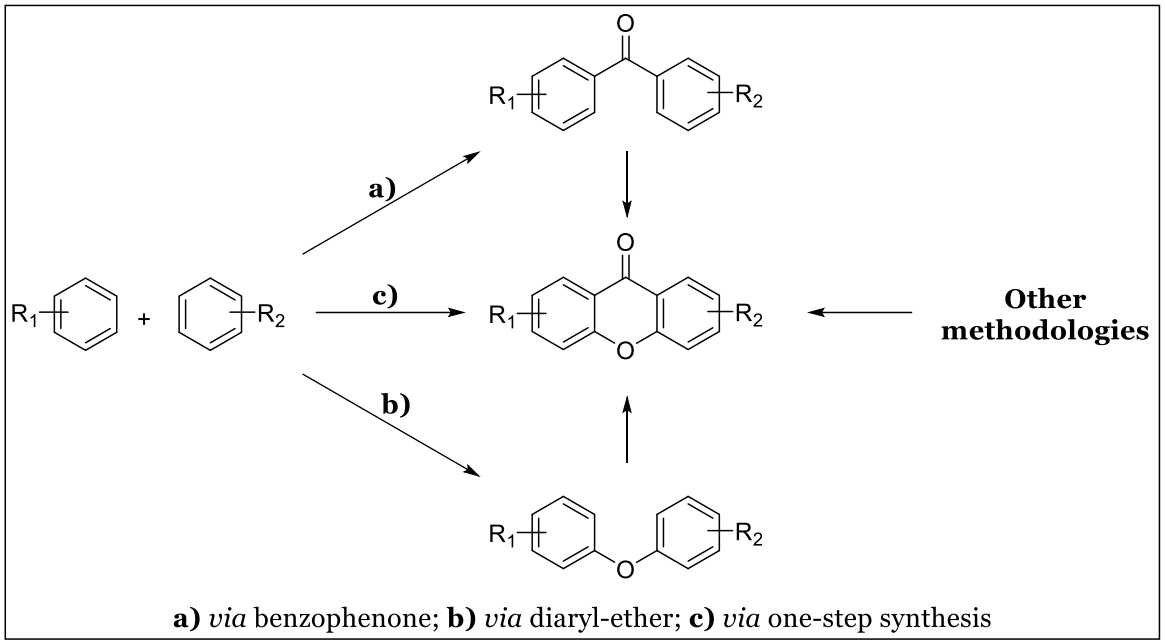

a) *via* benzophenone; **b)** *via* diaryl-ether; **c)** *via* one-step synthesis

Scheme 1. *Commonly used synthetic routes to obtain xanthone derivatives (adapted from [138])*

3.1.1. *Via* Benzophenone intermediate

The synthesis of XDs *via* benzophenone intermediate is the most commonly used pathway. It is based in a two-step synthesis including the synthesis of a benzophenone intermediate and subsequent intramolecular cyclisation. The synthesis of the benzophenone intermediate can be achieved through several methods, such as by photoacylation reaction between a benzaldehyde and *p*-quinone, by the addition of a lithium-substituted aryl group to a carbonyl group or by Friedel-Crafts acylation [126, 134].

The Friedel-Crafts acylation is the most used synthetic pathway to the formation of benzophenone intermediates, and it is based in an electrophilic aromatic substitution between a phenol or protected phenol derivative and an acyl chloride [126, 134]. The benzophenone is generally obtained in good yields, however, this reaction may present some limitations such as a restricted applicability with certain functional groups, due to the acidic conditions in which it is performed, and its lack of regioselectivity, allowing for both *ortho* and *para* positions to be acylated.

Then, the cyclization of the benzophenone derivatives may be achieved by an Ullman-coupling reaction, by oxidative coupling, oxidation and conjugate addition, and by nucleophilic aromatic substitution under alkaline conditions [126].

3.1.2. *Via* diaryl-ether intermediate

The synthesis of XDs *via* diaryl ether intermediate is also based in a two-step synthesis: the formation of the diaryl ether and subsequent intramolecular cyclization to obtain the correspondent xanthone [138].

The synthesis of diaryl ether intermediates can be achieved by a conjugate substitution of a 1,4-halobenzoquinone and a phenol derivative or by Ullman-coupling reaction between a benzoic acid bearing a halogen group in the *ortho* position and a phenol derivative. Ullman-coupling reactions are the most commonly used reactions for obtaining a diaryl ether derivative, however, this copper-catalysed reaction often present low yields, the reaction times are long, and are carried out at high temperatures [139-140].

Then, the cyclization of the diaryl ether derivatives can be achieved mainly by intramolecular acylation, by base-catalysed intramolecular anionic cycloacylation or by acid-catalysed intramolecular electrophilic cycloacylation [134, 138].

3.1.3. One-step synthesis

One-step synthesis of XDs is not commonly used because of the harsh conditions required. This synthesis may be achieved by three different approaches: by acid-catalysed condensation of salicylic acid or salicylic ester derivatives with a phenol derivative, by condensation of a salicylic ester with an aryne intermediate or by Palladium-catalysed reaction of salicylaldehyde with 1,2-dibromophenyl derivatives [138].

3.1.4. Other methodologies

Other non-conventional methodologies to the synthesis of XDs are described in literature, such as *via* chromen-4-ones, *via* benzoquinone, *via* Claisen cyclization of poly-β-ketides, among others [134, 138].

II. Aims

The main aim of this dissertation was the preparation of new chiral stationary phases (CSPs) for liquid chromatography (LC) based on xanthone derivatives (XDs) and polysaccharides.

The specific aims of this dissertation concerning the preparation of a new CSP comprising a chiral derivative of xanthone (CDX) as small molecule chiral selector (**Figure 8**), were:

- Total synthesis of a suitable functionalized XD as building block by a multi-step pathway;
- Synthesis of a CDX by coupling reaction of the synthetized XD with a enantiomerically pure building block;
- Synthesis of a silylated derivative of CDX and further covalent bound to the chromatographic support;
- Structure elucidation of the silylated derivative of CDX, CDX, XD and all the intermediates by spectroscopic techniques;
- Pack of the CSP in a HPLC column and evaluation of its enantioresolution performance using different chiral analytes.

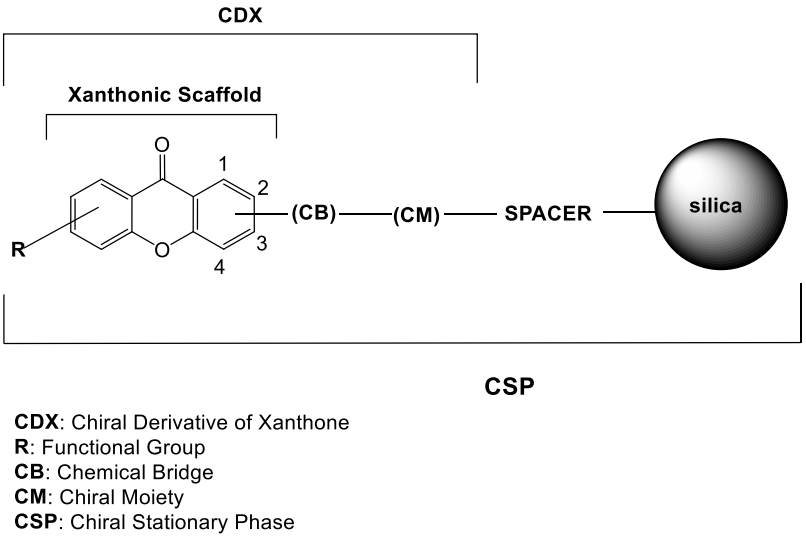

***Figure 8**. Schematic representation of a CSP based on CDX.*

The specific aims concerning the preparation of CSPs comprising polysaccharide derivatives as chiral selector (**Figure 9**), were:

- Synthesis of 3,5-dimethylphenylcarbamates of polysaccharides;
- Coating the obtained derivatives onto aminopropylsilica;
- Pack of the CSPs in a HPLC column and evaluation of their enantioresolution performance using different chiral analytes.

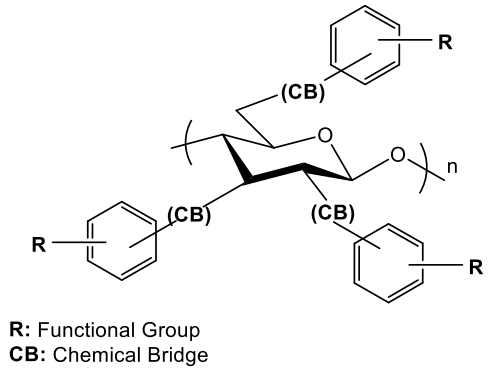

Figure 9. *Schematic representation of a chiral selector based on polysaccharide derivative.*

The specific aims concerning the preparation of a new CSP comprising a xanthone-polysaccharide derivative as chiral selector (**Figure 10**), were:

- Total synthesis of a suitable functionalized XD as building block by a multi-step pathway;
- Synthesis of a xanthone-polysaccharide derivative by bonding the XD to the polysaccharide;
- Coating the obtained derivative onto aminopropylsilica;
- Pack of the CSP in a HPLC column and evaluation of its enantioresolution performance using different chiral analytes.

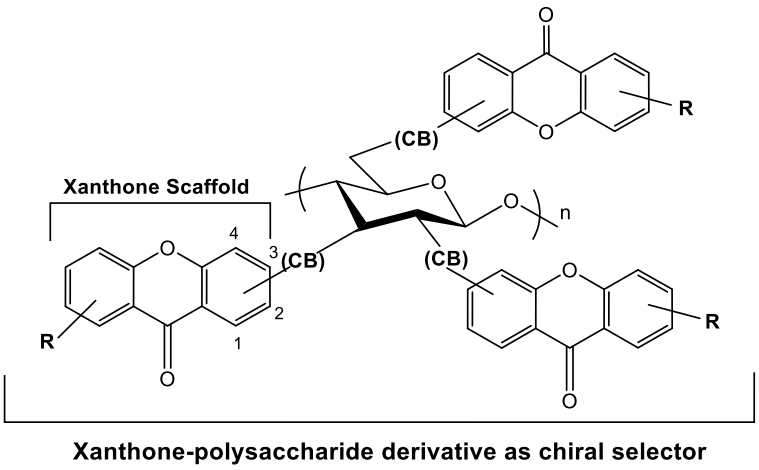

Figure 10. *Schematic representation of a chiral selector based on a xanthone-polysaccharide derivative.*

III. Results and Discussion

A. SYNTHESIS AND STRUCTURE ELUCIDATION

In this chapter are described and discussed the steps for preparation of chiral stationary phases (**CSPs 1-4**) (**92-95**) as well as the full synthetic pathways of the chiral selectors used and the xanthone derivatives (XD). Several attempts of binding XDs to amylose, cellulose, chitin and chitosan are also described and discussed.

CSP-1 comprises a chiral derivative of xanthone (CDX) covalently bonded to silica, **CSP-2** and **CSP-3** comprise the 3,5-dimethylphenylcarbamate of amylose and cellulose, respectively, coated in Aminopropylsilica (APS) and **CSP-4** comprises of *N*-derivated chitosan with a XD coated in APS.

Firstly, the 5,7-dimethyl-9-oxo-9*H*-xanthene-2-carboxilic acid (XD-1) was chosen to prepare **CSP-1** due to its structural similarity to the 3,5-dimethylphenyl moiety of the ADMPC and CDMPC CSPs, commercially available.

CSPs-2 and **-3** were then prepared to optimize the derivatization reaction of amylose and cellulose with 3,5-dimethylphenylisocyanate.

Several attempts of binding the XD-1 were then performed with four polysaccharides through coupling reactions or *via* benzoyl chloride, however none of the attempts were successful. One of the possible reasons for the failure of theses reaction attempts may be due to steric hindrance effects that blocks the ester/amide formation. Therefore 2-((9-oxo-9*H*-xanthen-3-yl)oxy)acetic acid (XD-2) was chosen to proceed the binding attempts of a XD to the polysaccharides.

The **CSP-4** was prepared by derivatizing the amine group of chitosan with XD-2 through reaction with the correspondent benzoyl chloride and further with 3,5-dimethylphenylisocyanate.

Finally, several further binding attempts were performed between XD-2 and the polysaccharides cellulose and chitosan, however none of the binding attempts were successful.

The structure elucidation of the synthesized compounds and CSPs evaluation in the resolution of some racemates are also discussed.

1. Preparation of a CSP with a small molecule as chiral selector (CSP-1) (92)

The preparation of **CSP-1** (**92**) was carried out using 5,7-dimethyl-9-oxo-9*H*-xanthene-2-carboxilic acid (XD-1) (**96**) as building block (**Scheme 2**). The XD-1 (**96**) was coupled with the chiral amino-alcohol (*R*)-(-)-phenylglycinol (**97**) using *O*-(benzotriazol-1-yl)-*N,N,N′,N′*-tetramethyluronium tetrafluoroborate (TBTU) affording the xanthonic chiral selector (*R*)-*N*-(2-hydroxy-2-phenylethyl)-5,7-dimethyl-9-oxo-9-*H*-xanthene-2-

carboxamide (CDX-1) (**98**). The strategy used to bond the chiral selector to the chromatographic support was through the synthesis of a derivative that allowed the covalent linkage to the silica. Consequently, the CDX-1 (**98**) was reacted with 3-(triethoxysilyl)propylisocyanate (**99**) to give the silylated derivative (*R*)-*N*-(2-hydroxy-2-phenylethyl)-5,7-dimethyl-9-oxo-9-*H*-xanthene-2-carboxamido)-1-phenylethyl(3-(triethoxysilyl)propyl)carbamate (SilCDX-1) (**100**). Then, the SilCDX-1 (**100**) was covalently bonded to silica giving the **CSP-1** (**92**).

The general strategy for preparation of **CSP-1** was based on pathways previously described in literature [141-142].

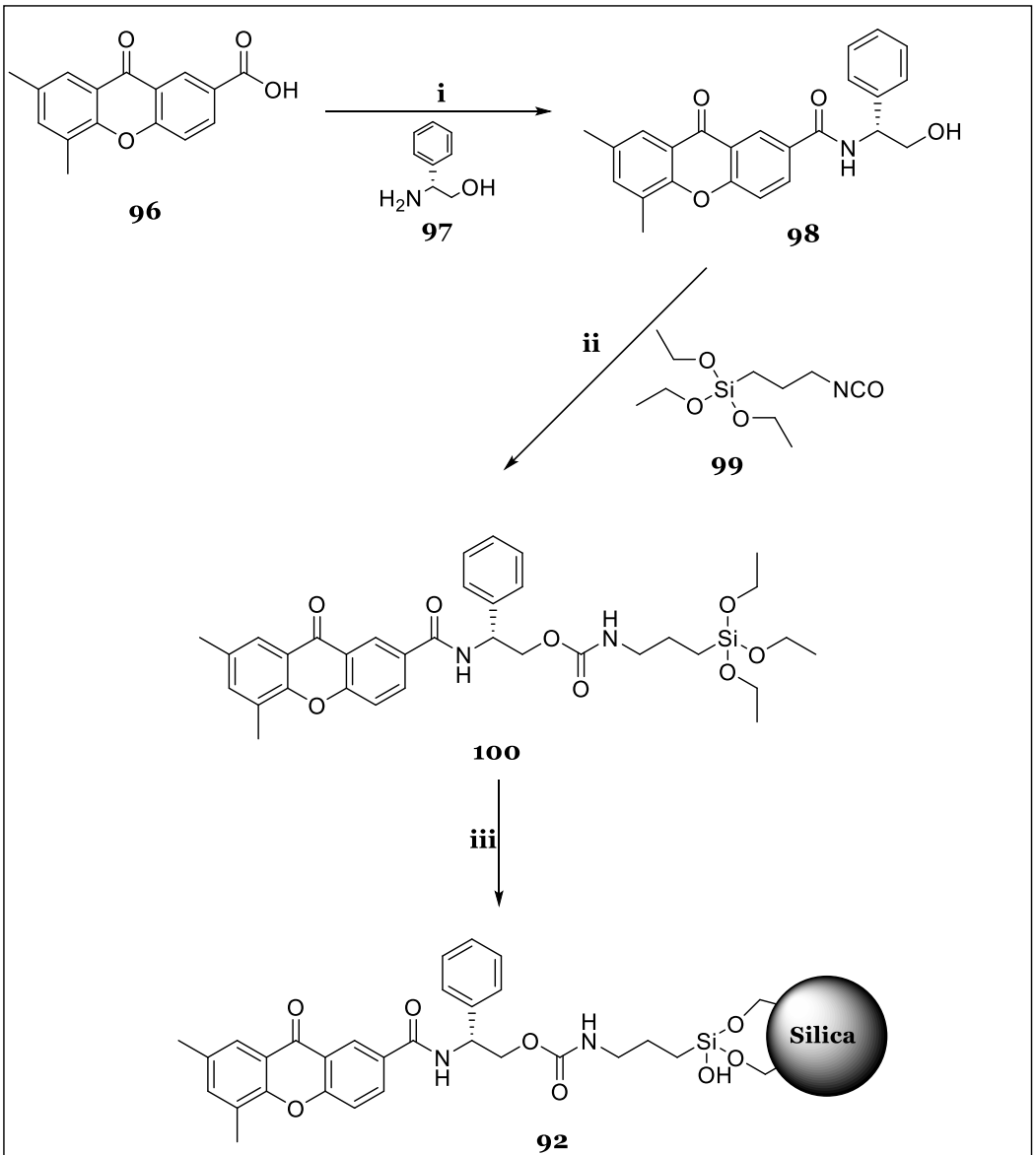

i- TBTU, TEA and THF, room temperature, 1.5 h;
ii- TEA and dry Toluene, reflux, 76 h;
iii- Silica gel (Nucleosil 100 A-5µm), dry Toluene, reflux, 76 h

***Scheme 2**.Preparation of CSP1 (**92**).*

1.1. Synthesis of 5,7-dimethyl-9-oxo-9*H*-xanthene-2-carboxilic acid (XD-1) (96)

To obtain the **CSP-1** (**92**), the total synthesis of 5,7-dimethyl-9-oxo-9*H*-xanthene-2-carboxilic acid (**XD-1**) (**96**) was firstly performed, following a 4-step synthetic pathways as represented in **Scheme 3** and based on described procedure [140].

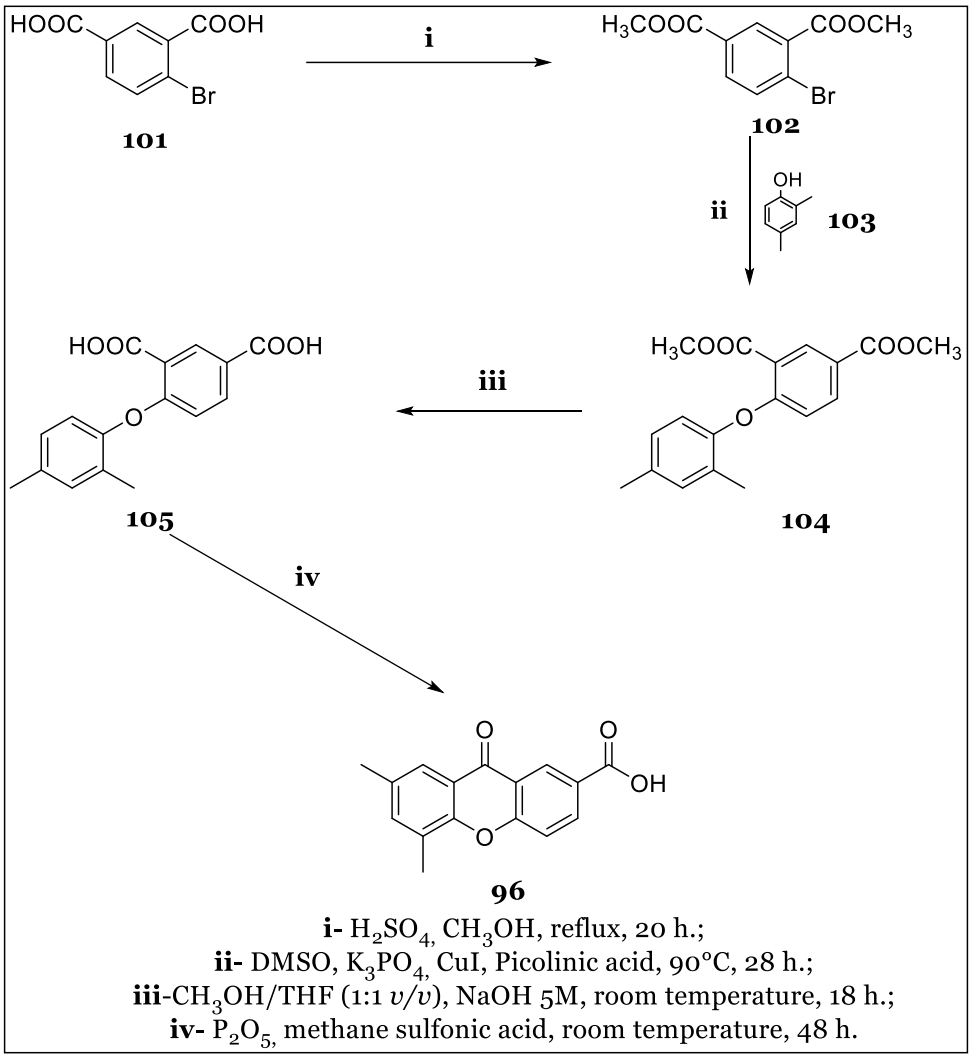

***Scheme 3**. Synthesis of XD-1 (**96**).*

The first reaction step (reaction i, **Scheme 3**) comprised of a Fischer esterification of 4-bromoisophtalic acid (**101**) with methanol and concentrated H_2SO_4 to give dimethyl 4-bromoisophtalate (**102**). Dimethyl 4-bromoisophtalate (**102**) was then reacted with 2,4-dimethylphenol (**103**) *via* Ullman reaction using picolinic acid and CuI as catalyst, in an alkaline medium with K_3PO_4 and dimethylsulfoxide (DMSO) (reaction ii, **Scheme 3**) [139] to give dimethyl 4-(2,4-dimethylphenoxy)isophtalate (**104**).

The next reaction step comprised a hydrolysis of the ester groups of dimethyl 4-(2,4-dimethylphenoxy)isophtalate (**104**) under alkaline conditions, using 5M NaOH, to achieve the 4-(2,4-dimethylphenoxy)isophtalic acid (**105**) (reaction iii, **Scheme 3**).

The last step for the synthesis of XD-1 (**96**) comprised an intramolecular acylation under acidic conditions using phosphorous pentoxide and methane sulfonic acid (Eaton's reagent) at room temperature to afford XD-1 (**96**) (reaction iv, **Scheme 3**).

The structure elucidation of XD-1 (**96**) and its intermediates was carried out as described in sections **1.1.1.** to **1.1.4.**

1.1.1. Structure elucidation of dimethyl 4-bromoisophtalate (102)

Dimethyl 4-bromoisophtalate (**102**) was obtained through esterification of 4-bromoisophtalic acid (**101**). The structure elucidation of compound **102** was achieved by ^{1}H NMR, ^{13}C NMR and IR.

Regarding the ^{1}H NMR spectrum, it is important to point out the presence of two distinct singlets, with integration for three protons each, with chemical shifts at 3.93 and 3.95 ppm corresponding to the protons of the methyl groups of the two esters (**Table 1**).

In ^{13}C NMR spectrum, it is important to highlight the presence of two signals with chemical shifts at 52.5 and 52.7 ppm, corresponding to the carbons of the methyl groups of the two esters of the molecule (**102**) (**Table 1**).

Table 1. *^{1}H NMR and ^{13}C NMR assignments of compound **102**.*

^{1}H NMR chemical shifts δ (ppm)		**^{13}C NMR chemical shifts δ (ppm)**	
2-H	*d,* 8.43 (*J*=2.2)	1	127.0
5-H	*d,* 7.75 (*J*=8.3)	2	132.3
6-H	*d,* 7.95 (*J*=2.2)	3	129.3
2'-C<u>H</u>$_3$	*s,* 3.93	4	134.7
2"-C<u>H</u>$_3$	*s,* 3.95	5	132.2
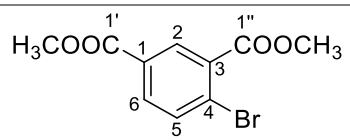		6	133.0
		1' and 1"	165.7 and 165.5
		1' and 1" – O<u>C</u>H$_3$	52.5 and 52.7

J values in Hz

The IR spectrum of compound **102** was collected and compared to the IR spectrum of compound **101** (**Table 2**). By comparison it is important to highlight that two characteristic bands at 2880 and 2625 cm^{-1}, corresponding to O-H bond of carboxylic acids,

are only present on spectrum of compound **101**. Additionally, the shift of the band at 1687 cm^{-1} to 1754 cm^{-1} confirmed that the synthesis of compound **102** was successful.

***Table 2**. IR data of compounds **101** and **102**.*

Bond	υ (cm^{-1})	
	(101)	**(102)**
C=C (aromatic)	930	929
C=O (acid/ester)	1687	1754
O-H	2625 and 2880	---
C-O (acid/ester)	1255	1253
O-CH_3 (ester)	---	1309

1.1.2. Structure elucidation of dimethyl 4-(2,4-dimethylphenoxy) isophtalate (104)

Dimethyl 4-(2,4-dimethylphenoxy)isophtalate (**104**) was obtained *via* Ullman reaction of dimethyl 4-bromoisophtalate (**102**) and 2,4-dimethylphenol (**103**). The structure elucidation of compound **104** was achieved by ^{1}H NMR, ^{13}C NMR and IR.

The ^{1}H and ^{13}C NMR spectra data obtained are consistent to the proposed structure of compound **104** (**Table 3**). Considering the ^{1}H NMR spectrum, the presence of two singlets with chemical shifts at 2.07 and 2.29 ppm with integration for three protons each, corresponding to the protons of the methyl groups, confirmed that the synthesis of compound **104** was successful. It is also confirmed by the presence of two signals, in the ^{13}C NMR spectrum, with chemical shifts at 20.4 and 21.0 ppm, corresponding to the carbons of the referred groups.

***Table 3**. ^{1}H NMR and ^{13}C NMR assignments of compound **104**.*

^{1}H NMR chemical shifts δ (ppm)		**^{13}C NMR chemical shifts δ (ppm)**	
2-H	*d*, 8.35 (*J*=2.2)	1 and 3	165.0 and 165.2
5-H	*d*, 6.70 (*J*=8.7)	2	134.2
6-H	*dd*, 8.00 (*J*=8.7 and 2.2)	4	160.4
2'-C$\underline{H}_3$	*s*, 2.29	5	120.3
3'-H	*s*, 7.17	6	134.9
4'-C$\underline{H}_3$	*s*, 2.07	1'	124.9
5'-H	*d*, 6.89 (*J*=8.2 Hz)	2' and 4'	116.2 and 116.3
6'-H	*d*, 7.08 (*J*=8.2 Hz)	3'	124.4

*Table 3. 1H NMR and 13C NMR assignments of compound **104**. (Cont.)*

^{1}H NMR chemical shifts δ (ppm)		^{13}C NMR chemical shifts δ (ppm)	
1" and 1"' -C<u>H</u>$_3$	*s*, 3.84	5'	121.9
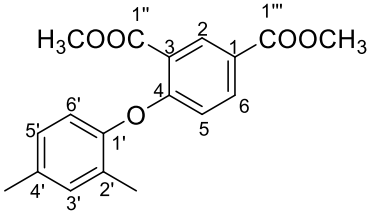		6'	120.3
		2' and 4' – <u>C</u>H$_3$	21.0 and 20.4
		1" and 1"'	166.0 and 166.1
		1" and 1"' – O<u>C</u>H$_3$	52.3 and 52.4

J values in Hz

Concerning IR spectrum of compound **104** it is important to highlight the presence of a band at 1259 cm^{-1} corresponding to the ether bond formation which confirms the success of the desired transformation. The remaining IR bands are assigned in **Table 4**.

*Table 4. IR data of compound **104**.*

Bond	*υ* (cm^{-1})
C=C (aromatic)	1436
C=O (ester)	1717
C-O-C (ether)	1259

1.1.3. Structure elucidation of 4-(2,4-dimethylphenoxy)isophtalic acid (105)

4-(2,4-Dimethylphenoxy)isophtalic acid (**105**) was obtained through hydrolysis of methyl esters of compound **104**. The data obtained from ^{1}H NMR, ^{13}C NMR and IR allowed its structure elucidation

Comparing the ^{1}H NMR spectra data of compound **105** (**Table 5**) to its precursor (**104**) (**Table 3**), it is important to highlight the absence of two singlets with chemical shift at 3.84 ppm corresponding to the protons of the two ester methyl groups of compound **104**.

Furthermore, the absence in the ^{13}C NMR spectrum of compound **105**, of two signals corresponding to the carbons of ester methyl groups (δ=52.3 and 52.4 ppm) confirmed that the reaction was successful. The remaining ^{1}H NMR and ^{13}C NMR assignments are described in **Table 5**.

*Table 5. ^{1}H NMR and ^{13}C NMR assignments of compound **105**.*

^{1}H NMR chemical shifts δ (ppm)		**^{13}C NMR chemical shifts δ (ppm)**	
2-H	*d,* 8.33 (*J*=2.2)	1 and 3	164.2 and 165.1
5-H	*d,* 6.67 (*J*=8.7)	2	134.4
6-H	*dd,* 7.97 (*J*=8.7 and 2.2)	4	160.0
2'-C$\underline{H}_3$	*s,* 2.29	5	120.3
3'-H	*s,* 7.16	6	132.9
4'-C$\underline{H}_3$	*s,* 2.07	1'	128.2
5'-H	*d,* 6.87 (*J*=8.1)	2' and 4'	118.1 and 116.3
6'-H	*d,* 7.07 (*J*=8.1)	3'	124.4
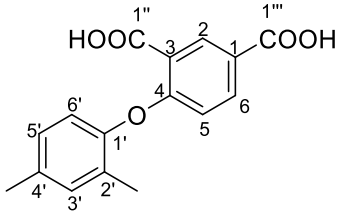		5'	122.0
		6'	120.3
		2' and 4' – $\underline{C}H_3$	20.4 and 15.6
		1" and 1"'	166.2 and 166.3

J values in Hz

Comparing the IR data of compounds **105** (**Table 4**) and **104** (**Table 6**), it is possible to observe the shift of the band correspondent to the carbonyl bond at 1717 cm^{-1} to 1613 cm^{-1}, associated to the transformation of $COOCH_3$ to COOH. Moreover, the presence in the IR spectrum of compound **105,** of a broad band at 2923 cm^{-1} correspondent to the O-H bond of the carboxylic acid moiety confirmed that the reaction occurred with success.

*Table 6. IR data of compound **105**.*

Bond	***v* (cm^{-1})**
C=C (aromatic)	1491 and 1604
C=O (ester/acid)	1613
O-H (acid)	2923
C-O-C (ether)	1257

1.1.4. Structure elucidation of 5,7-dimethyl-9-oxo-9*H*-xanthene-2-carboxilic acid (XD-1) (96)

5,7-Dimethyl-9-oxo-9*H*-xanthene-2-carboxilic acid (XD-1) (**96**) resulted from an intramolecular acylation of 4-(2,4-dimethylphenoxy)isophtalic acid (**105**). The structure elucidation of compound **96** was achieved by ^{1}H NMR, ^{13}C NMR and IR.

In the ^{1}H NMR spectrum of compound **96**, it is shown the signals corresponding to the six protons of the two methyl groups and five signals corresponding to the aromatic protons of the xanthone scaffold (**Table 7**).

The ^{13}C NMR spectrum of compound **96** showed a new signal with chemical shift at 176.8 ppm corresponding to the carbonyl group of the xanthone scaffold, confirming the success of the reaction.

The full signal assignment of ^{1}H NMR and ^{13}C NMR spectra are described in **Table 7**.

Table 7. *^{1}H NMR and ^{13}C NMR assignments of compound **96**.*

^{1}H NMR chemical shifts δ (ppm)		**^{13}C NMR chemical shifts δ (ppm)**	
1-H	*d,* 8.61 (*J*=2.1)	1	128.0
3-H	*dd,* 8.23 (*J*=8.7 and 2.2)	2	126.3
4-H	*d,* 7.59 (*J*=8.7)	2 - COOH	166.2
5-$C\underline{H}_3$	*s,* 2.39	3	134.9
6-H	*s,* 7.02	4	118.2
7-$C\underline{H}_3$	*s,* 2.74	5	117.2
8-H	*s,* 7.23	6	128.6
		7	121.7
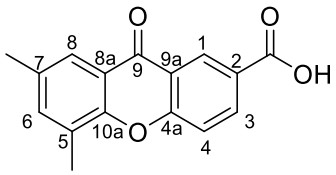		8	116.0
		8a	140.8
		9	176.8
		10a	145.8
		5 and 7 – $\underline{C}H_3$	21.2 and 22.6
		4a and 9a	156.8 and 157.2

J values in Hz

The IR spectrum of XD-1 (**96**) showed the presence of absorption bands corresponding to the C=O bond (at 1667 cm^{-1}) and aromatic C=C bonds (at 1475 and 1421 cm^{-1}) associated with the xanthone scaffold (**Table 8**) that confirmed the success of the reaction.

Table 8*. IR data of compound **96**.*

Bond	***υ* (cm^{-1})**
C=O (xanthone)	1667
C=C (aromatic)	1475 and 1421
C=O (acid)	1611
O-H (acid)	2920

1.2. Synthesis of (*R*)-*N*-(2-hydroxy-2-phenylethyl)-5,7-dimethyl-9-oxo-9-*H*-xanthene-2-carboxamide (CDX-1) (98)

Based on described procedure [126, 137, 140], the synthesized **XD-1** (**96**) was coupled with the chiral amino-alcohol (*R*)-(-)-phenylglycinol (**97**) using *O*-(benzotriazol-1-yl)-*N,N,N′,N′*-tetramethyluronium tetrafluoroborate (TBTU) and a catalytic amount of TEA in THF for 1.5 hours at room temperature, to give (*R*)-*N*-(2-hydroxy-2-phenylethyl)-5,7-dimethyl-9-oxo-9-*H*-xanthene-2-carboxamide (**CDX-1**) (**98**) (**Scheme 4**).

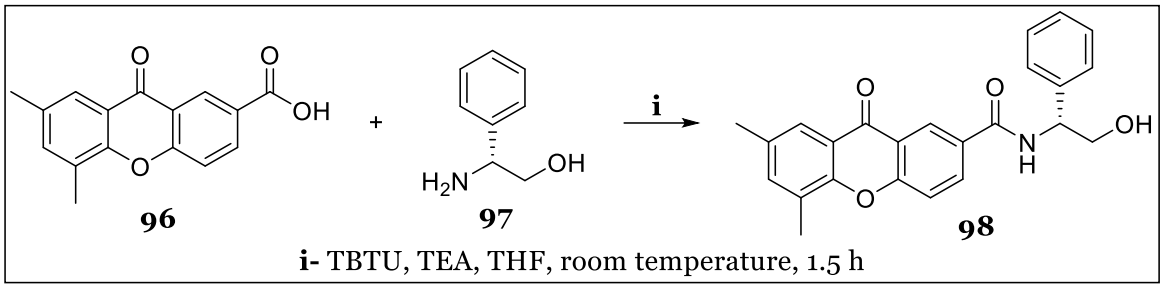

***Scheme 4**. Synthesis of CDX-1.*

O-(Benzotriazol-1-yl)-*N,N,N′,N′*-tetramethyluronium tetrafluoroborate (TBTU), is one of the most commonly used coupling reagents for amide bond formation. It is very efficiency and presents low tendency towards racemization [143]. TBTU reacts with the carboxylic acid group of XD-1 (**96**) forming an active ester that then reacts with the amine group of the amino alcohol to form an amide bond [143].

1.2.1. Structure elucidation of (*R*)-*N*-(2-hydroxy-2-phenylethyl)-5,7-dimethyl-9-oxo-9-*H*-xanthene-2-carboxamide (*CDX-1*) (98)

The ^{1}H and ^{13}C NMR (**Table 9**) and IR (**Table 10**) data allowed the structure elucidation of CDX-1 (**98**).

In ^{1}H NMR spectrum, it is important to highlight the presence of new signals correspondent to the protons of the chiral moiety, when compared to the ^{1}H NMR spectrum data of compound **96** (**Table 7**), which confirmed the success of the coupling reaction. It is also important to point out the presence of new signals correspondent to the carbons of the chiral moiety in the ^{13}C NMR.

***Table 9**. [1]H NMR and [13]C NMR assignments of compound **98**.*

[1]H NMR chemical shifts δ (ppm)		**[13]C NMR chemical shifts δ (ppm)**	
1-H	*d,* 8.63 (*J*=2.2)	1	129.5
3-H	*dd,* 8.25 (*J*=2.2 and 8.8)	2	124.7
4-H	*d,* 7.53 (*J*=8.7)	2-C=O	166.3
5-CH_3	*s,* 2.42	3	133.8
6-H	*s,* 7.26	4	121.0
7-CH_3	*s,* 2.49	4a	157.7
8-H	*s,* 7.90	5-CH_3	20.8
1'-H	*m,* 5.34	7-CH_3	15.7
2'-CH_2	*d,* 4.06 (*J*=5.2)	5	134.4
2'-OH	*s,* 1.74	6	128.0
2", 3", 4", 5" and 6"	*m,* 7.36	7	137.6
		8	118.8
		8a	120.6
		9	177.2
		9a	123.6
		10a	152.6
		1'	56.5
		2'	66.4
		1"	138.8
		2" and 6"	127.1
		3" and 5"	129.0
		4"	126.9

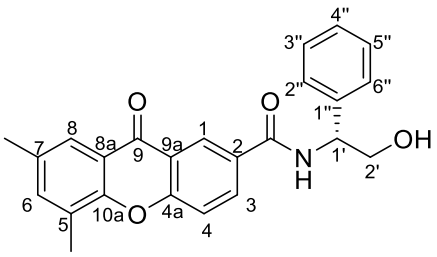

J values in Hz

In the IR spectrum of compound **98** it is observed an intense band at 3431 cm^{-1} corresponding to the N-H of the amide bond and a broad band at 3105-3661 cm^{-1} corresponding to the O-H bond of the compound (**Table 10**). Furthermore, when comparing to the IR spectrum data of compound **96** (**Table 8**), it is important to point out the shift of the carbonyl band at 1667 cm^{-1} to 1652 cm^{-1} corresponding to the transformation from carboxylic acid to amide.

Table 10. *IR data of compound* ***98****.*

Bond	υ (cm^{-1})
C=O (xanthone)	1652
C=C (aromatic)	1540 and 1474
C=O (amide)	1615
O-H	3105-3661(*br*)
N-H (amide)	3431

1.3. Synthesis of (*R*)-*N*-(2-hydroxy-2-phenylethyl)-5,7-dimethyl-9-oxo-9-*H*-xanthene-2-carboxamido)-1-phenylethyl(3-(triethoxysilyl) propyl)carbamate (SilCDX-1) (100)

CDX-1 (**97**) was reacted with 3-(triethoxysilyl)propylisocyanate (**99**) using a catalytic amount of TEA in dry toluene to afford the derivative (*R*)-*N*-(2-hydroxy-2-phenylethyl)-5,7-dimethyl-9-oxo-9-*H*-xanthene-2-carboxamido)-1-phenylethyl(3-(triethoxysilyl)propyl)carbamate (SilCDX-1) (**100**) (**Scheme 5**).

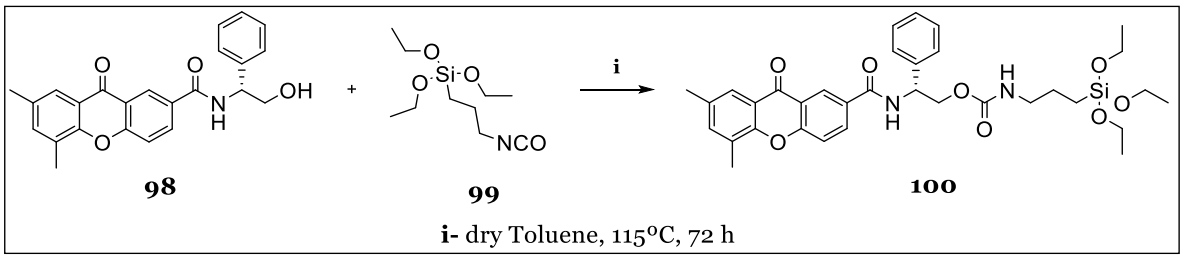

Scheme 5. *Synthesis of the silylated derivative of CDX-1, SilCDX-1 (****100****).*

This reaction was performed under anhydrous conditions due to the instability of the isocyanate in contact with water that lead to the formation of urea [144]. The crude product was purified by flash chromatography.

1.3.1. Structure elucidation of (*R*)-*N*-(2-hydroxy-2-phenylethyl)-5,7-dimethyl-9-oxo-9-*H*-xanthene-2-carboxamido)-1-phenylethyl(3-(triethoxysilyl)propyl)carbamate (SilCDX-1)

SilCDX-1 (**98**) was analysed by ^{1}H NMR (**Table 11**). This data allowed for the structure elucidation of SilCDX-1 (**98**).

In the ^{1}H NMR spectrum, it is important to highlight the presence of new signals correspondent to the protons of the silylated carbamate moiety, when compared to the ^{1}H NMR spectrum data of compound **96** (**Table 9**), which confirmed the success of the reaction.

Table 11. *^{1}H NMR and ^{13}C NMR assignments of compound* ***100****.*

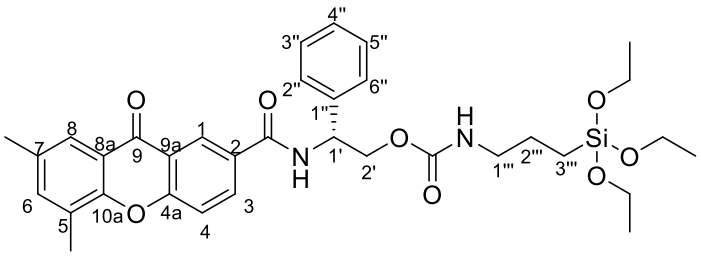

^{1}H NMR chemical shifts δ (ppm)	
1-H	*d,* 8.75 (*J*=2.2)
3-H	*dd,* 8.29 (*J*=2.0 and 8.6)
4-H	*d,* 7.61 (*J*=8.9)
5-C<u>H</u>$_3$	*s,* 2.45
6-H	*s,* 7.55
7-C<u>H</u>$_3$	*s,* 2.55
8-H	*s,* 7.98
1'-H	*m,* 5.14
2'-C<u>H</u>$_2$	*m,* 4.63
2", 3", 4", 5" and 6"	*m,* 7.71
1"'	*m,* 3.23
2"'	*m,* 2.14
3"'	*m,* 0.61
Si-OC<u>H</u>$_2$CH$_3$	*m,* 4.22
Si-OCH$_2$C<u>H</u>$_3$	*m,* 2.04

J values in Hz

1.4. Covalent bonding of (*R*)-*N*-(2-hydroxy-2-phenylethyl)-5,7-dimethyl-9-oxo-9-*H*-xanthene-2-carboxamido)-1-phenylethyl(3-(triethoxysilyl)propyl)carbamate (SilCDX-1) to Nucleosil 100 silica gel

SilCDX-1 (**100**) and silica Nucleosil® (5µm, 100 Å) were previously dried for 24 h in a desiccator with phosphorous pentoxide. SilCDX-1 (**100**) was dissolved in anhydrous toluene and the silica was added, the reaction was stirred for 40 h at 110ºC and the reaction product was thoroughly washed with several organic solvents to obtain **CSP-1** (**92**).

The **CSP-1** (**92**) was dried in the desiccator with phosphorous pentoxide for 24 h and then sieved and packed into a 4.6 mm × 150 mm HPLC column with *n*-hexane/isopropanol (90:10 *v/v*) as packing solvent at 6000 psi.

1.5. Calculation of silica loading capacity percentage

The **CSP-1** (**92**) was analysed through elemental analysis, and the percentage values obtained were as follows: C=8.81%, N=0.90% and H=1.18%. With these values it was possible to calculate the silica loading capacity percentage of SilCDX-1 (**98**). This parameter is calculated through the **Equation 1** that gives the moles of compound **98** bonded *per* area of the silica particles surface, $N_{M,}$ expressed in μmol m^{-2} [145].

$$\boldsymbol{N}_{\mathrm{M}} = \frac{10^6 \times \%C}{S \times [(100 \times n \times 12) - (\%C \times M_w)]} \quad \textbf{Equation 1}$$

In which S is the surface area of the silica particles, %C the percentage of carbons obtained through elemental analysis, n the number of carbon atoms in SilCDX-1, and M_w the molecular wheight of SilCDX-1. The value obtained for N_M was 0.87 μmol m^{-2}. Comparing to the values obtained from literature it was possible to obtain the percentage of silica hydroxyl groups derivated with compound **98**. In literature, it is stated that the concentration of hydroxyl groups in underivatized silica particles is 7.3 μmol m^{-2}, measured through thermogravimetric analysis (TGA)[146]. Therefore, it is possible to conclude that in **CSP-1**, 12% of the hydroxyl groups of the silica particles were derivated. This percentage may be explained due to the fact that only approximately 50% of the hydroxyl groups can be derivated, due to steric hindrance effects[147].

2. Preparation of CSPs with polysaccharide derivatives as chiral selectors

Two polysaccharide-based CSPs (**CSPs-2** and **CSP-3**) (**93** and **94**), already described in literature [20, 39, 41], were prepared. These CSPs are the most commonly used CSPs and are obtained by derivatization of amylose or cellulose with 3,5-dimethylphenyl isocyanate, respectively.

2.1. Preparation of CSP-2 (93)

The preparation of CSP-2 (**93**) was obtained from the reaction of amylose (**106**) with 3,5-dimethylphenylisocyanate (**107**) at reflux for 76 h to give amylose *tris*(3,5-dimethylphenylcarbamate) (ADMPC) (**108**) (**Scheme 6**) [20, 39, 41].

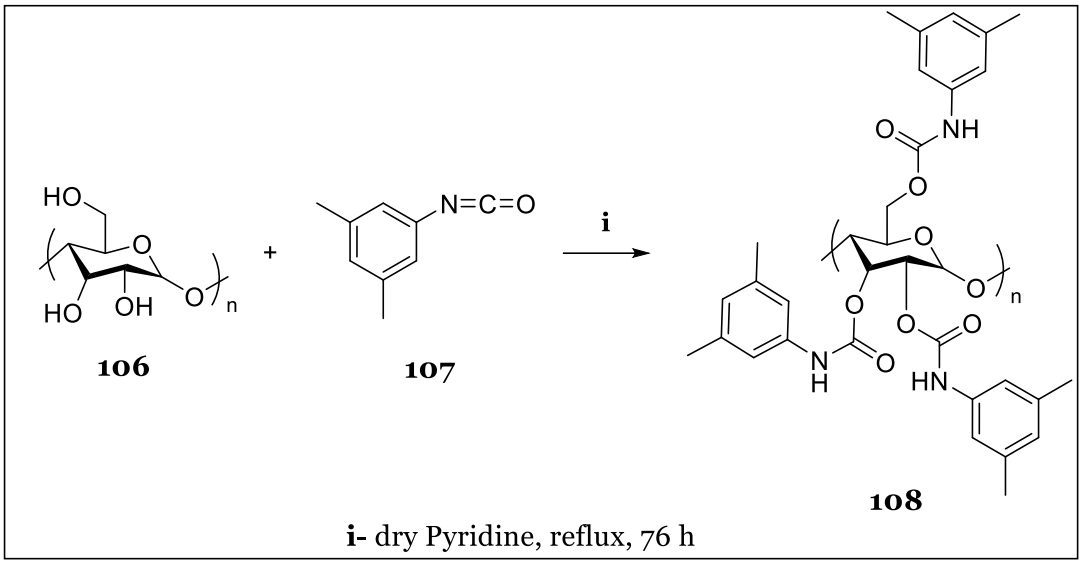

Scheme 6. *Synthesis of amylose tris(3,5-dimethylphenylcarbamate).*

Then, ADMPC (**108**) and the aminopropylsilica (APS) were dried in the desiccator with phosphorous pentoxide for 24 h and, then, the APS was refluxed with THF and gentle stirring for 30 min. ADMPC (**108**) was dissolved in THF and added to the suspended APS. The coating was achieved by stirring and slowly evaporating the solvent under reduced pressure in the rotatory evaporator. The coated silica gel was completely dried, sieved (180 μm sieve) and packed into a 4.6 mm × 150 mm HPLC column to give **CSP-2** (**93**). The coating method procedure was performed to give **CSP-2** (**93**) with a chiral selector 20% w/w loading capacity.

The column packing was achieved by a slurry mode with *n*-hexane/isopropanol (50:50 *v/v*) and *n*-hexane/isopropanol (80:20 *v/v*) as packing solvent, at 6000 psi.

2.1.1. Analysis of ADMPC (108) by IR and elemental analysis

Amylose 3,5-dimethylphenylcarbamate (ADMPC) (**108**) was analysed by, IR and Elemental Analysis.

The IR spectrum for ADMPC was obtained and compared to the IR spectrum of amylose (**106**). It is important to highlight the presence of three intense bands in the IR spectrum of ADMPC (**108**), that are not present in the IR spectrum of amylose (**106**), corresponding to characteristic bonds of carbamate group as well as the absence of the broad band corresponding to the O-H stretching of the hydroxyl groups of amylose (**Table 12**). This data allowed to conclude that the reaction occurred and a large number of amylose hydroxyl groups were derivatized with the isocyanate **107**.

Table 12. *IR data of compound* ***108*** *and amylose (****106****).*

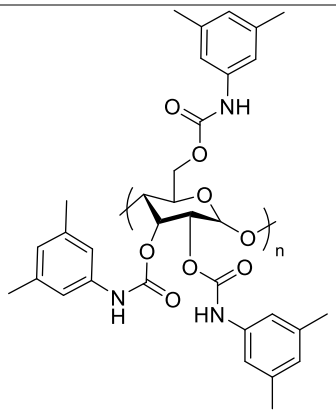

Bond	**υ (cm^{-1})**	
	(106)	**(108)**
O-H	3422 (br)	absent
N-H (carbamates)	---	3292
C=O (carbamates)	---	1713
C=C (aromatic)	---	1614

Elemental analysis of the final product was also performed (**Table 13**). The results obtained were compared to the theoretical data. By comparison, it was concluded that the amylose hydroxyl groups were quantitatively substituted by 3,5-dimethylphenylisocyanate.

Table 13. *Experimental and theoretical values of elemental analysis for compound* ***108****.*

	%C	**%N**	**%H**
Experimental	62.32	6.18	6.19
Theoretical	62.37	6.20	6.25

2.2. Preparation of CSP-3 (94)

The preparation of CSP-3 (**94**) was carried out by reaction of cellulose (**109**) with 3,5-dimethylphenylisocyanate (**106**) at reflux for 76 h to give cellulose *tris*(3,5-dimethylphenylcarbamate) (CDMPC) (**110**) (**Scheme 7**) [20, 39, 41].

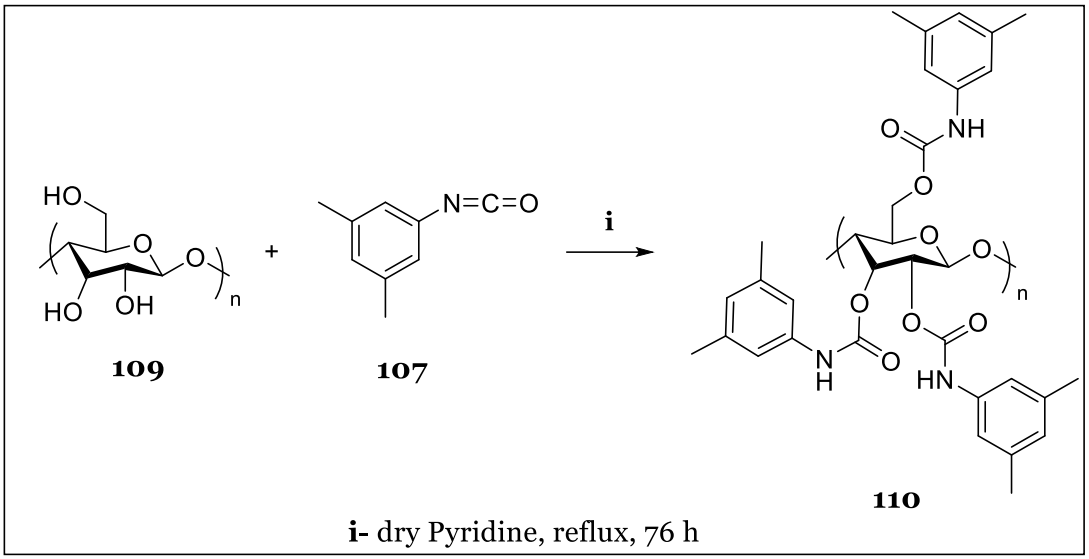

Scheme 7. *Synthesis of cellulose tris(3,5-dimethylphenylcarbamate).*

CDMPC (**110**) coating was performed as described previously for CSP-2 (**93**) in section **2.1**. to give CSP-3 (**94**)

The column packing was achieved by a slurry mode with n-hexane/isopropanol (50:50 *v/v*) and n-hexane/isopropanol (80:20 *v/v*) as mobile phase, at 6000 psi.

2.2.1. Analysis of CDMPC (110) by IR and elemental analysis

CDMPC (**110**) was analysed by, IR and elemental analysis. The IR spectrum obtained for the CDMPC (**110**) was compared to the IR spectrum of cellulose (**109**). It is important to highlight the presence of three intense bands in the IR spectrum of CDMPC (**110**), that are not present in the IR spectrum of cellulose (**109**), corresponding to characteristic bonds of carbamate group as well as the absence of the broad band corresponding to the O-H stretching of the hydroxyl groups of cellulose (**109**) (**Table 14**). This data allowed to conclude that the reaction occurred and a large number of amylose hydroxyl groups were derivatized with the isocyanate **107.**

Table 14. *IR data of compounds* ***109*** *and* ***110****.*

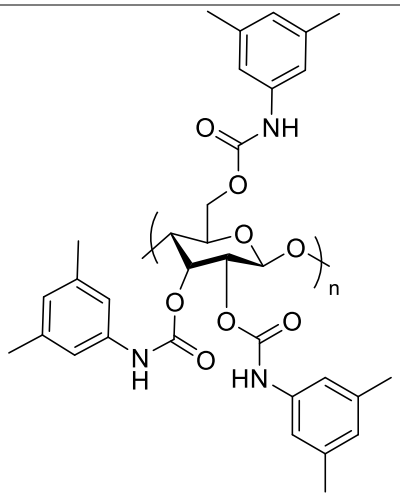

Bond	***v*** **(cm^{-1})**	
	(109)	**(110)**
O-H	3354 (*br*)	absent
N-H (carbamates)	---	3296
C=O (carbamates)	---	1732
C=C (aromatic)	---	1615

Elemental analysis of the final product was also performed (**Table 15**). The results obtained were compared to the theoretical data. By comparison, it was concluded that the cellulose hydroxyl groups were quantitatively substituted by 3,5-dimethylphenylisocyanate.

Table 15. *Experimental and theoretical values of elemental analysis for compound* ***110****.*

	%C	**%N**	**%H**
Experimental	65.06	7.08	6.33
Theoretical	62.37	6.20	6.25

3. Preparation of CSPs with xanthone-polysaccharide derivatives as chiral selectors

Following the preparation of three successful CSPs, the next step was to develop new CSPs comprising xanthone–polysaccharide derivatives as chiral selectors.

The first step in the preparation of these new CSPs was to bind a suitable functionalized XD to a polysaccharide through an ester/amide bond. The ester/amide bond could be achieved through coupling reactions or by reaction between a xanthone derivative benzoyl chloride and the alcohol/amine groups present in the backbone of the polysaccharides.

Several binding attempts were made with four different polysaccharides, namely amylose (**106**), cellulose (**109**), chitin (**111**) and, chitosan (**112**) and two XDs.

Firstly, attempts were carried out in binding XD-1 (**96**) to the four polysaccharides, being described in sections **3.1.1** to **3.1.4**. These attempts were not successful, and it was proposed that steric hindrance could be one of the main causes for the failure of these reactions. Therefore, another XD was chosen comprising the carboxylic acid group in a flexible lateral chain, and without substituents groups in the xanthone scaffold. Binding attempts of 2-((9-oxo-9*H*-xanthen-3-yl)oxy)acetic acid (XD-2) (**113**) with the polysaccharides cellulose (**109**) and chitosan (**112**) were performed and are described in sections **3.2.2.** and **3.2.3.**

Consequently, a xanthone-chitosan derivative was successfully prepared by reaction of XD-2 (**113**) with chitosan (**112**) through previous synthesis of XD-2 benzoyl chloride, as described in section **3.2.4.**

3.1. Attempts of synthesis of a xanthone-polysaccharide derivative using XD-1 (96) as building block

XD-1 (**96**) was firstly chosen due to its structural similarity to the most used carbamates of amylose and cellulose (3,5-dimethylphenylcarbamates).

Several binding methods between the synthesized XD-1 (**96**), and the polysaccharides amylose (**106**), cellulose (**109**), chitin (**111**) and chitosan (**112**) were tested.

3.1.1. Attempt reactions of XD-1 (96) with amylose (106)

Firstly, it was attempted the linkage of XD-1 (**96**) to amylose (**106**) through coupling reactions with the coupling reagents TBTU, (1-Cyano-2-ethoxy-2-oxoethylidenaminooxy)dimethylamino-morpholino-carbenium hexafluorophosphate (COMU) and Dicyclohexylcarboxamide with *N*-Hydroxysuccinimide as additive (DCC/NHS). The linkage was also tested through the reaction of the respective benzoyl chloride of XD-1 with the polysaccharide (**Scheme 8**).

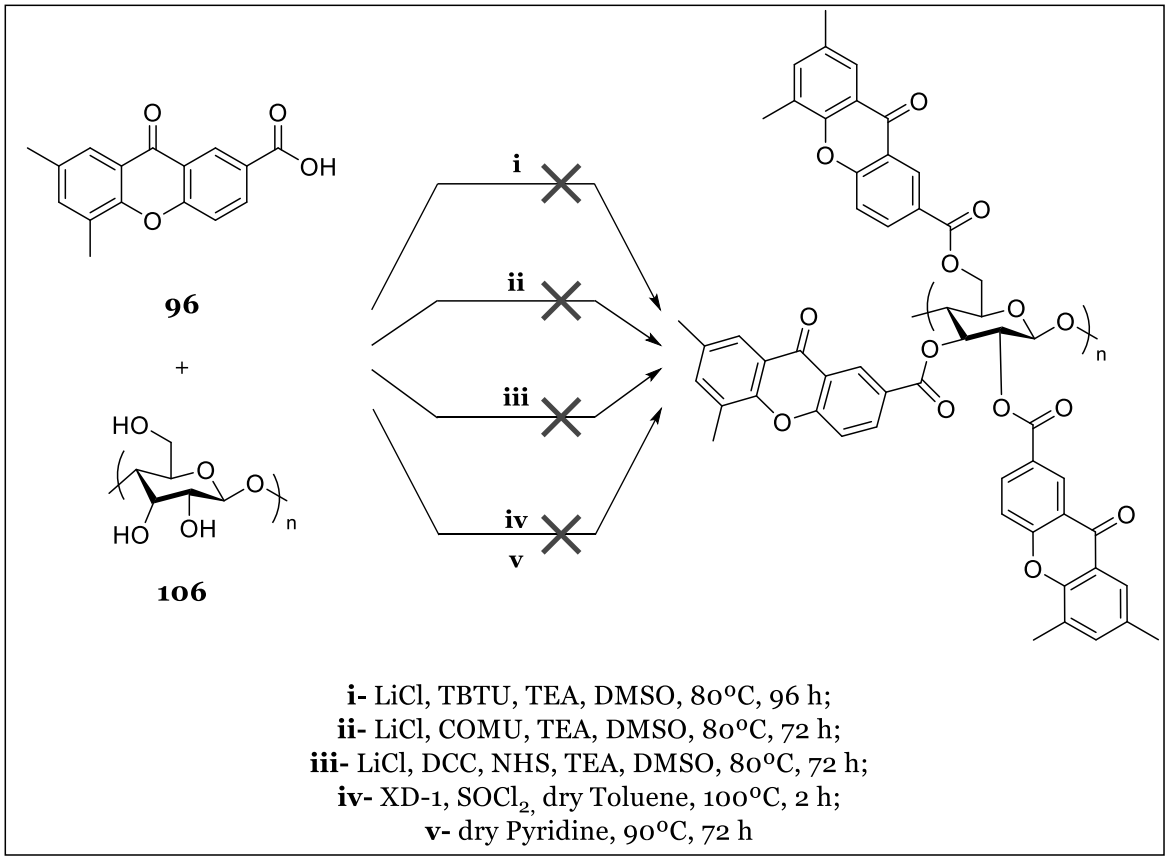

***Scheme 8**. Binding attempts of XD-1 (**96**) to amylose (**106**).*

In the coupling reactions, XD-1 (**96**) was dissolved in DMSO or THF and the correspondent coupling reagent was added in excess with a catalytic amount of TEA. This mixture was stirred for 30 min at room temperature. Amylose (**106**) was dissolved in DMSO and added to XD-1 (**96**) mixture with the coupling reagent. The mixture was allowed to react for 48 h at room temperature and was controlled by TLC. No evolution of the reaction was observed, and the reaction was set for 80°C for an additional 76 h.

The XD-1 benzoyl chloride was obtained by reaction of XD-1 (**96**) with thionyl chloride in dry toluene for 3 h at reflux. The reaction was controlled by TLC and toluene and thionyl chloride were evaporated under nitrogen atmosphere. The polysaccharide previously suspended in dry pyridine, was added to the benzoyl chloride residue and was allowed to react for 24 h at 80°C.

The crude products of the reactions were insolubilized in methanol, filtered under reduced pressure and analysed trough IR. By analysis of IR data, it was concluded that the reactions were not successful, since the IR spectra of the final products were similar to that of amylose. It was possible to notice as well as that there was no alteration on the intensity and shape of the band correspondent to the hydroxyl groups of the polysaccharide, which indicates that the formation of the ester bonds was not successful.

3.1.2. Attempted reactions of XD-1 (96) with cellulose (109)

The linkage of the same XD (**96**) to cellulose (**109**) through coupling reaction using the coupling reagent TBTU as well as through the reaction of the respective benzoyl chloride with the polysaccharide (**Scheme 9**) was also tested.

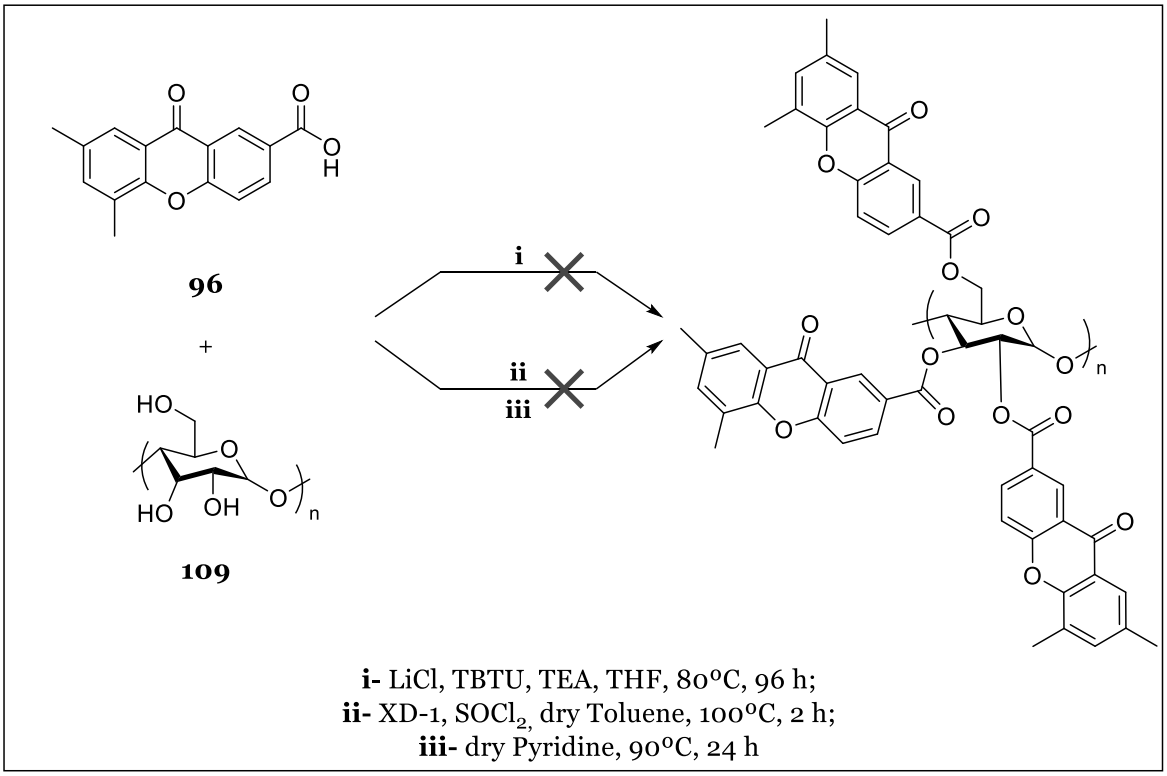

Scheme 9. *Binding attempts of XD-1 (**96**) to cellulose (**109**).*

In the coupling reaction, XD-1 (**96**) was dissolved in THF and TBTU was added in excess with a catalytic amount of TEA. This mixture was stirred for 30 min at room temperature. Cellulose (**109**) was suspended in dry pyridine and added to XD-1 (**96**) mixture with the coupling reagent. The mixture was allowed to react for 24 h at room temperature. After a TLC control, no evolution of the reaction was observed, and the reaction was set for 80°C for additional 72 h.

The XD-1 benzoyl chloride was synthesized by reaction of XD-1 (**96**) with thionyl chloride in dry toluene for 2 h at reflux. The reaction was controlled by TLC and toluene and thionyl chloride were evaporated under nitrogen atmosphere. The polysaccharide, previously suspended in dry pyridine, was added to the benzoyl chloride residue and was allowed to react for 24 h at 90°C.

The crude products of the reactions were insolubilized in methanol, filtered under reduced pressure and analysed trough IR. The IR spectra of the products of both reactions were similar to that of cellulose, presenting a broad band corresponding to O-H stretching from cellulose hydroxyl groups and presenting no characteristic bands of the XD, allowing to conclude that the reactions were not successful.

3.1.3. Attempt reaction of XD-1 (96) with chitin (111) through coupling reaction with TBTU

The linkage of XD-1 (**96**) to chitin (**111**) using the coupling reagent TBTU was tested (**Scheme 10**). This polysaccharide has a similar structure to cellulose, however, the hydroxyl group in the 2 position is replaced by an acetamide group. This polysaccharide presents only two available groups for the establishment of ester bonds with the carboxylic groups of XDs.

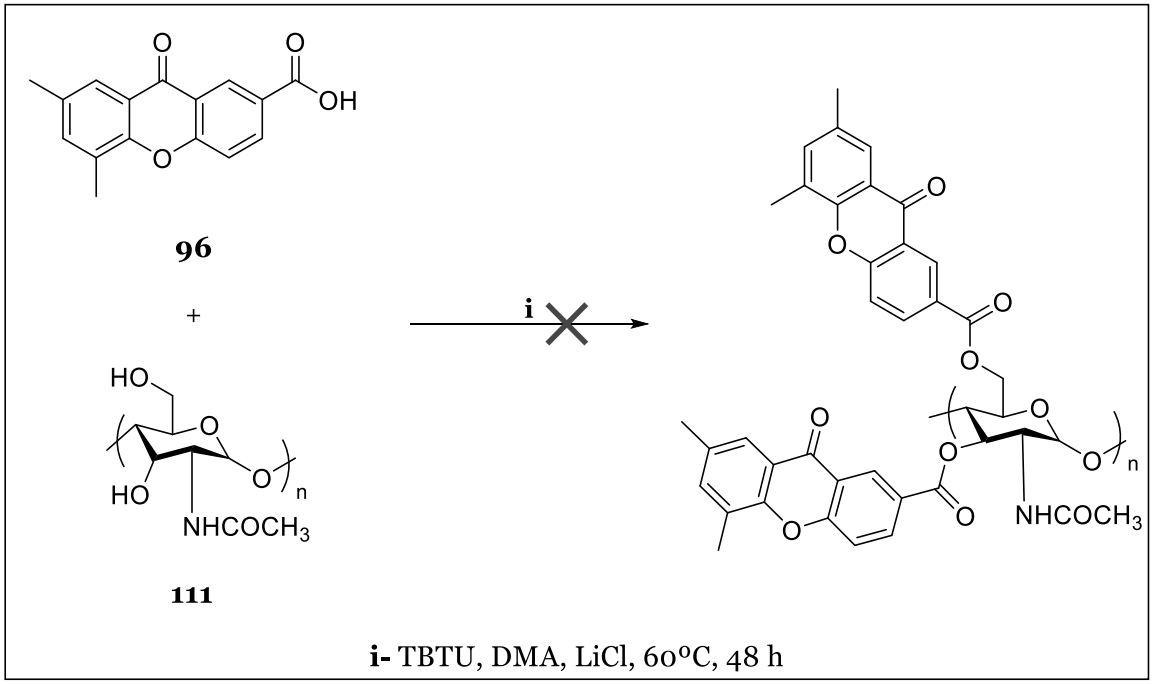

***Scheme 10**. Binding attempt of XD-1 (**96**) to chitin (**111**).*

XD-1 (**96**) was dissolved in dimethylacetamide (DMA) and TBTU was added in excess. The mixture stirred for 30 min at room temperature and then chitin (**110**), previously suspended in DMA with LiCl, was added. The mixture was allowed to react 60°C for 48 h.

The product was insolubilized in methanol, filtered under reduced pressure and analysed trough IR. Once again, regarding the obtained IR data, it was concluded that the reaction was not successful.

3.1.4. Attempt reaction of XD-1 (96) with chitosan (112) through coupling reactions with TBTU and DCC/NHS

The linkage between XD-1 (**96**) and the polysaccharide chitosan (**112**) was tested (**Scheme 11)**. This polysaccharide is obtained through the deacetylation of chitin (**111**)

presenting a similar structure to cellulose, however with an amine group in the 2 position, instead of a hydroxyl group.

Amine groups are more reactive than hydroxyls, so the binding of the carboxylic acid to the amine group in chitosan (**112**) to form an amide bond, may be easier to occur. Consequently, it was expected that in this case the coupling reactions would be more probable to occur in chitosan's amine group. Therefore, the synthetic strategy for obtained xanthone-chitosan derivatives was first by the formation of amide bonds between the polysaccharide (**Scheme 11**).

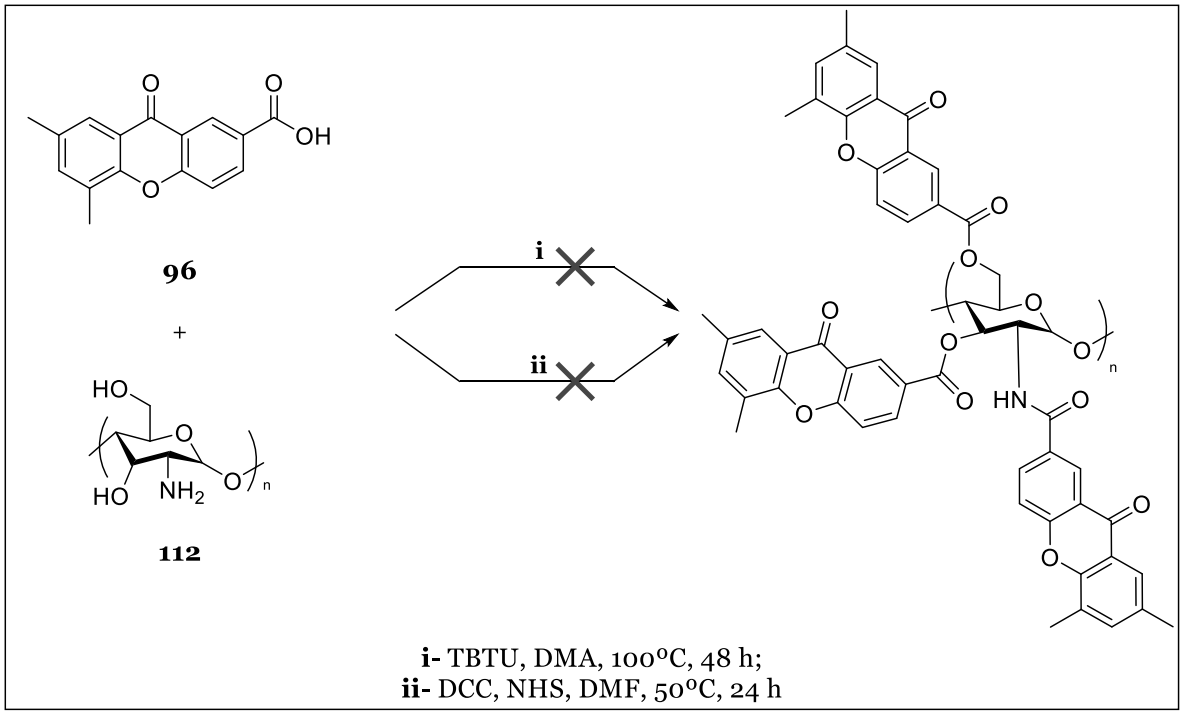

***Scheme 11**. Binding attempts of XD-1 (**96**) to chitosan (**112**).*

In the coupling reaction with TBTU, XD-1 (**96**) was dissolved in DMA and TBTU was added in excess. The mixture stirred for 30 min at room temperature and then chitosan (**112**) previously suspended in DMA was added. The mixture was allowed to react for 48h hours at 100°C.

Later, the coupling reaction with DCC/NHS was tested. In this coupling reaction, XD-1 (**96**) was dissolved in DMF and DCC and NHS [148] were added in excess. The mixture stirred for 12 h at room temperature and centrifuged and filtrated under reduced pressure to remove the insoluble product formed, dicyclohexylurea (DHU). The obtained solution was then added to a solution of chitosan (**112**) dissolved in acetic acid previously stirred at room temperature for 12 h. The reaction was allowed to run at 50°C for 24 h

The products were insolubilized in methanol or ethanol, filtered under reduced pressure and analysed trough IR. Regarding the IR data it was concluded that the reactions were not successful.

3.2. Synthesis of a xanthone-polysaccharide derivative using 2-((9-oxo-9*H*-xanthen-3-yl)oxy)acetic acid (XD-2) (113) as building block

3.2.1. Synthesis of 2-((9-oxo-9*H*-xanthen-3-yl)oxy)acetic acid (XD-2) (113)

For the execution of the binding attempts of XD-2 (**113**) to the polysaccharides cellulose (**109**) and chitosan (**112**), the total synthesis of 2-((9-oxo-9*H*-xanthen-3-yl)oxy)acetic acid (**XD-2**) (**113**) was firstly performed following a 5-step synthetic pathway, as represented in **Scheme 12** [126].

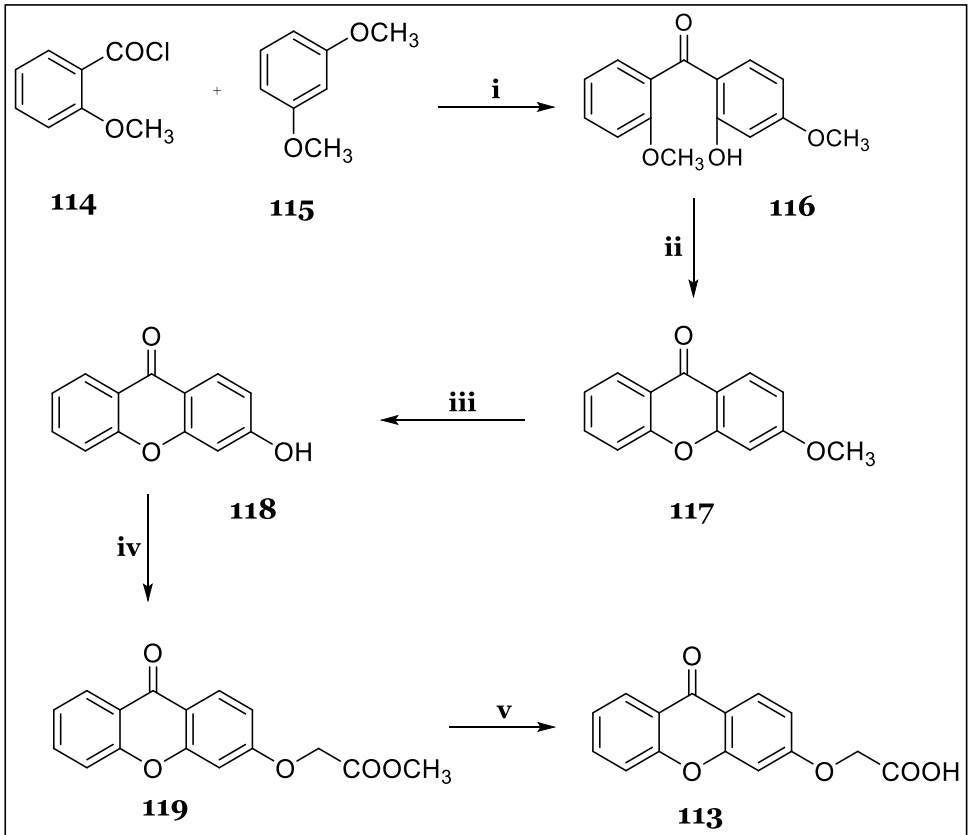

Scheme 12. *Synthesis of XD-2 (**113**).*

The total synthesis of XD-2 (**113**) was achieved based on described procedure [140, 149]. The first step was the formation of a benzophenone intermediate by a Friedel-Crafts acylation of 2-methoxybenzoyl chloride (**114**) with 1,3-dimethoxyphenyl (**115**) under catalytic action of aluminium chloride (reaction i, **Scheme 12**). The 2-hydroxy-2',4-dimethoxybenzophenone (**116**) suffers an intramolecular aromatic nucleophilic substitution under alkaline conditions to give 3-methoxy-9*H*-xanthen-9-one (**117**). This

reaction was performed under microwave radiation affording a significant reduction of the reaction time and higher yield, when comparing to the conventional method [126] (reaction ii, **Scheme 12**).

The next reaction step comprised the demethylation under the catalytic action of aluminium chloride to give 3-hydroxy-9*H*-xanthen-9-one (**118**) (reaction iii, **Scheme 12**). Then, the 3-hydroxy-9*H*-xanthen-9-one (**118**) reacted with methyl bromoacetate *via* Williamson reaction using potassium carbonate as base, to give methyl 2-((9-oxo-9*H*-xanthen-3-yl)oxy)acetate (**122**) (reaction iv, **Scheme 12**).

The last step comprised the hydrolysis of the methyl ester under alkaline conditions with NaOH to afford XD-2 (**113**) (reaction v, **Scheme 12**).

The structure elucidation of XD-2 (**113**) and all its intermediates was performed as described in sections **3.2.1.1.** to **3.2.1.5.**

3.2.1.1. Structure elucidation of 2-hydroxy-2',4-dimethoxybenzophenone (116)

2-Hydroxy-2',4-dimethoxybenzophenone (**116**) was obtained through Friedel-Crafts acylation of 2-methoxybenzoyl chloride (**114**) with 1,3-dimethoxyphenyl (**115**). The structure elucidation of compound **116** was achieved by ^{1}H NMR, ^{13}C NMR and IR.

Concerning the ^{1}H NMR spectra, there are signals that are important to point out, such as the presence of two singlets with integration for three protons each, with chemical shifts 3.79 and 3.83 ppm corresponding to the two methoxy group protons in and the presence of a singlet with chemical shift 12.48 ppm, corresponding to the hydroxyl group in C4a.

In the ^{13}C NMR, it is important to highlight the presence of two signals with chemical shifts 55.8 and 55.6 ppm, corresponding to the carbons of the methoxy groups in C4 and C10a, as well as a signal with chemical shift 166.1 corresponding to C9.

The remaining chemical shifts are described and assigned in **Table 16**.

Table 16. *^{1}H NMR and ^{13}C NMR assignments of compound **116**.*

^{1}H NMR chemical shifts δ (ppm)		**^{13}C NMR chemical shifts δ (ppm)**	
1-H	*d,* 7.15 (*J*=8.9)	1	131.8
2-H	*dd,* 6.47 (*J*=2.5 and 8.9)	2	128.2
3-OC$\underline{H}_3$	*s,* 3.73	3	199.6
4-H	*d,* 6.54 (*J*=2.5)	4	100.8
4a-O$\underline{H}$	*s,* 12.48	4a	164.6
5-H	*dd,* 7.30 (*J*=1.7 and 7.5)	5	113.9

*Table 16. ^{1}H NMR and ^{13}C NMR assignments of compound **116**. (Cont.)*

^{1}H NMR chemical shifts δ (ppm)		^{13}C NMR chemical shifts δ (ppm)	
6-H	*ddd,* 7.08 (*J*=1.4, 7.4 and 8.0)	6	135.1
7-H	*ddd,* 7.53 (*J*=1.0, 7.4 and 7.6)	7	127.5
8-H	*d,* 7.19 (*J*=8.2)	8	126.2
10a-$OC\underline{H}_3$	*s,* 3.83	8a	120.5
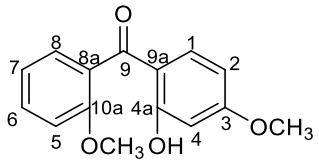		9	166.1
		9a	111.9
		10a	155.7
		10a and 3 – OCH_3	55.8 and 55.6

J values in Hz

The IR bands of compound **116** are presented in **Table 17**. It is important to highlight the formation of the carbonyl group of the benzophenone, confirmed by the presence of a band at 1621 cm^{-1} that further confirms the success of the reaction.

*Table 17. IR data of compound **116**.*

Bond	*v* (cm^{-1})
C=O (xanthone)	1621
C=C (aromatic)	1507, 1487 and 1462
O-H	3094-2833 (*br*)
Ar-OCH_3	1255 and 1201

3.2.1.2. Structure elucidation of 3-methoxy-9*H*-xanthen-9-one (117)

3-Methoxy-9*H*-xanthen-9-one (**117**) was obtained by an intramolecular aromatic nucleophilic substitution of 2-hydroxy-2',4-dimethoxybenzophenone (**116**). The structure elucidation of the compound was achieved by ^{1}H NMR, ^{13}C NMR and IR.

Comparing the ^{1}H NMR spectrum of compounds **116** and **117**, it is important to point out the absence of one of the singlets with integration for three protons correspondent to the and the absence of the singlet correspondent to the hydroxyl group of compound **116**, that confirms the cyclization of compound **116**.

Comprising the ^{13}C NMR, it is important to highlight the absence of a signal corresponding to a methoxy group of compound **116** and the shift of C4a signal from δ=164.4 ppm to δ=157.57 ppm.

The remaining chemical shifts are described and assigned in **Table 18**.

***Table 18**. [1]H NMR and [13]C NMR assignments of compound **117**.*

[1]H NMR chemical shifts δ (ppm)		**[13]C NMR chemical shifts δ (ppm)**	
1-H	*d,* 8.10 (*J*=8.9)	1	127.3
2-H	*dd,* 7.06 (*J*=2.4 and 8.9)	2	113.7
3-OC<u>H</u>$_3$	*s,* 3.94	3	165.0
4-H	*d,* 7.17 (*J*=2.4)	3-O<u>C</u>H$_3$	56.2
5-H	*dd,* 7.63 (*J*=1.1 and 8.7)	4	100.6
6-H	*ddd,* 7.85 (*J*=1.7, 7.8 and 8.7)	4a	157.6
7-H	*ddd,* 7.47 (*J*=1.1, 7.8 and 8.0)	5	117.9
8-H	*dd,* 8.17 (*J*=1.7 and 8.0)	6	135.1
		7	124.3
		8	125.9
		8a	121.2
		9	174.9
		9a	114.9
		10a	155.5

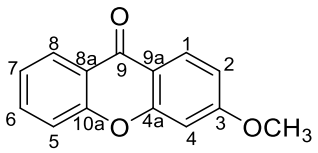

J values in Hz

The IR spectrum data of 3-methoxy-9*H*-xanthen-9-one (**117**) is presented in **Table 18** and comparing with the IR spectra of compound **116** (**Table 19)**, it is important to highlight the absence of the bands correspondent to the hydroxyl group and one methoxy group bonds, this data further confirms the success of the cyclization.

***Table 19.** IR data of compound **117**.*

Bond	***υ* (cm^{-1})**
C=O (xanthone)	1620
C=C (aromatic)	1502, 1466 and 1438
Ar-OCH$_3$	1277
O-H	---

3.2.1.3. Structure elucidation of 3-hydroxy-9*H*-xanthen-9-one (118)

3-Hydroxy-9*H*-xanthen-9-one (**118**) was obtained by hydrolysis of the methoxy moiety of 3-methoxy-9*H*-xanthen-9-one (**117**). The structure elucidation of the compound was achieved by [1]H NMR, [13]C NMR and IR.

Comparing the [1]H NMR spectra of compounds **117** and **118** (**Table 20**), it is important to point out the presence of a new the singlet with chemical shift of 11.00 ppm,

correspondent to the hydroxyl group in C3 of compound **118**. It is also observed the absence of the singlet corresponding to the three protons of the methoxy group present in compound 117. This data confirms the hydrolysis of the methoxy group of compound **117**.

Considering the ^{13}C NMR, it is important to highlight the absence of the signal corresponding to the methoxy group of compound **117** with chemical shift 56.2 ppm (**Table 18**).

The remaining chemical shifts are described and assigned in **Table 20**.

Table 20. *^{1}H NMR and ^{13}C NMR assignments of compound **118**.*

^{1}H NMR chemical shifts δ (ppm)		**^{13}C NMR chemical shifts δ (ppm)**	
1-H	*d,* 8.14 (*J*=8.5)	1	128.0
2-H	*dd,* 6.89 (*J*=2.2 and 8.5)	2	113.7
3-O<u>H</u>	*s,* 11.00	3	164.0
4-H	*d,* 6.93 (*J*=2.2)	4	102.1
5-H	*dd,* 7.61 (*J*=1.0 and 8.7)	4a	157.6
6-H	*ddd,* 7.82 (*J*=1.7, 7.8 and 8.7)	5	117.9
7-H	*ddd,* 7.44 (*J*=1.0, 7.8 and 8.0)	6	134.8
8-H	*dd,* 8.15 (*J*=1.7 and 8.0)	7	124.1
		8	125.8
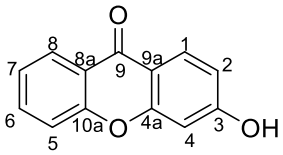		8a	121.2
		9	174.8
		9a	114.1
		10a	155.6

J values in Hz

The IR spectrum data of 3-hydroxy-9*H*-xanthen-9-one (**118**) is presented in **Table 21** and comparing with the IR spectra of compound **117** (**Table 19),** it is important to highlight the absence of the bands corresponding to the methoxy group bond and the presence of a new broad band at 3085cm^{-1} corresponding to the hydroxyl group of compound **118**, confirming the hydrolysis was successful.

Table 21. *IR data of compound **118**.*

Bond	**υ (cm^{-1})**
C=O (xanthone)	1613
C=C (Aromatic)	1566, 1480 and 1451
Ar-OCH_3	---
O-H	3085 (*br*)

3.2.1.4. Structure elucidation of methyl 2-((9-oxo-9*H*-xanthen-3-yl)oxy)acetate (119)

methyl 2-((9-oxo-9*H*-xanthen-3-yl)oxy)acetate (**119**) was obtained by the reaction of 3-hydroxy-9*H*-xanthen-9-one (**118**) with methyl-bromoacetate. The structure elucidation of the compound was achieved by ^{1}H NMR, ^{13}C NMR and IR.

Regarding the ^{1}H NMR (**Table 22**) it is important to highlight the presence of new signals with chemical shifts of 5.05 ppm and 3.74 ppm corresponding to two protons of the ether group (O-C<u>H</u>$_2$-) and t three protons of the ester group (-COOC<u>H</u>$_3$), respectively. The absence of the singlet corresponding to the proton of the hydroxyl group present in compound **118** is also observed.

Regarding the ^{13}C NMR, it is important to point out the presence of three new signals with chemical shifts, 52.0, 65.0 and 168.6 ppm, corresponding to the carbon of the ester group (C1'-OCH$_3$), to the carbon of the ether group (C2', -OCH$_2$-) and to the carbon of the ester carbonyl group (C1', <u>C</u>OOCH$_3$), respectively.

__Table 22__. ^{1}H NMR and ^{13}C NMR assignments of compound __119__.

^{1}H NMR chemical shifts δ (ppm)		**^{13}C NMR chemical shifts δ (ppm)**	
1-H	*d,* 8.12 (*J*=8.9)	1	127.7
2-H	*dd,* 7.10 (*J*=2.4 and 8.9)	2	113.8
4-H	*d,* 7.19 (*J*=2.4)	3	163.2
5-H	*dd,* 7.64 (*J*=1.0 and 8.6)	4	101.6
6-H	*ddd,* 7.86 (*J*=1.7, 8.0 and 8.6)	4a	157.3
7-H	*ddd,* 7.48 (*J*=1.0, 7.5 and 8.0)	5	117.9
8-H	*dd,* 8.18 (*J*=1.7 and 7.5)	6	135.2
2'-C<u>H</u>$_2$	*s,* 5.05	7	124.4
1'-OC<u>H</u>$_3$	*s,* 3.74	8	125.9
		8a	121.2
		9	174.9
		9a	115.5
		10a	155.6
		1'	168.6
		2'	65.0
		1'-OCH$_3$	52.0

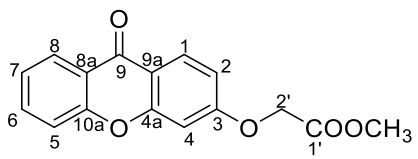

J values in Hz

Considering the IR spectra of compound **119** (**Table 23**), it is important to highlight the presence of the bands corresponding to the methoxy group bond and the ester carbonyl

group. It is also important to point out the absence of the broad band corresponding to the hydroxyl group in compound **118** (**Table 21**), further confirming the reaction was successful.

***Table 23**. IR data of compound **119**.*

Bond	υ (cm^{-1})
C=O (xanthone)	1648
C=C (Aromatic)	1622, 1452
C=O (ester)	1739
Ar-OCH2	1236
O-H	---

3.2.1.5. Structure elucidation of 2-((9-oxo-9*H*-xanthen-3-yl)oxy)acetic acid (XD-2) (113)

XD-2 (**113**) was obtained by the reaction of methyl 2-((9-oxo-9*H*-xanthen-3-yl)oxy)acetate (**119**). The structure elucidation of the compound was achieved by ^{1}H NMR, ^{13}C NMR (**Table 24**) and IR (**Table 25**).

Comparing the ^{1}H NMR spectra of compounds **113** and **119**, it is important to highlight the absence of the singlet with integration for three protons with chemical shift 3.74 ppm, corresponding to the protons of the ester group (C1'-OCH_3) (**Table 22**) and the presence of a new the singlet with chemical shift 12.74 ppm, corresponding to the proton of the hydroxyl group of compound **113**.

Considering the ^{13}C NMR, it is important to highlight the absence of the signal corresponding to the carbon of the methoxy group (C1'-OCH_3) of compound **119** with chemical shift 52.0 ppm (**Table 22**).

***Table 24.** ^{1}H NMR and ^{13}C NMR assignments of compound **113**.*

^{1}H NMR chemical shifts δ (ppm)		^{13}C NMR chemical shifts δ (ppm)	
1-H	*d,* 8.11 (*J*=8.8)	1	127.7
2-H	*dd,* 7.08 (*J*=2.4 and 8.8)	2	113.8
4-H	*d,* 7.19 (*J*=2.4)	3	163.4
5-H	*dd,* 7.62 (*J*=3.3 and 8.4)	4	101.5
6-H	*ddd,* 7.85 (*J*=1.5, 6.8 and 8.4)	4a	157.3
7-H	*ddd,* 7.47 (*J*=3.3, 6.4 and 8.4)	5	117.9
8-H	*dd,* 8.17 (*J*=1.7 and 8.4)	6	135.1
1'-C<u>H</u>$_2$	*s,* 4.91	7	124.4
2'-O<u>H</u>	*s,* 12.74	8	125.9
		8a	121.2

Table 24. ^{1}H NMR and ^{13}C NMR assignments of compound **113. (Cont.)**

^{1}H NMR chemical shifts δ (ppm)	^{13}C NMR chemical shifts δ (ppm)	
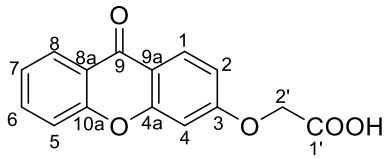	9	174.9
	9a	115.3
	10a	155.6
	1’	65.0
	2’	169.5
***J* values in Hz**		

The IR spectrum data of XD-2 (**113**) is presented in **Table 25** and comparing with the IR spectra of compound **119** (**Table 23**), it is important to highlight the presence of a new broad band at 3442cm^{-1} corresponding to the hydroxyl group of the carboxylic acid of XD-2 (**113**), confirming the hydrolysis of the ester was successful.

Table 25. *IR data of compound* ***113****.*

Bond	*v* (cm^{-1})
C=O (xanthone)	1645
C=C (Aromatic)	1464, 1447 and 1420
Ar-OCH$_2$	1233
O-H (acid)	3442 (*br*)
C=O (ester/acid)	1714

3.2.2. Attempted reaction of XD-2 (113) with cellulose (109) through coupling reaction with TBTU

Firstly, the linkage of XD-2 (**113**) to cellulose (**109**) through coupling reaction with TBTU was tested (**Scheme 13**).

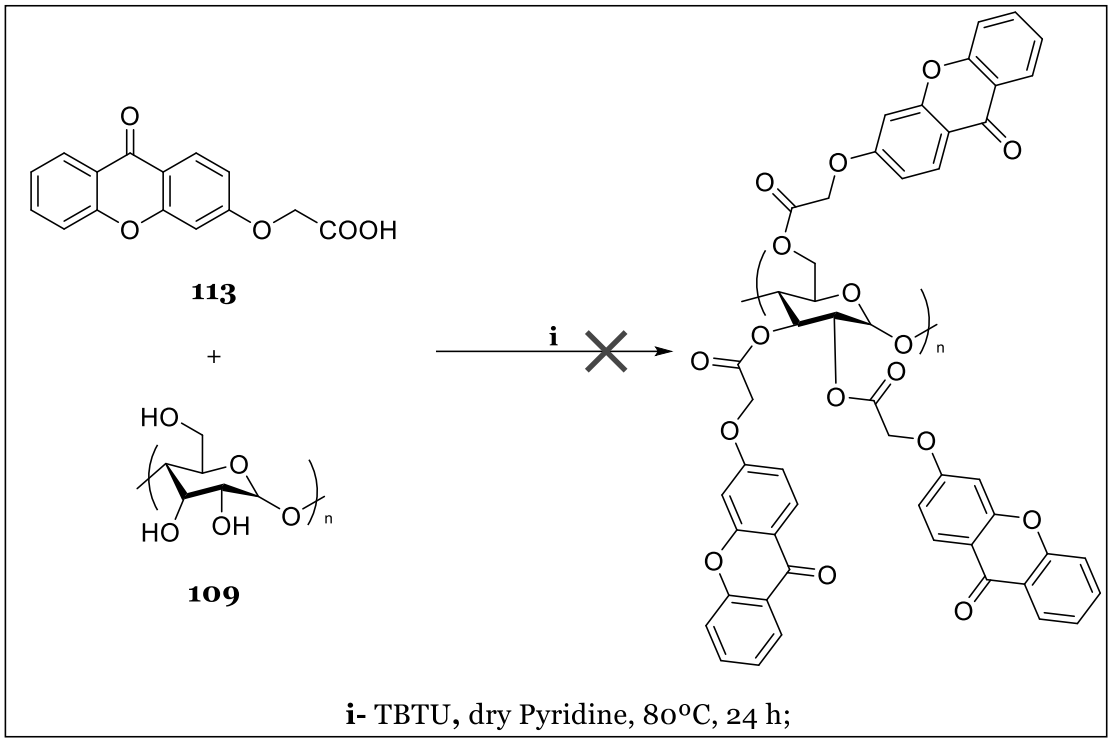

Scheme 13. *Binding attempt of XD-2 (**113**) to cellulose (**109**).*

XD-2 (**113**) was dissolved in dry pyridine and TBTU was added in excess. The mixture stirred for 30 min at room temperature and then cellulose (**109**) previously suspended in dry pyridine was added. The mixture was allowed to react for 48h hours at 80°C. The solid was filtered under reduced pressure and thoroughly washed with methanol. The isolated product IR spectrum was obtained, analysed and it was concluded that the reaction was not successful.

3.2.3. Attempt reaction of XD-2 (113) with chitosan (112) through coupling reactions with TBTU and DCC/NHS

It was further tested the linkage of XD-2 (**113**) to chitosan (**112**) through coupling reactions with TBTU and DCC/NHS (**Scheme 14**).

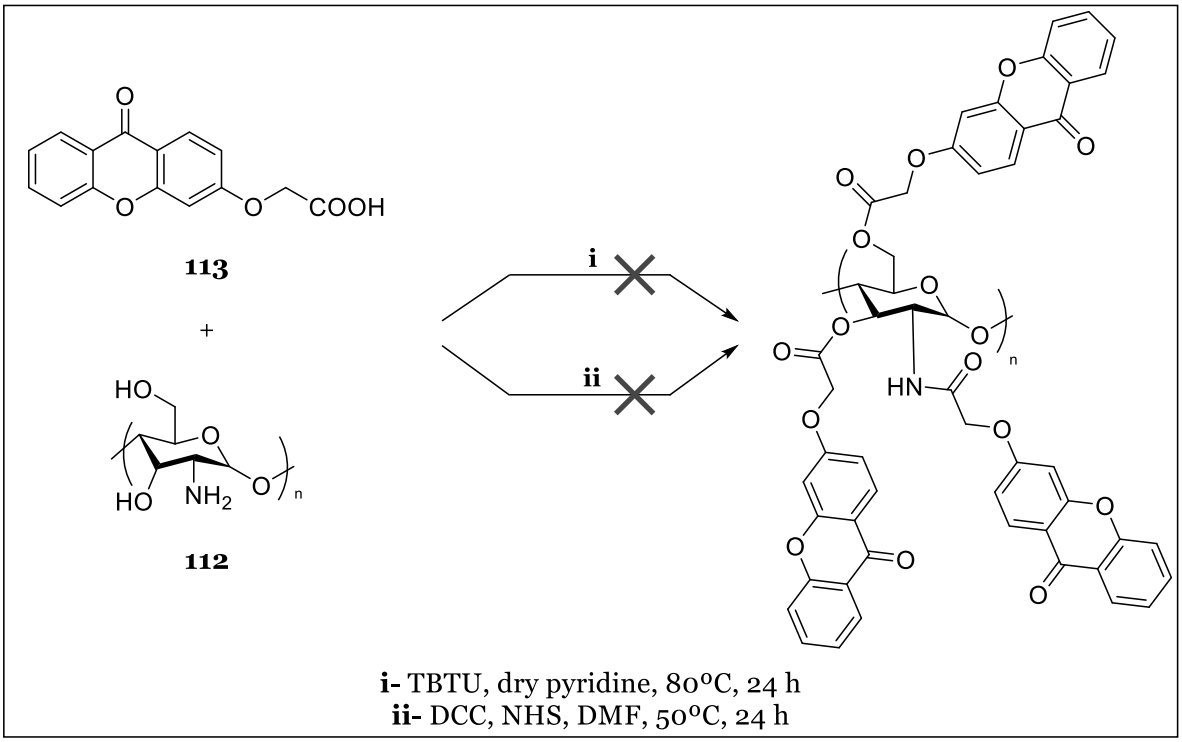

Scheme 14. *Binding attempts of XD-2 (**113**) to chitosan.*

In the coupling reaction with TBTU, the XD-2 (**113**) was dissolved in dry pyridine and TBTU was added in excess. The mixture stirred for 30 min at room temperature and then chitosan (**112**) previously suspended in dry pyridine was added. The mixture was allowed to react for 24h hours at 80°C. After 24h it was noticed that a white solid had precipitated. The solid was filtered under reduced pressure and thoroughly washed with methanol

In the coupling reaction with DCC/NHS, the XD-2 (**113**) was dissolved in DMF and DCC and NHS [148] were added in excess. The mixture stirred for 12 h at room temperature and then centrifuged and filtrated under reduced pressure to remove the insoluble product formed, dicyclohexylurea (DHU). The obtained solution was then added to a solution of chitosan (**112**) dissolved in acetic acid previously stirred at room temperature for 12 h. The reaction was allowed to run at 50°C for 24 h. The reaction mixture was poured in ethanol and the obtained insoluble product IR spectra analysed.

Regarding the obtained IR data, it was concluded that the reaction with the coupling reagent DCC/NHS was not successful.

The IR spectrum for the product obtained in the reaction with TBTU presented several XD-2 (**113**) characteristic bands. It is important to highlight the presence of an intense band at 1660 cm^{-1} corresponding to the C=O stretching of the xanthonic ketone as well as the bands corresponding to the aromatic C=C and O-CH_2 stretchings at 1465, 1445 and 1417 cm^{-1} and 1231 cm^{-1}, respectively. Due to these results, further ^1H NMR and elemental analysis to this product were made.

The ^{1}H NMR results are presented in **Table 26**. In the ^{1}H NMR spectra it is important to highlight the presence of characteristic signals of XD-2 (**113**), however due to the absence of signals of chitosan as well as the absence of a N-H signal it was concluded that the reaction was not successful.

***Table 26**. ^{1}H NMR and ^{13}C NMR assignments of the product obtained through coupling reaction of chitosan and XD-2 (**113**) with TBTU.*

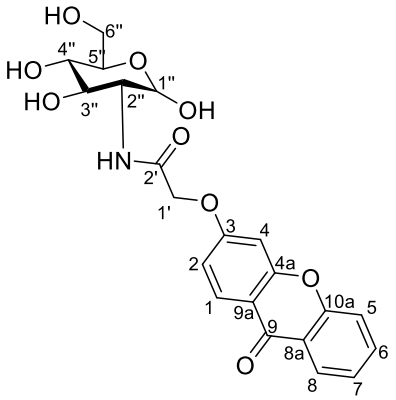

^{1}H NMR chemical shifts δ (ppm)	
1'-H, 1'-OH, 2'-H, 2'-NH, 3'-H, 3'-OH, 3'-H, 4'-OH, 5'-H, 6'-CH_2, 6'-OH	absent
1'-CH_2	*s,* 4.57
1-H	*d,* 8.09 (*J*=9.0)
2-H	*m,* 7.01
4-H	absent
5-H	*d,* 7.64 (*J*=9.0)
6-H	*m,* 7.85
7-H	*m,* 7.47
8-H	*dd,* 8.17 (*J*=3.0 and 9.0)

J values in Hz

3.2.4. Preparation of CSP-4 (115)

The preparation of 3,5-DMPC-XD-2-chitosan CSP (**CSP-4**) (**95**) was achieved using XD-2 (**113**) as building block. The XD-2 (**113**) was firstly converted into the correspondent acyl chloride (**120**) and then reacted with chitosan (**112**) to give chitosan *N*-2-((9-oxo-9*H*-xanthen-3-yl)oxy)acetamide (**121**). This compound (**121**) was then reacted with 3,5-dimethylphenylisocyanate (**107**) to give chitosan 3,6-*bis*(3,5-dimethylphenylcarbamate)-2-((9-oxo-9*H*-xanthen-3-yl)oxy)acetamide) (**3,5-DMPC-XD-2-chitosan**) (**122**).

The preparation of 3,5-DMPC-XD-2-chitosan (**122**) is presented in **Scheme 15**.

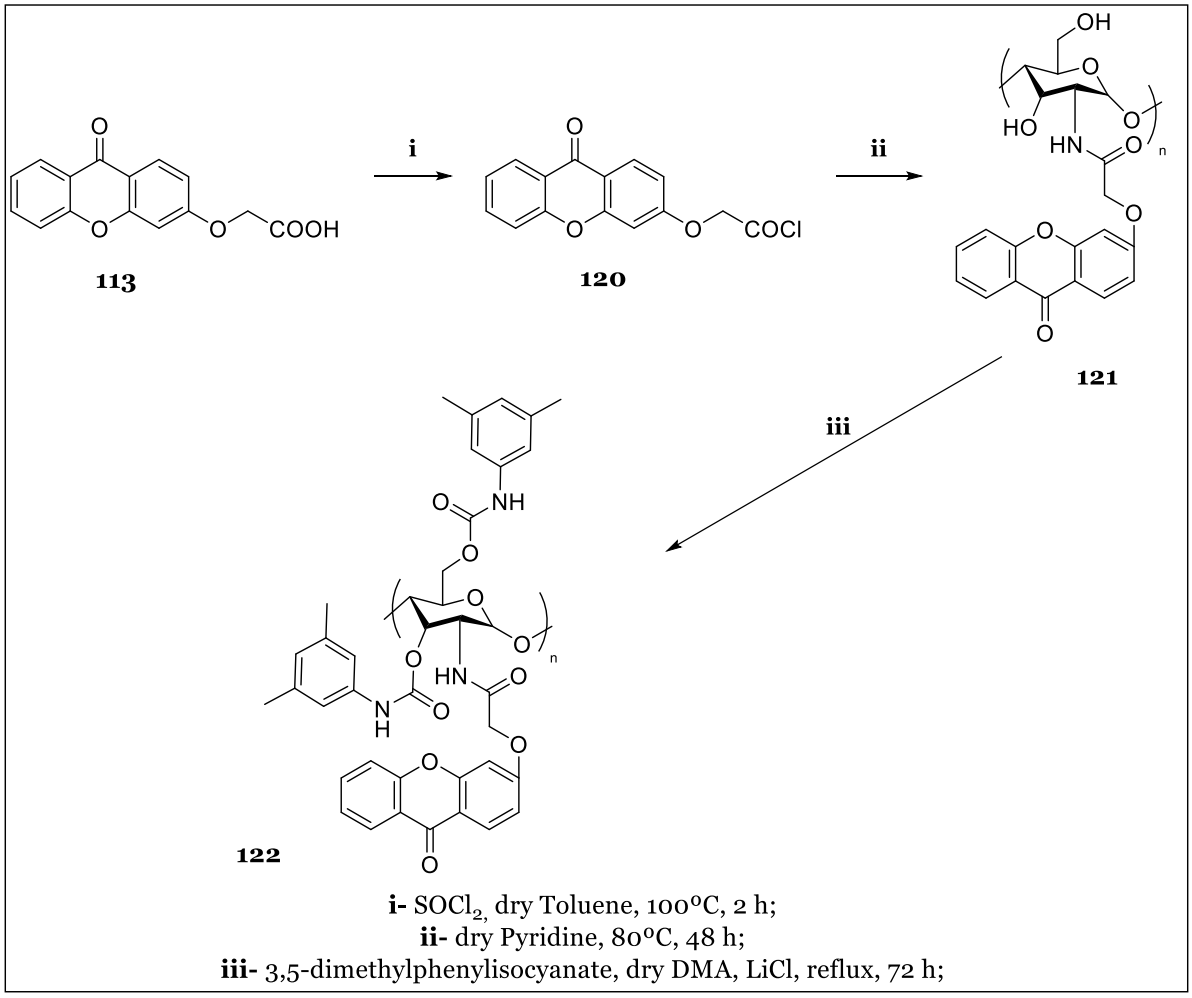

Scheme 15. *Preparation of chitosan 3,6-*bis*(3,5-dimethylphenylcarbamate)-2-((9-oxo-9*H*-xanthen-3-yl)oxy)acetamide CSP (CSP4).*

3.2.4.1. Synthesis of chitosan *N*-2-((9-oxo-9*H*-xanthen-3-yl)oxy)acetamide (121)

Chitosan *N*-2-((9-oxo-9*H*-xanthen-3-yl)oxy)acetamide (**121**) was synthesized by reaction of **XD**-2 benzoyl chloride (**120**) with chitosan (**112**) (**Scheme 16**). Firstly, XD-2 (**113**) was converted in the corresponding acyl chloride (**120**) through reaction with thionyl chloride in dry toluene. The acyl chloride was then reacted with chitosan previously suspended in dry DMA with LiCl to give chitosan *N*-2-((9-oxo-9*H*-xanthen-3-yl)oxy)acetamide (**121**).

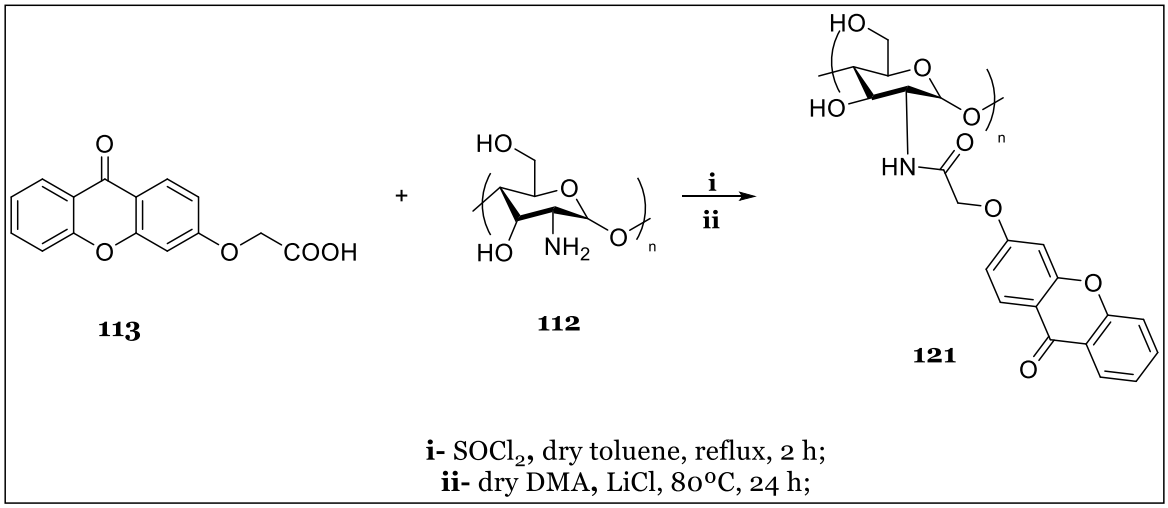

Scheme 16. *N-2-((9-oxo-9H-xanthen-3-yl)oxy)acetamide synthesis.*

Both steps in this reaction were performed under anhydrous conditions due to the instability of the acyl halide intermediate that in contact with water converts back to the corresponding carboxylic acid.

3.2.4.1.1. Analysis of chitosan *N*-2-((9-oxo-9*H*-xanthen-3-yl)oxy)acetamide (121) by IR and elemental analysis

The IR spectral data of compound **121** is presented in **Table 27** and compared to the IR data for chitosan (**112**) and XD-2 (**113**). It is important to highlight the presence of characteristic bands from both starting blocks in the final product, mainly the presence of the bands corresponding to the ketone C=O bond at 1653 cm^{-1}, the ether Ar-OCH_2 bond at 1230 cm^{-1} and to the aromatic C=C bonds at 1463 and 1440 cm^{-1}. The results allowed us to conclude that the reaction had been successful.

Table 27*. IR data of compounds* ***112*** *and* ***121****.*

Bond	***υ* (cm^{-1})**	
	(112)	**(121)**
O-H	3447 (*br*)	3447 (*br*)
N-H (chitosan)	absent	absent
C=O (xanthone)	---	1653
C=C (aromatic)	---	1463 and 1440
Ar-OCH_2	---	1230
C=O (amide)	---	absent

Furthermore, the elemental analysis results showed similar values for the percentage of carbons and hydrogens of compound **121** when compared to the theoretical

values (**Table 28**). Moreover, the presence of a greater percentage of nitrogen atoms in compound **121** when compared to the theoretical value, indicate that not all chitosan (**112**) units were successfully derivatized. An additional study was made, and it was predicted that the XD was linked to chitosan (**112**) in an irregularly alternated derivatization, *i.e.* approximately every, one in two chitosan (**112**) units was successfully derivatized.

***Table 28**. Experimental and theoretical values of elemental analysis for compound **121**.*

	%C	%N	%H
Experimental	54.85	4.31	4.52
Theoretical (fully derivatized)	58.47	3.25	4.91
Theoretical (alternate derivatization)	56.09	4.85	5.30

3.2.4.2. Synthesis of chitosan 3,6-*bis*(3,5-dimethylphenylcarbamate)-2-((9-oxo-9*H*-xanthen-3-yl)oxy)acetamide) (3,5-DMPC-XD-2-Chitosan) (122)

The preparation of 3,5-DMPC-XD-2-Chitosan CSP (**122**) was obtained from the reaction of chitosan *N*-2-((9-oxo-9*H*-xanthen-3-yl)oxy)acetamide (**121**) with 3,5-dimethylphenylisocyanate (**107**) at reflux for 76 h (**Scheme 17**), as described in literature [113, 115, 117, 119-121].

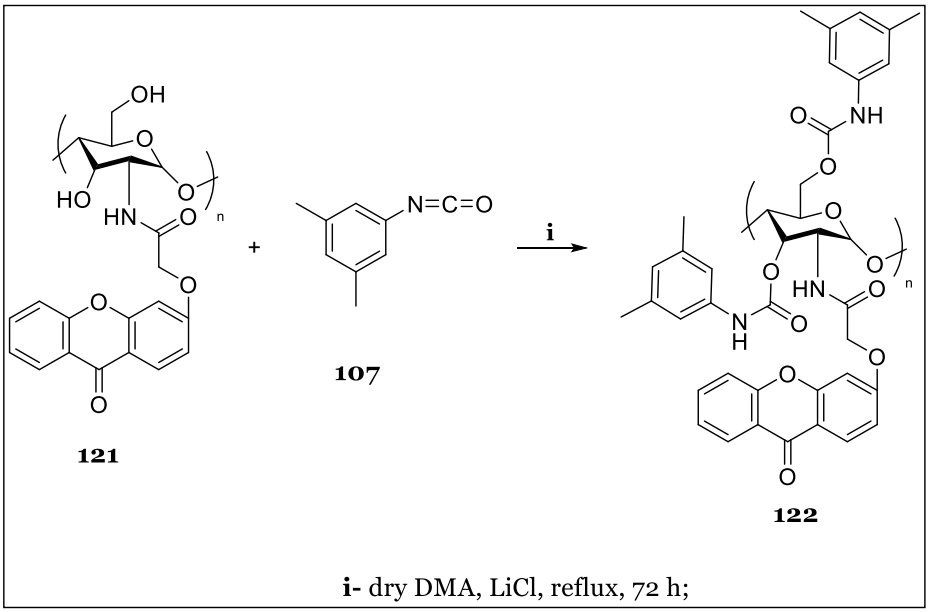

***Scheme 17.** 3,5-DMPC-XD-2-Chitosan synthesis.*

Chitosan 3,6-*bis*(3,5-dimethylphenylcarbamate)-2-((9-oxo-9*H*-xanthen-3-yl)oxy)acetamide (**122**) coating was performed as described previously for CSP-2 (**93**) in section **2.1**., however, due to the low solubility of compound **122**, DMF was used as the coating solvent. CSP-4 (**95**) was then packed into a 4.6 mm × 150 mm HPLC column.

The column packing was achieved by a slurry mode with n-hexane/isopropanol/paraffin oil (50:50:0.01 *v/v/v*) and n-hexane/isopropanol (80:20 *v/v*) as mobile phase, at 6000 psi.

3.2.4.2.1. Analysis of chitosan 3,6-*bis*(3,5-dimethylphenylcarbamate)-2-((9-oxo-9*H*-xanthen-3-yl)oxy)acetamide) (3,5-DMPC-XD-2-Chitosan) (122) by IR and elemental analysis

The IR spectra data of compound **122** is presented in **Table 29** and comparing to the IR data for compound **121** (**Table 27**), it is important to highlight the presence of characteristic bands of compound **121** in the final product, the absence of the broad band at 3447 cm^{-1} corresponding to the O-H bond of chitosan (**112**) and the presence of a new band at 3290 cm^{-1} corresponding to the N-H bond present in carbamates and amides. This data allowed us to conclude that the reaction had been successful.

Table 29. *IR data of compound* ***122****.*

Bond	***v*** **(cm^{-1})**
O-H	absent
C=O (xanthone)	1636
C=C (aromatic)	1449
Ar-OCH_2	1229
C=O (amide)	absent
N-H (amide and carbamates)	3290

Moreover, the elemental analysis of the final product shows that the percentages of carbon and hydrogen atoms are close to the theoretical value, however the percentage of nitrogen atoms is much higher (**Table 30**). This situation can be explained due to the fact the full derivatization of chitosan (**116**) amine groups with XD-2 (**113**) was not achieved and free amine groups were allowed to react with the isocyanate to form carbamates that increase the overall nitrogen atoms percentage.

***Table 30**. Experimental and theoretical values of elemental analysis for compound **122**.*

	%C	%N	%H
Experimental	65.29	9.03	6.71
Theoretical	64.54	5.79	5.42

B. EVALUATION OF ENANTIORESOLUTION BY LIQUID CHROMATOGRAPHY

The LC enantioresolution ability of all prepared CSPs (CSP1-CSP4) was evaluated using various chiral analytes (A1-A39) including commercially available standard racemates (**Figure 11**), as well as several enantiomeric mixtures of CDXs synthesized "in-house" (**Figure 12**) [126, 137, 140].

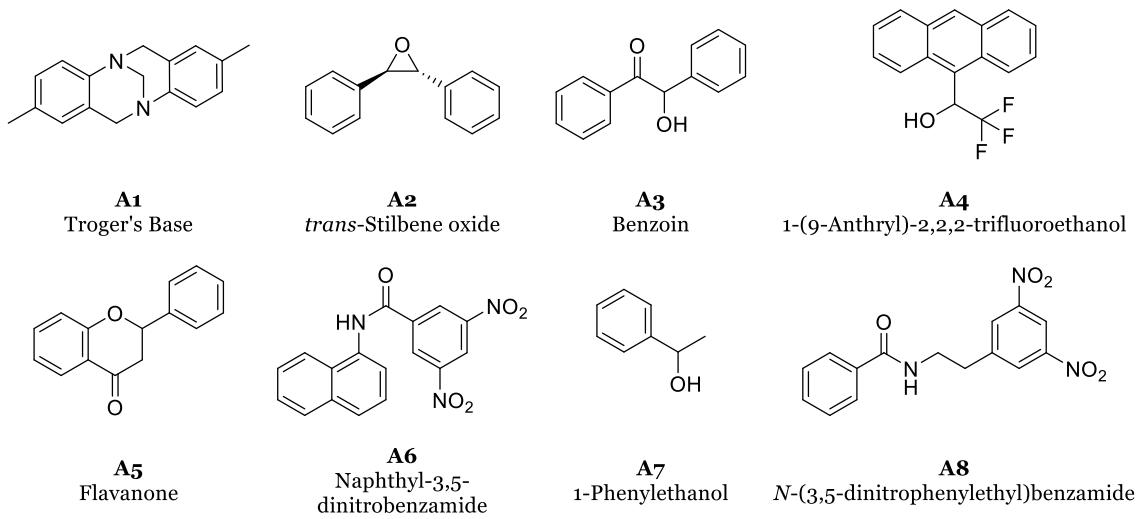

A1 Troger's Base

A2 *trans*-Stilbene oxide

A3 Benzoin

A4 1-(9-Anthryl)-2,2,2-trifluoroethanol

A5 Flavanone

A6 Naphthyl-3,5-dinitrobenzamide

A7 1-Phenylethanol

A8 *N*-(3,5-dinitrophenylethyl)benzamide

***Figure 11**. Chemical structures of commercially available standard racemic analytes (A1-A8).*

The chromatographic parameters, retention factor (k), separation factor (α) and resolution (Rs), were calculated for the different analytes, according to the equations described in Experimental chapter (page 86). The four CSPs were tested using two distinct elution mode conditions: normal phase using *n*-hexane/2-propanol (9:1 *v/v*) and *n*-hexane/ethanol (9:1 or 8:2 *v/v*) as mobile phases, and polar organic mode using methanol (100%) as mobile phase. The rate flow chosen was 0.5 mL/min and the analysis were performed at room temperature and UV detection at 254 nm.

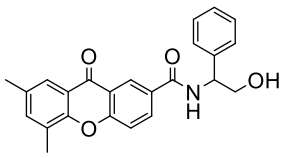

A9

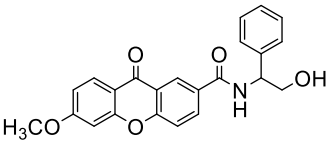

A10

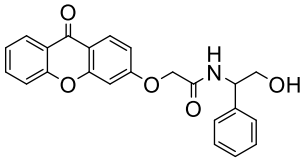

A11

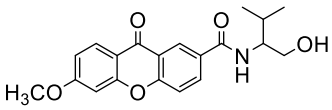

A12

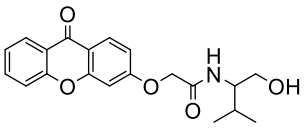

A13

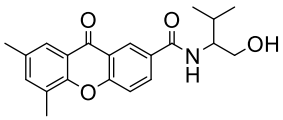

A14

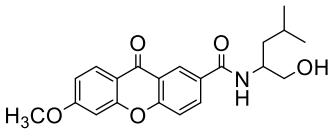

A15

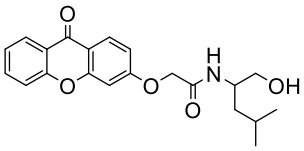

A16

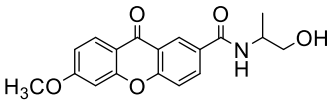

A17

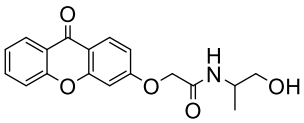

A18

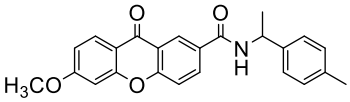

A19

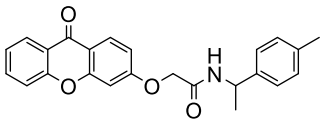

A20

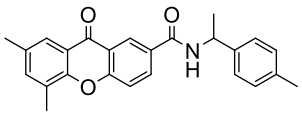

A21

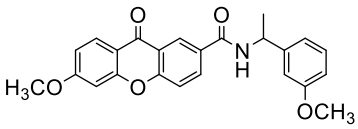

A22

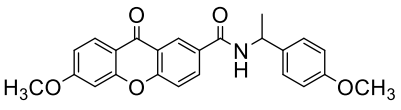

A23

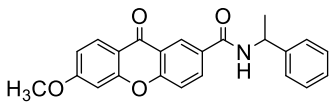

A24

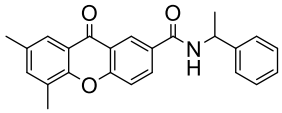

A25

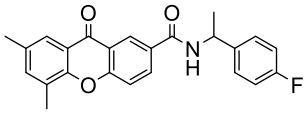

A26

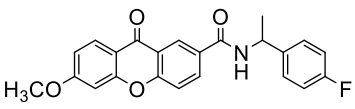

A27

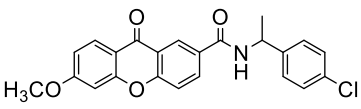

A28

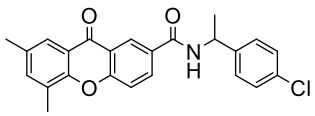

A29

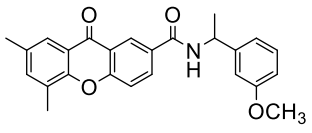

A30

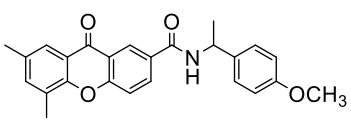

A31

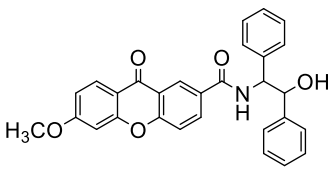

A32 (*S,R/R,S*)

A33 (*R,R/S,S*)

Figure 12. *Chemical structures of enantiomeric mixtures of CDXs A9-A33).*

1. Enantioresolution performance of CSP-1

The chiral resolution evaluation of CSP-1 was performed through the analysis of some commercially available racemates (**Figure 11**), using *n*-hexane/2-propanol (9:1 *v/v*) as mobile phase. Considering the racemates A4 and A6, their enantioresolution ability was tested using *n*-hexane/ethanol (9:1 *v/v*) and racemate A6 was also tested using *n*-hexane/ethanol (8:2 *v/v*) as mobile phases. The preliminary results are presented in **Table 31**.

Table 31. *Enantioresolution performance of CSP-1.*

Analytes	k_1	k_2	α	Rs	Mobile Phase
A1	1.81	1.96	1.08	<1.00	A
A2	0.14	0.14	1.00	---	
A3	1.83	1.96	1.08	<1.00	
A4	0.17	0.27	1.62	<1.00	C
A6	2.33	2.67	1.14	2.00	B
	6.16	7.28	1.18	2.66	C
A9	4.85	5.39	1.11	1.21	B
A10	8.10	8.79	1.08	<1.00	B
	23.92	25.86	1.08	<1.00	C
A11	7.76	7.76	1.00	---	B
A12	4.67	4.67	1.00	---	
A13	4.39	4.39	1.00	---	
A14	3.15	5.31	1.69	5.56	
A15	4.02	4.32	1.07	<1.00	B
	10.67	11.56	1.08	1.10	C
A16	3.70	3.87	1.05	<1.00	B
	10.20	10.77	1.06	<1.00	C
A17	4.68	4.68	1.00	---	B
A18	4.36	4.36	1.00	---	
A19	3.77	4.01	1.06	<1.00	B
	8.83	9.43	1.07	<1.00	C
A20	4.03	4.23	1.05	<1.00	B
	8.72	9.19	1.05	<1.00	C
A21	2.26	2.39	1.05	<1.00	B
A22	5.71	5.95	1.04	<1.00	B
	13.99	14.66	1.05	<1.00	C

Table 31. *Enantioresolution performance of CSP-1* ***(Cont.).***

Analytes	k_1	k_2	α	Rs	Mobile Phase
A23	5.84	6.05	1.04	<1.00	B
	13.83	14.36	1.04	<1.00	C
A24	2.48	4.41	1.78	7.79	B
A25	2.59	2.73	1.05	< 1.00	
A26	2.51	2.74	1.09	1.09	
A27	4.36	4.76	1.09	1.25	
A28	3.96	4.33	1.09	1.41	
A29	2.65	2.93	1.11	1.25	
A30	3.69	3.84	1.04	<1.00	
A31	3.93	3.93	1.00	---	
A32	9.56	9.56	1.00	---	
A33	9.52	9.52	1.00	---	

Mobile Phases: A – *n*-hexane/2-propanol (9:1 *v/v*), B – **n**-hexane/ethanol (8:2 *v/v*); C – *n*-hexane/ethanol (9:1 *v/v*)

It is possible to observe in **Table 31** that the racemates A1, A3 and A4 were separated with α values of 1.08, 1.08 and 1.62, respectively, however, due to the lower efficiency of separation, their resolution was not calculated. Racemate A6 presented good resolution (**Figure 13**) in *n*-hexane/ethanol (8:2 and 9:1 *v/v*) with α values of 1.14 and 1.18 and *Rs* values of 2.00 and 2.66, respectively.

The theoretical plate number *N* of **CSP-1** (**92**) is 1444 being calculated using the racemate A6 in *n*-hexane/ethanol (8:2 *v/v*). This data allowed to conclude that the CSP-1 was well packed and presents efficiency in the resolution of racemates.

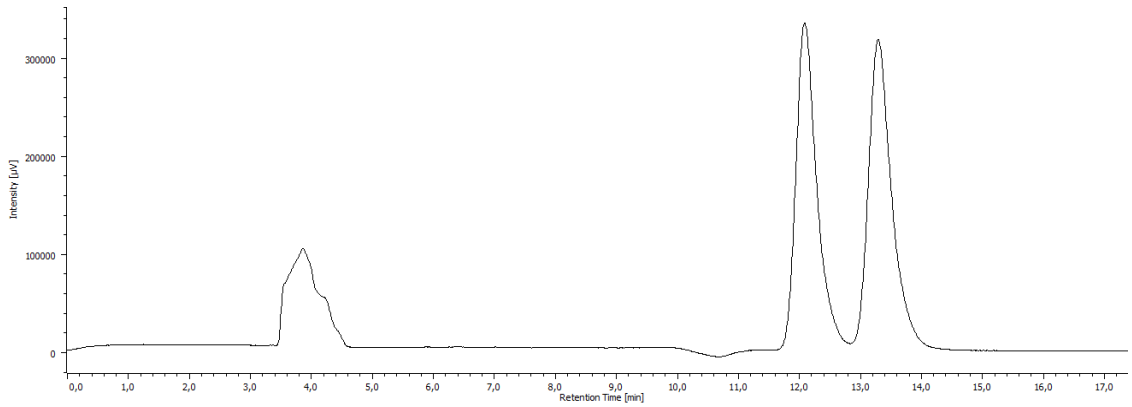

Figure 13*. Chromatogram of naphthyl-3,5-dinitrobenzamide (A6) enantioresolution on CSP-1. Mobile phase, n-hexane/ethanol (8:2 v/v); Flow rate, 0.5 mL/min.; detection, 254 nm.*

Furthermore, according to the results obtained, most of the analytes tested were separated. Moreover, it is important to highlight the high enantioresolution of A14 and A24 with α values of 1.69 and 1.79 and *Rs* values of 5.56 and 7.79, respectively. **Figure 14** presents the obtained chromatogram for the resolution of A24 using *n*-hexane/ethanol (8:2 *v/v*) as mobile phase.

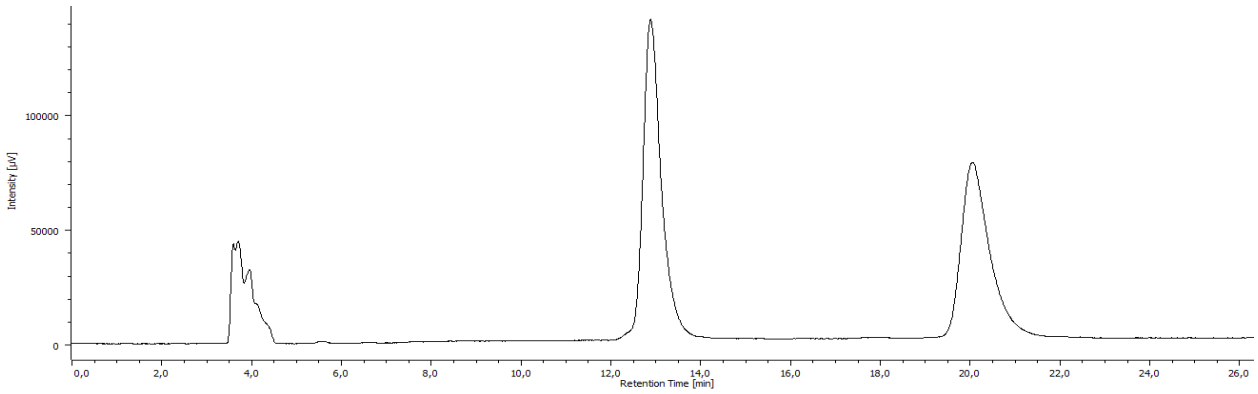

Figure 14. *Chromatogram of CDXA24 enantioresolution on CSP-1. Mobile phase, n-hexane/ethanol (8:2 v/v) Flow rate, 0.5 mL/min.; detection, 254 nm.*

These promising preliminary results lead us to predict that CSP-1 is efficient in resolving a wide variety of compounds, namely those with similar structures to those of the commercially available racemates as well as CDXs. These results also allowed to conclude that the mobile phases are equally important for the chiral discrimination of this CSP.

2. Enantioresolution performance of CSP-2

The chiral resolution evaluation of ADMPC (**CSP-2**) was performed through the analysis of some commercially available racemates, using *n*-hexane/2-propanol (9:1 *v/v*) as mobile phase. Furthermore, CSP-2 was tested with a library of CDXs with methanol (100%) as mobile phase. The LC evaluations were performed with chromatographic conditions based on the literature [39, 86] and the results are presented in **Table 32**.

Table 32. *Enantioresolution performance of CSP-2.*

Analytes	k_1	k_2	α	Rs	Mobile Phase
A1	1.17	1.59	1.36	<1.00	A
A2	0.93	0.93	1.00	---	
A3	1.27	1.58	1.24	<1.00	
A9	0.17	0.27	1.62	<1.00	B
A10	1.03	10.82	10.52	4.88	
A13	0.36	0.61	1.68	<1.00	

Table 32. *Enantioresolution performance of CSP-2* ***(Cont.).***

Analytes	k_1	k_2	α	Rs	Mobile Phase
A15	0.65	7.56	11.71	3.8	B
A16	0.34	0.51	1.50	<1.00	
A17	1.13	7.56	6.70	3.98	
A19	1.72	8.52	4.95	3.81	
A20	1.33	1.69	1.27	<1.00	

Mobile Phases: A – *n*-hexane/2-propanol (9:1 *v/v*); B - methanol (100%)

It is possible to observe in **Table 32** that racemate A2 was not separated, moreover the racemates A1 and A3 were separated with α values of 1.36, 1.24, respectively.

According to the results obtained, all further analytes tested were separated using methanol (100%) as mobile phase. It is important to highlight the enantioresolution of A10, A15, A17 and A19 with *α* values of 10.52, 11.71, 6.70 and 4.95 and *Rs* values of 4.88, 3.8, 3.98 and 3.81, respectively. **Figure 15** presents the obtained chromatogram for the enantioresolution of A19.

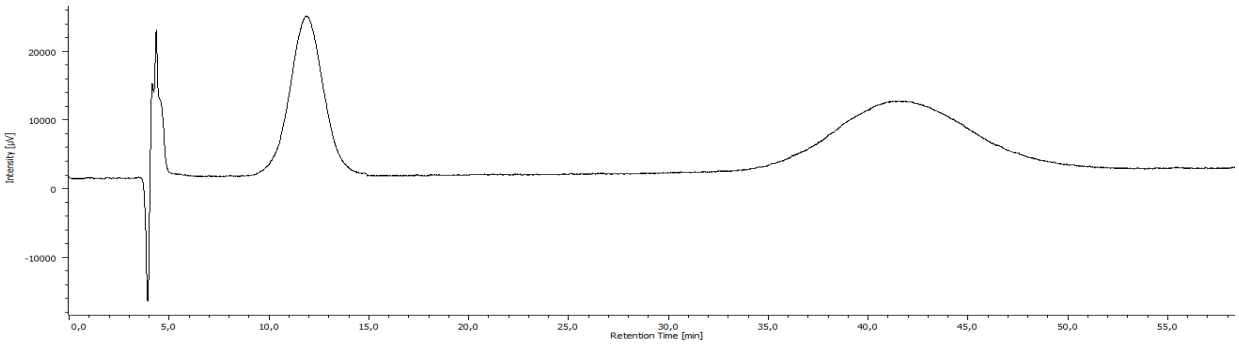

Figure 15*. Chromatogram of CDXA19 enantioresolution on CSP-2. Mobile phase, Methanol (100%); Flow rate, 0.5 mL/min.; detection, 254 nm.*

The theoretical plate number *N* of **CSP-2** is 211 being calculated using A19 in methanol (100%). CSP-2 was well packed and presents efficiency in the enantioresolution of racemates.

3. Enantioresolution performance of CSP-3

The chiral resolution evaluation of CDMPC (**CSP-3**) was performed through the analysis of some commercially available racemates, using *n*-hexane/2-propanol (9:1 *v/v*) as mobile phase. Furthermore, CSP-3 was tested with a library of CDXs (A9-A33) with *n*-hexane/ethanol (8:2 *v/v*) and methanol (100%) as mobile phases. The LC evaluations were performed with specific chromatographic conditions according to the literature [39, 86] and the results are presented in **Table 33**.

Table 33. *Enantioresolution performance of CSP-3.*

Analytes	k_1	k_2	α	Rs	Mobile Phase
A1	0.78	1.32	1.69	3.15	A
A2	0.53	0.79	1.49	3.08	
A3	2.51	3.34	1.33	2.11	
A7	0.78	0.78	1.00	---	
A11	8.84	11.89	1.34	1.78	B
A13	3.99	6.74	1.69	3.12	
A16	3.63	6.53	1.80	3.53	C
A17	2.10	2.40	1.14	<1.00	B
A19	1.99	2.30	1.16	1.54	C
A20	0.72	1.03	1.44	1.57	
A21	1.08	1.30	1.21	<1.00	

Mobile Phases: A – ***n***-hexane/2-propanol (9:1 *v/v*);
B – ***n***-hexane/ethanol (8:2 *v/v*); C – methanol (100% *v/v*)

It is possible to observe that the racemates A1, A2 and A3 were successfully separated with α values of 1.69, 1.49 and 1.33 and *Rs* values of 3.15, 3.08 and 2.11, respectively. The theoretical plate number *N* of this CSP is 246 being calculated using racemate A3 in *n*-hexane/2-propanol (9:1 *v/v*) (**Figure 16**).

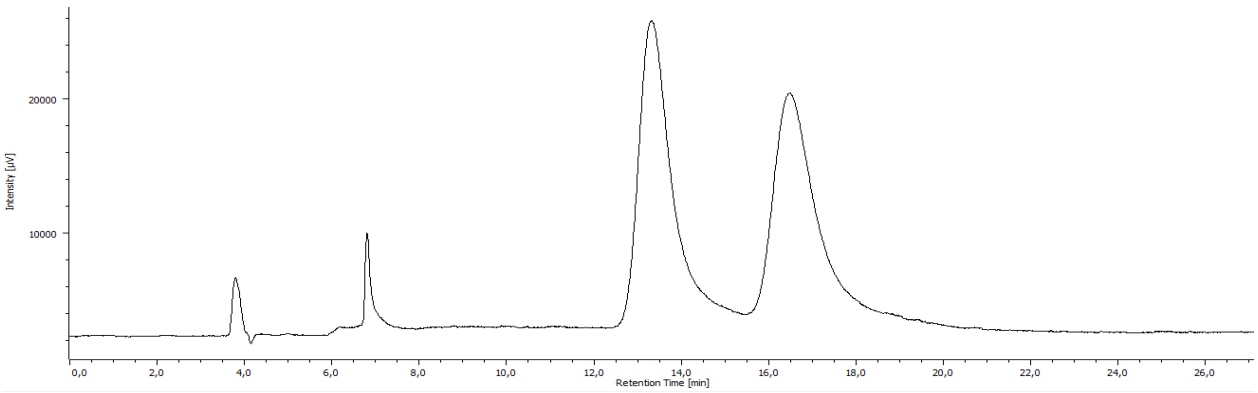

Figure 16. *Chromatogram of benzoin (A3) enantioresolution on CSP-3. Mobile phase, n-hexane/2-propanol (9:1 v/v); Flow rate, 0.5 mL/min.; detection, 254 nm.*

According to the results obtained, all further analytes were enantioseparated however, A17 and A21 presented low resolution values indicating an inefficient enantioresolution of the analytes in this CSP. Moreover, A13 and A16 were resolved using *n*-hexane/ethanol (8:2 *v/v*) or 100% methanol as mobile phase, presenting *α* values of 1.69

and 1.80 and *Rs* values of 3.12 and 3.53, respectively. **Figure 17** presents the obtained chromatogram for the enantioresolution of A13 using *n*-hexane/ethanol (8:2 *v/v*).

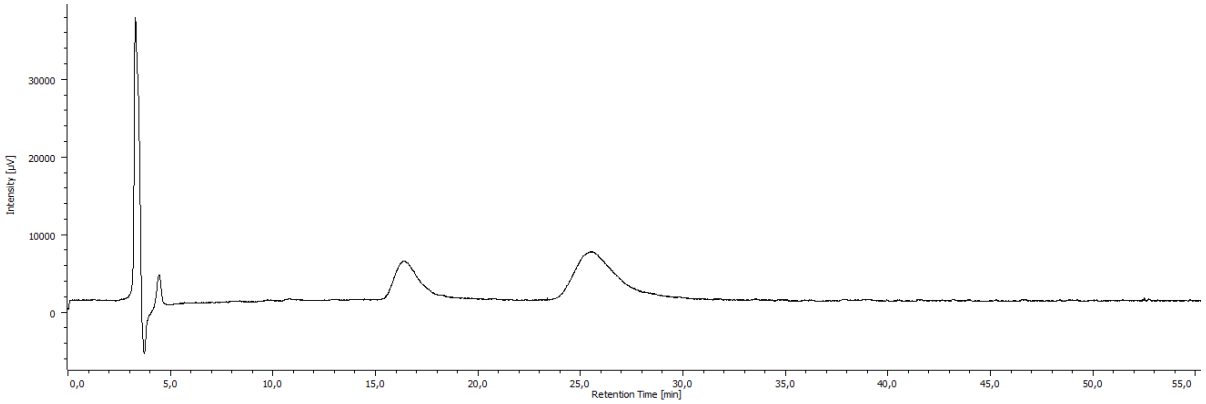

Figure 17. *Chromatogram of CDXA13 enantioresolution on CSP-3. Mobile phase, n-hexane/Ethanol (8:2 v/v), Flow rate, 0.5 mL/min.; detection, 254 nm.*

These promising results allowed to predict that **CSP-3** is efficient in resolving a wide variety of compounds, namely those with similar structures to those of the commercially available racemates as well as CDXs.

4. Enantioresolution performance of CSP-4

The chiral resolution evaluation of 3,5-DMPC-XD-2-Chitosan CSP (**CSP-4**) was performed through the analysis of some commercially available racemates, as well as some enantiomeric mixtures of CDXs synthesized "in house".

CDX A24 could be enantioresolved in this CSP, using *n*-hexane/ethanol (9:1, 8:2 and 7:3 *v/v*) as mobile phases with excellent values of enantioselectivity (α= 2.68, 2.35 and 1.73, respectively) and resolution (*Rs*= 2.81, 2.18 and 1.86, respectively). Even though this good result, the remaining analytes tested were not enantioseparated by **CSP-4**. In **Figure 18** it is shown the chromatogram for the CDX A24 using *n*-hexane/ethanol (7:3 *v/v*) as mobile phase.

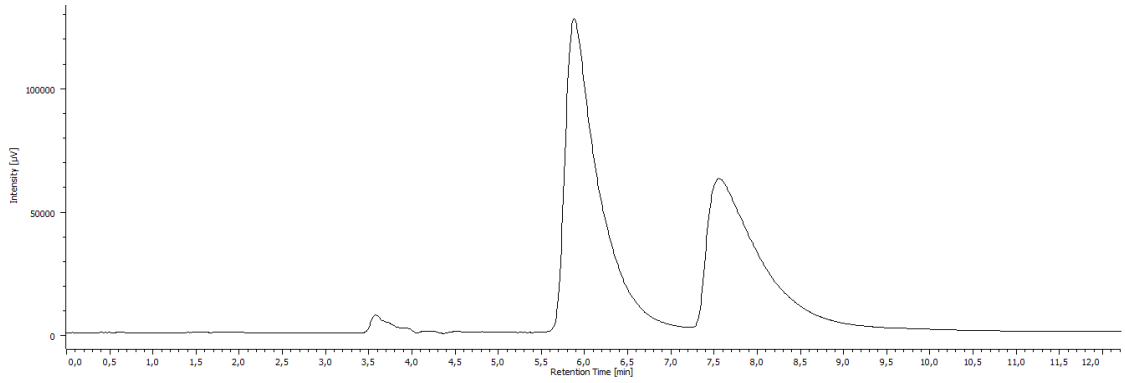

Figure 18. *Chromatogram of CDX A24 enantioresolution on CSP-4. Mobile phase n-hexane/ethanol (7:3 v/v) Flow rate, 0.5 mL/min.; detection, 254 nm.*

IV. Experimental

A. SYNTHESIS AND STRUCTURE ELUCIDATION

1. General Methods

The commercial available reagents were purchased from Sigma Aldrich Co., TCI and Fluka.

The solvents were *pro analysis* or HPLC grade from Sigma-Aldrich, ACROS and Fluka.

All the reactions were controlled by thin-layer chromatography (TLC) using Merck silica gel 60 (GF_{254}) plates, with appropriate mobile phases and UV detection at 254 and 365 nm.

Microwave (MW) reactions were performed using a MicroSYNTH 1600 from Millestone (ThermoUnica*m,* Portugal) synthesizer in sealed reaction vessels.

The solvents were evaporated on a rotary evaporator under reduced pressure (rotative evaporator Büchi).

Purifications of compounds were carried out by flash chromatography using Merck™ silica gel 60 (0.04-0.063 mm), liquid-liquid extraction and crystallization.

Melting points were obtained in a Köfler microscope and are uncorrected.

Optical rotation measurements were carried out on a Polartronic Universal polarimeter (ADP 410 polarimeter).

IR spectra were recorded in a KBr microplate in a FTIR spectrometer Nicolet iS10 from Thermo Scientific (Waltha*m,* MA, USA) with Smart OMNI-Transmission accessory (Software 188 OMNIC 8.3).

^{1}H and ^{13}C NMR spectra were performed in University of Aveiro, Department of Chemistry, and were taken in $CDCl_3$ or DMSO-d_6, at room temperature and/or 90ºC, on Bruker Avance 300 instrument (300.13 MHz for ^{1}H and 75.47 MHz for ^{13}C). ^{13}C NMR assignments were made by 2D HSQC and HMBC experiments (long-range C, H coupling constants were optimized to 7 and 1 Hz). Chemical shifts are expressed in ppm values relative to tetramethylsilane (TMS) as an internal reference. Coupling constants are reported in hertz (Hz).

Elemental analysis was performed in Centro de Apoio Científico e Tecnolóxico á Investigation (CACTI, University of Vigo, Spain).

2. Preparation of CSP with CDX as small molecule chiral selector (CSP-1) (92)

2.1. Synthesis of XD 5,7-dimethyl-9-oxo-9*H*-xanthene-2-carboxilic acid (XD-1) (96)

2.1.1. Synthesis of dimethyl 4-bromoisophtalate (102)

4-Bromoisophtalic acid (**101**) (10.49 g, 42.83 mmol) was dissolved in methanol (330 mL) and concentrated H_2SO_4 (7 mL) was added. The reaction was stirred under reflux for 20 h. Then, the methanol was evaporate*d,* and water (65 mL) was added. The crude product was extracted with diethyl ether (3 x 70 mL), and the organic layer was washed with water (2 x 50 mL), saturated $NaHCO_3$ solution (3 x 100 mL) and water (2 x 70 mL), successively. The organic layer was then dried with anhydrous Na_2SO_4, filtered and the solvent evaporated under reduced pressure. During overnight at room temperature white crystals of 4-bromoisophtalate (**102**) were obtained. Yield: 84 %; m.p. 56-58°C; IR ν_{max} (cm^{-1}) (KBr): 1754, 1309, 1253, 929, 565; ^{1}H NMR ($CDCl_3$, 300MHz) δ: 8.43 (1H, *d, J*=2.2 Hz, 2-H), 7.95 (1H, *d, J*=2.2 Hz, 6-H), 7.75 (1H, *d, J*=8.3 Hz, 5-H), 3.95 (3H, *s*, 1'-C$\underline{H}_3$), 3.93 (3H, *s*, 1"-C$\underline{H}_3$); ^{13}C NMR ($CDCl_3$, 75.47 MHz) δ: 127.0 (C-1), 132.3 (C-2), 129.3 (C-3), 134.7 (C-4), 132.2 (C-5), 133.0 (C-6), 165.7 (C-1'), 165.5 (C-1"), 52.5 (O$\underline{C}H_3$-1'), 52.7 (O$\underline{C}H_3$-1").

2.1.2. Synthesis of dimethyl 4-(2,4-dimethylphenoxy) isophtalate (104)

Dimethyl 4-bromoisophtalate (**102**) (9.50 g, 34.80 mmol), picolinic acid (0.41 g, 3.30 mmol), K_3PO_4 (14.26 g, 67.17 mmol) and CuI (0.32 g, 1.65 mmol) were added to a sealed twin-neck bottom round flask. The flask was then purged and backfilled with nitrogen three times. 2,4-Dimethylphenol (**103**) (10.0 mL, 82.67 mmol) and DMSO (66 mL) were added. The reaction was heated to 80°C and stirred for 28 h. Then, it was cooled at room temperature, filtered and extracted with ethyl acetate (3 x 100 mL) and water (30 mL). The aqueous layer was then extracted with chloroform (3 x 100 mL). The combined organic layers were dried with anhydrous Na_2SO_4, filtered and the solvent evaporated under reduced pressure, to afford the dimethyl 4-(2,4-dimethylphenoxy) isophtalate (**104**) as a dark-brown oil. Yield: 63 %; m.p. 97-99°C; IR ν_{max} (cm^{-1}) (KBr): 1717, 1436, 1259; ^{1}H NMR ($CDCl_3$, 300MHz) δ: 8.35 (1H, *d, J*= 2.2Hz, 2-H), 8.00 (1H, *dd, J*= 8.7 and 2.2 Hz, 6-H), 7.17 (1H, s, 3'-H), 7.08 (1H, *d, J*=8.2 Hz, 6'-H), 6.89 (1H, *d, J*= 8.2 Hz, 5'-H), 6.70 (1H, *d, J*= 8.7 Hz, 5-H), 2.29 (3H, s, 2'-C$\underline{H}_3$), 2.07 (3H,s, 4'-C$\underline{H}_3$); ^{13}C NMR ($CDCl_3$, 75.47 MHz) δ: 165.0 (C-1), 134.2 (C-2),165.5 (C-3), 160.4 (C-4), 120.3 (C-5), 134.9 (C-6), 124.9 (C-1'), 116.2 (C-2'), 124.4 (C-3'), 116.3 (C-4'), 121.9 (C-5'), 120.3 (C-6'), 21.0 (O$\underline{C}H_3$-2'), 20.4 (O$\underline{C}H_3$-4'), 166.0 (C-1"), 166.1 (C-1'"), 52.3 (O$\underline{C}H_3$-1"), 52.4 (O$\underline{C}H_3$-1'").

2.1.3. Synthesis of 4-(2,4-dimethylphenoxy)isophtalic acid (105)

Dimethyl 4-(2,4-dimethylphenoxy) isophtalate (**104**) (8.00 g, 25.45 mmol) was dissolved in methanol/THF (200 mL, 1:1 *v/v*) and 5M NaOH solution (30 mL, 774.40 mmol) was added. The reaction mixture was stirred at room temperature for 18 h. Then, the solvents were evaporated under reduced pressure and water (50 mL) was added. The crude product was washed with ethyl acetate (4 x 50 mL) and the organic layer extracted with water (3 x 100 mL). The combined aqueous layers were acidified with 5M HCl solution and the precipitate was filtered under reduced pressure and washed with cooled water, to afford the 4-(2,4-dimethylphenoxy) isophtalic acid (**105**) as a dark-brown solid. Yield: 61 %; m.p. 240-242 °C; IR ν_{max} (cm^{-1}) (KBr): 2923, 1613, 1604, 1491, 1257; ^{1}H NMR ($CDCl_3$, 300MHz) δ: 8.33 (1H, *d, J*= 2.2Hz, 2-H), 7.97 (1H, *dd, J*= 8.7 and 2.2 Hz, 6-H), 7.16 (1H, s, 3'-H), 7.07 (1H, *d, J*=8.1 Hz, 6'-H), 6.87 (1H, *d, J*= 8.1 Hz, 5'-H), 6.67 (1H, *d, J*= 8.7 Hz, 5-H), 2.29 (3H, s, 2'-C$\underline{H}_3$), 2.07 (3H,s, 4'-C$\underline{H}_3$); ^{13}C NMR ($CDCl_3$, 75.47 MHz) δ: 164.2 (C-1), 134.4 (C-2), 165.1 (C-3), 160.0 (C-4), 120.3 (C-5), 132.9 (C-6), 128.2 (C-1'), 118.1 (C-2'), 124.4 (C-3'), 116.3 (C-4'), 122.0 (C-5'), 120.3 (C-6'), 20.4 ($\underline{C}H_3$-2'), 15.6 ($\underline{C}H_3$-4'), 166.2 (C-1''), 166.3 (C-1''').

2.1.4. Intramolecular acylation of 4-(2,4-dimethylphenoxy)isophtalic acid (96)

4-(2,4-Dimethylphenoxy) isophtalic acid (**105**) (0.63 g, 2.18 mmol) was dissolved in methane sulfonic acid (9 mL, 140 mmol) and phosphorous pentoxide (0.99 g, 3.50 mmol) was added. The reaction mixture was stirred at room temperature for 22 h and then poured over ice. The product formed was filtered under reduced pressure and dried at room temperature, to afford the 5,7-dimethyl-9-oxo-9*H*-xanthene-2-carboxilic acid (**96**) as a brown solid. Yield: 72 %; m.p. >300 °C; IR ν_{max} (cm^{-1}) (KBr): 2920, 1667, 1611, 1475, 1421, 768, 680; ^{1}H NMR ($CDCl_3$, 300MHz) δ: 8.61 (1H, *d, J*= 2.1 Hz, 1-H), 8.23 (1H, *dd, J*= 8.7 and 2.2 Hz, 3-H), 7.59 (1H, *d, J*=8.1 Hz, 4-H), 7.23 (1H, s, 8-H), 7.02 (1H, s, 6-H), 2.74 (3H, s, 7-C$\underline{H}_3$), 2.39 (3H,s, 5-C$\underline{H}_3$); ^{13}C NMR ($CDCl_3$, 75.47 MHz) δ: 128.0 (C-1), 126.3 (C-2), 166.2($\underline{C}$OOH-2), 134.9 (C-3), 118.2 (C-4), 156.8 (C-4a), 117.2 (C-5), 128.6 (C-6), 121.7 (C-7), 116.0 (C-8), 140.8 (C-8a), 176.8 (C-9), 157.2 (C-9a), 145.8 (C-10a), 21.2 ($\underline{C}H_3$-5), 22.6 ($\underline{C}H_3$-7).

2.2. Synthesis of CDX (*R*)-*N*-(2-hydroxy-2-phenylethyl)-5,7-dimethyl-9-oxo-9-*H*-xanthene-2-carboxamide (98)

5,7-Dimethyl-9-oxo-9*H*-xanthene-2-carboxylic acid (XD-1) (**96**) (100 mg, 0.37 mmol) was dissolved in THF (20 mL) and TEA (103 mL, 0.74 mmol) was added. Then,

TBTU (120 mg, 0.37 mmol) and (*R*)-phenylglycinol (**97**) (0.37 mmol) were added. The reaction was stirred at room temperature for 1.5 h. The solvent was evaporated under reduced pressure and the crude product was dissolved in dichloromethane (50 mL). This solution was washed with 1M HCl (2 x 25 mL), saturated solution of $NaHCO_3$ (2 x 30 mL) and water (3 x 50 mL). The organic layer was dried with anhydrous Na_2SO_4, filtered and the solvent evaporated under reduced pressure, to afford the (*R*)-*N*-(2-hydroxy-2-phenylethyl)-5,7-dimethyl-9-oxo-9-*H*-xanthene-2-carboxamide (**98**) as a white solid. Yield: 83 %; m.p. 184-186°C; $[\alpha]_{D^{25^{\circ}C}}$ =+128.3°; IR ν_{max} (cm^{-1}) (KBr): 3431, 1652, 1615, 1540, 1474; ^{1}H NMR ($CDCl_3$, 300MHz) δ: 8.63 (1H, *d, J*= 2.2 Hz, 1-H), 8.25 (1H, *dd, J*= 8.8 and 2.2 Hz, 3-H), 7.90 (1H, s, 8-H), 7.53 (1H, *d, J*=8.7 Hz, 4-H), 7.36 (5H, *m,* 20-H, 2", 3", 4", 5" and 6"-H), 7.26 (1H, s, 6-H), 5.34 (1H, *m,* 1'-H), 4.06 (2H, *d, J*=5.2 Hz, 2'-C$\underline{H}_2$), 2.49 (3H, s, 7-C$\underline{H}_3$), 2.42 (3H,s, 5-C$\underline{H}_3$), 1.74 (1H, s, 2'-O$\underline{H}$); ^{13}C NMR ($CDCl_3$, 75.47 MHz) δ: 129.5 (C-1), 124.7 (C-2), 166.3 ($\underline{C}$=O-2), 133.8 (C-3), 121.0 (C-4), 157.7 (C-4a), 134.4 (C-5), 20.8 ($\underline{C}H_3$-5), 128.0 (C-6), 137.6 (C-7), 15.7 ($\underline{C}H_3$-7), 118.8 (C-8), 120.6 (C-8a), 177.2 (C-9), 123.6 (C-9a), 152.6 (C-10a), 56.5 (C-1'), 66.4 (C-2'), 138.8 (C-1"), 127.1 (C-2" and C-6"), 129.0 (C-3" and 5"), 126.9 (C-4").

2.3. Synthesis of silylated CDX (*R*)-*N*-(2-hydroxy-2-phenylethyl)-5,7-dimethyl-9-oxo-9-*H*-xanthene-2-carboxamido)-1-phenylethyl(3-(triethoxysilyl) propyl)carbamate (100)

The (*R*)-*N*-[(2-hydroxy-1-phenyl)ethyl]-3,5-dimethylxanthone-2-carboxamide (**98**) was dissolved in anhydrous toluene (30 mL), and TEA (1 mL) and 3-triethoxysylilpropyl isocyanate (**99**) (670 µL, 2.71 mol) were added. The mixture was stirred at reflux for 76 h. The solvent was evaporated under reduced pressure and the crude product was purified by flash chromatography (Merck™ silica gel 5 g/25 mL, *n*-hexane/ethyl acetate in gradient), to afford the (*R*)-*N*-(2-hydroxy-2-phenylethyl)-5,7-dimethyl-9-oxo-9-*H*-xanthene-2-carboxamido)-1-phenylethyl(3-(triethoxysilyl)propyl)carbamate (**100**). Yield: 16 %. ^{1}H NMR ($CDCl_3$, 300MHz) δ: 8.75 (*d, J*= 2.2 Hz, 1-H), 8.31 (*d, J*= 2.0 Hz, 3-H), 7.98 (s, 8-H), 7.71 (*m,* 2", 3", 4", 5" and 6"-H), 7.69 (*s,* 4-H), 7.55 (s, 6-H), 5.14 (*m,* 1'-H), 4.63 (2H, *m,* 2'-C$\underline{H}_2$), 4.22 (*q, J*=, Si-OC$\underline{H}_2$CH$_3$), 3.23 (*m,* 1"'- CH$_2$), 2.55 (s, 7-C$\underline{H}_3$), 2.45 (s, 5-C$\underline{H}_3$), 2.14 (*m,* 2"'- CH$_2$), 2.04 (*m,* Si-OCH$_2$C$\underline{H}_3$), 0.61 (*m,* 3"'- CH$_2$).

2.4. Covalent bonding of silylated CDX-1 (*R*)-*N*-(2-hydroxy-2-phenylethyl)-5,7-dimethyl-9-oxo-9-*H*-xanthene-2-carboxamido)-1-phenylethyl(3-(triethoxysilyl)propyl)carbamate (92) to silica gel

Silica gel Nucleosil® (3 g, 100 Å-5µ*m,* Merck), previously dried in a desiccator under vacuum with phosphorus pentoxide for 24 h, was suspended in anhydrous toluene (30 mL). Then, (*R*)-*N*-(2-hydroxy-2-phenylethyl)-5,7-dimethyl-9-oxo-9-*H*-xanthene-2-carboxamido)-1-phenylethyl(3-(triethoxysilyl)propyl)carbamate (**100**) (700mg, 1.18 mmol) dissolved in the same solvent (30mL) was added. The reaction mixture was gently stirred at reflux for 76 h. The obtained product was filtered and washed successively with toluene, methanol, acetone, ethyl acetate, dichloromethane and *n*-hexane (100 mL). The bonded phase was dried in a desiccator under vacuum for 24 h, yielded 3.68 g of CSP-1. Elemental analysis of CSP-1 (C, 8.81%; H, 1.18%; N, 0.90%).

2.5. HPLC column packing

CSP-1 (**92**) (2.30 g) was mixed with *n*-hexane/isopropanol (50:50 *v/v*) (50 mL), and then was sonicated for 3 min. The suspension was poured into the chamber of a column packer and was packed into empty HPLC column (150 x 4.6 mm i.d.) with *n*-hexane/isopropanol (90:10 *v/v*) as packing solvent, under the pressure of 6000 psi.

3. Preparation of CSPs with polysaccharide derivatives as chiral selectors (CSP-2 and CSP-3)

3.1. Synthesis of amylose *tris*(3,5-dimethylphenyl) carbamate (3,5-ADMPC) (108)

Amylose (**106**) (1.60 g, 8.32 mmol) was suspended in dry pyridine (20 mL, 249.70 mmol) and the mixture was stirred under reflux for 24 h in nitrogen atmosphere. 3,5-dimethylisocyanate (**107**) (4.90 g, 33.30 mmol) was added to the mixture and the reaction was stirred under reflux for 72 h. Then, the reaction mixture was concentrated and poured over methanol. The solid was filtered under reduced pressure and washed abundantly with methanol, to afford the amylose *tris*(3,5-dimethylphenyl) carbamate (**108**) as a white-brown solid. Yield: 85 %; IR ν_{max} (cm^{-1}) (KBr): 3292, 1713, 1614; Elemental analysis (C, 62.37%; H, 6.20%; N, 6.25%).

3.2. Synthesis of cellulose *tris*(3,5-dimethylphenyl) carbamate (3,5-CDMPC) (110)

Cellulose (**109**) (1.60 g, 8.32 mmol) was suspended in dry pyridine (16 mL, 197.70 mmol) and the mixture was stirred under reflux for 24 h in nitrogen atmosphere. 3,5-dimethylisocyanate (**107**) (4.90 g, 33.30 mmol) was added to the mixture and the reaction was stirred under reflux for 72 h. The reaction mixture was concentrated and poured over methanol. The solid was filtered under reduced pressure and washed abundantly with methanol, to afford the cellulose *tris*(3,5-dimethylphenyl) carbamate (**110**) as a white-brown solid. Yield: 93 %; IR ν_{max} (cm^{-1}) (KBr): 3296, 1732, 1615. Elemental analysis (C, 65.06%; H, 6.33%; N, 7.08%).

3.3. General procedure of silica coating

Aminopropylsilica (2.7 g, 100 Å, 5 μm) was suspended in THF (30 mL) and refluxed for 30 min. Amylose *tris*(3,5-dimethylphenyl) carbamate (**108**) or cellulose 3,5-dimethylphenylcarbamate (**110**) (0.675 g, 1.07 mmol) was dissolved in THF and added to the aminopropylsilica. Then, the solvent was slowly evaporated under reduced pressure. The coated phase was dried in a desiccator under vacuum for 24 h, yielded 3.3 g of CSP-2 (**93**) or 3.4 g of CSP-3 (**94**). Elemental analysis of CSP-2 (C, 8.70%; H, 1.30%; N, 1.39%). Elemental analysis of CSP-3 (C, 15.86%; H, 1.99%; N, 2.11%).

3.4. General procedure of HPLC column packing

CSP-2 (**93**) (2.3 g) or CSP-3 (**94**) (2.3 g) was mixed with n-hexane/isopropanol (50:50 v/v) (50 mL), and then was sonicated for 3 min. The suspension was poured into the chamber of a column packer and was packed into empty HPLC column (150 x 4.6 mm i.d.) with *n*-hexane/isopropanol/paraffin oil (80:20:0.01 *v/v/v*) as packing solvent, under the pressure of 6000 psi.

4. Preparation of CSP with xanthone-polysaccharide derivative as chiral selector (CSP-4) (95)

4.1. Attempts of synthesis of a xanthone-polysaccharide derivative using 5,7-dimethyl-9-oxo-9*H*-xanthene-2-carboxilic acid (XD-1) (96) as building block

4.1.1. General procedure of attempt reaction of XD-1 (96) with amylose using coupling reagents

A mixture of XD-1 (**96**) (50 mg, 184.9 μmol) and the coupling reagent TBTU (15 mg, 61.7 μmol) or COMU (42.3 mg, 98.7 μmol) or DCC (19.08 mg, 92.5 μmol) was dissolved in DMSO (5 mL) and TEA (17 μL, 123.3 μmol) was added. The mixture was stirred for 30 min. Amylose (**106**) (12 mg, 61.7 μmol) dissolved in the same solvent (10 mL) was added to the mixture and the reaction was stirred at room temperature for 24 h. Then, the reaction was stirred at 90°C for 72 h, or 80°C for 76 h, or 35°C for 24h, when using TBTU, COMU or DCC, respectively. The crude product was poured over methanol and the solid was filtrated under reduced pressure.

4.1.2. Attempt reaction of XD-1 (96) with amylose through previous preparation of XD-1 benzoyl chloride

XD-1 (**96**) (50 mg, 184.9 μmol) was dissolved in dry toluene (10 mL) and $SOCl_2$ (0.5 mL, 6.89 mmol) was added. The mixture was stirred under reflux for 2 h. Toluene and $SOCl_2$ were evaporated under a distillation apparatus and amylose (**106**) (11mg, 57.2 μmol), previously suspended in pyridine (15 mL), was added. The mixture was stirred at 90°C for 72 h. The crude product was poured over methanol and the solid was filtrated under reduced pressure.

4.1.3. Attempt reaction of XD-1 (96) with cellulose through coupling reaction with TBTU

A mixture of XD-1 (**96**) (50 mg, 184.9 μmol) and TBTU (15 mg, 61.7 μmol) was dissolved in THF (20 mL) and TEA (17 μL, 123.3 μmol) was added. The mixture was stirred for 30 min. Cellulose (**109**) (12 mg, 61.7 μmol) suspended in pyridine (10 mL) was added and the mixture was stirred at room temperature for 24 h. Then, the reaction was stirred at 90°C for additional 72h. The crude product was poured over methanol and the solid was filtrated under reduced pressure.

4.1.4. Attempt reaction of XD-1 (96) with cellulose through previous preparation of XD-1 benzoyl chloride

XD-1 (**96**) (50 mg, 184.9 μmol) was dissolved in dry toluene (10 mL) and $SOCl_2$ (0.5 mL, 6.89 mmol) was added. The mixture was stirred under reflux for 2 h. Toluene and $SOCl_2$ were evaporated under a distillation apparatus and cellulose (**109**) (11 mg, 57.2 μmol),

previously suspended in pyridine (15 mL) were added. The reaction was stirred at 90ºC for 72 h. The crude product was poured over methanol and the solid was filtrated under reduced pressure.

4.1.5. General procedure of attempt reaction of XD-1 (96) with marine-derived polysaccharides through coupling reaction with TBTU

A mixture of XD-1 (**96**) (50 mg, 184.9 μmol) and TBTU (15 mg, 61.7 μmol) was dissolved in DMA (10 mL) and TEA (17 μL, 123.3 μmol) was added. The mixture was stirred for 30 min. Chitosan (**111**) or chitin (**112**) (12 mg, 61.7 μmol), previously dissolved in DMA (10 mL) with LiCl (20 mg, 470μmol) was added. The mixture was stirred at 60ºC for 48 h. Then, the crude product was poured over methanol and the solid was filtrated under reduced pressure.

4.1.6. Attempt reaction of XD-1 (96) with chitosan through coupling reaction with DCC/NHS

A mixture of XD-1 (**96**) (50 mg, 184.9 μmol), DCC (76.91 mg, 372.8 μmol) and NHS (21.5 mg, 186.4 μmol) was dissolved in DMF (5 mL) and stirred for 30 min at room temperature. Chitosan (**112**) (12 mg, 61.7 μmol), previously dissolved in acetic acid (5 mL, 10% *v/v*) and stirred at room temperature for 24 h, was added. The mixture was stirred at 35ºC for 24 h. The crude product was poured over ethanol and the solid was filtrated under reduced pressure.

4.2. Synthesis of a xanthone-polysaccharide derivative using 2-((9-oxo-9*H*-xanthen-3-yl)oxy)acetic acid (XD-2) (113) as building block

4.2.1. Synthesis of 2-((9-oxo-9*H*-xanthen-3-yl)oxy)acetic acid (XD-2) (113)

4.2.1.1. Synthesis of 2-hydroxy-2',4-dimethoxybenzophenone (116)

1,3-Dimethoxybenzene (**115**) (32.83 mmol, 4.3 mL) was dissolved in diethylether anhydrous (160 mL) and aluminium chloride anhydrous (10.63 g) was added to complete dissolution and cessation of gas formation. Then, 2-methoxybezoyl chloride (**114**) (30.23 mmol, 4.5 mL) was added dropwise. The solution was stirred at room temperature for 23 h. The crude product was poured into crushed ice, acidified (pH 2) with a 10% HCl solution and extracted with ethyl acetate (3 × 100 mL). The organic layer washed with water (3 × 100 mL), dried over Na_2SO_4 anhydrous and filtered. The organic solvent was evaporated under reduced pressure, to afford the 2-hidroxy-2',4-dimethoxybenzophenone (**116**) as a white solid. Yield: 93 %; m.p. 83-86 ºC; IR ν_{max} (cm^{-1}) (KBr): 3094-2833, 1621, 1507, 1487,

1462, 1255, 1201; ^{1}H NMR ($CDCl_3$, 300MHz) δ: 12.48 (1H, s, 4a-O<u>H</u>), 7.53 (1H, *ddd, J*= 1.0, 7.4 and 7.6 Hz, 7-H), 7.30 (1H, *dd, J*= 1.7 and 7.5 Hz, 5-H), 7.19 (1H, *d, J*=8.2 Hz, 8-H), 7.15 (1H, *d, J*=8.9 Hz, 1-H), 7.08 (1H, *ddd, J*=8.0, 7.4 and 1.4 Hz, 6-H), 6.47 (1H, *dd, J*= 2.5 and 8.9, 2-H), 6.54 (1H, *d, J*=2.5, 4-H), 3.83 (3H, s, 10a-OC<u>H</u>$_3$), 3.73 (3H, s, 3-OC<u>H</u>$_3$); ^{13}C NMR ($CDCl_3$, 75.47 MHz) δ: 131.8 (C-1), 128.2 (C-2), 199.6 (C-3), 100.8 (C-4), 164.6 (C-4a), 113.9 (C-5), 135.1 (C-6), 127.5 (C-7), 126.2 (C-8), 120.5 (C-8a), 166.1 (C-9), 111.9 (C-9a), 155.7 (C-10a), 55.8 (O<u>C</u>H$_3$-10a), 55.6 (O<u>C</u>H$_3$-3).

4.2.1.2. Synthesis of 3-methoxy-9*H*-xanthen-9-one (117)

2-Hidroxy-2',4-dimethoxybenzophenone (**116**) (6.83 g) was placed in a sealed Teflon microwave reactor vessel and a mixture of methanol/water (2:1 *v/v*, 150 mL) and sodium hydroxide (14.5 g) were added. The mixture was heated at 130ºC and stirred for 30 min at 300 W. The mixture was cooled to room temperature, water was added and left it overnight in the fridge. The solid obtained was filtered under reduced pressure and washed with cooled water, to afford the 3-methoxy-9*H*-xanthen-9-one (**117**) as a yellow solid. Yield: 83 %; m.p. 270-273 ºC; IR ν_{max} (cm^{-1}) (KBr): 1620, 1502, 1466, 1438, 1277; ^{1}H NMR ($CDCl_3$, 300MHz) δ: 8.17 (1H, *dd, J*= 1.7 and 8.0 Hz, 8-H), 8.10 (1H, *d, J*=8.9 Hz, 1-H), 7.85 (1H, *ddd, J*= 1.7, 7.8 and 8.7 Hz, 6-H), 7.63 (1H, *dd, J*=8.7and 1.1 Hz, 5-H), 7.47 (1H, *ddd, J*= 1.1, 7.8 and 8.0, 7-H), 7.17 (1H, *d, J*=2.4, 4-H), 7.06 (1H, *dd, J*=2.4 and 8.9, 2-H), 3.94 (3H,s, 3-OC<u>H</u>$_3$); ^{13}C NMR ($CDCl_3$, 75.47 MHz) δ: 127.3 (C-1), 113.7 (C-2), 165.0 (C-3), 56.2 (O<u>C</u>H$_3$-3), 100.6 (C-4), 157.6 (C-4a), 117.9 (C-5), 135.1 (C-6), 124.3 (C-7), 125.9 (C-8), 121.2 (C-8a), 174.9 (C-9), 114.9 (C-9a), 155.5 (C-10a).

4.2.1.3. Synthesis of 3-hydroxy-9*H*-xanthen-9-one (118)

3-Methoxy-9*H*-xanthen-9-one (**117**) (6.21 mmol, 1.40 g) was dissolved in toluene anhydrous (100 mL) and aluminium chloride (18.63 mmol, 2.36 g) was added. The reaction was stirred under reflux for 2.5 h. The mixture was cooled to room temperature and acidified (pH 1) with concentrated HCl. Water (50 mL) was added and the mixture was extracted with ethyl acetate (3 × 50 mL). The organic layer was washed with a 5% NaOH solution (3 × 50 mL), dried over Na_2SO_4 anhydrous and filtered. The organic solvent was evaporated under reduced pressure. The aqueous layer was acidified with a 20% HCl solution and extracted with ethyl acetate (3 × 50 mL). The organic layer was dried over Na_2SO_4 anhydrous and filtered. Then, the organic solvent was evaporated under reduced pressure, to afford the 3-hydroxy-9*H*-xanthen-9-one (**118**) as a yellow solid. Yield: 74 %; m.p. 240-242 ºC; IR ν_{max} (cm^{-1}) (KBr): 3085, 1613, 1566, 1480, 1451; ^{1}H NMR ($CDCl_3$, 300MHz) δ: 11.00 (3H,s, 3-O<u>H</u>), 8.15 (1H, *dd, J*= 1.7 and 8.0 Hz, 8-H), 8.14 (1H, *d, J*=8.5 Hz, 1-H), 7.82 (1H, *ddd, J*= 1.7, 7.8 and 8.7 Hz, 6-H), 7.61 (1H, *dd, J*=8.7 and 1.0 Hz, 5-H), 7.44 (1H, *ddd, J*= 1.0, 7.8 and 8.0, 7-H), 6.93 (1H, *d, J*=2.2, 4-H), 6.89 (1H, *dd, J*=2.2 and

8.5, 2-H); ^{13}C NMR ($CDCl_3$, 75.47 MHz) δ: 128.0 (C-1), 113.7 (C-2), 164.0 (C-3), 102.1 (C-4), 157.6 (C-4a), 117.9 (C-5), 134.8 (C-6), 124.1 (C-7), 125.8 (C-8), 121.2 (C-8a), 174.8 (C-9), 114.1 (C-9a), 155.5 (C-10a).

4.2.1.4. Synthesis of methyl 2-((9-oxo-9*H*-xanthen-3-yl)oxy)acetate (119)

3-Hidroxy-9*H*-xanthen-9-one (**118**) (6.42 mmol, 1.36 g) was dissolved in acetone anhydrous (55 mL) and potassium carbonate (7.54 mmol, 1.40 g) and methyl bromoacetate (5.17 mmol, 680 μL) were added. The reaction was stirred under reflux for 24 h. The reaction mixture was concentrated under reduced pressure and *n*-hexane (50mL) was added. The product obtained was filtered and crystallized from methanol, to afford the methyl 2-((9-oxo-9*H*-xanthen-3-yl)oxy)acetate (**119**) as a light brown solid. Yield: 67 %; m.p. 157-159 ºC; IR ν_{max} (cm^{-1}) (KBr): 1739, 1648, 1622, 1452, 1236; ^{1}H NMR ($CDCl_3$, 300MHz) δ: 8.18 (1H, *dd, J*= 1.7 and 7.5 Hz, 8-H), 8.12 (1H, *d, J*=8.9 Hz, 1-H), 7.86 (1H, *ddd, J*= 1.7, *J*=8.0 and 8.6 Hz, 6-H), 7.64 (1H, *dd, J*=8.6 and 1.0 Hz, 5-H), 7.48 (1H, *ddd, J*= 1.0, 7.5 and 8.0, 7-H), 7.19 (1H, *d, J*=2.4, 4-H), 7.10 (1H, *dd, J*=2.4 and 8.9, 2-H), 5.05 (2H, s, 1'-C$\underline{H}_2$), 3.74 (3H, s, 3-OC$\underline{H}_3$); ^{13}C NMR ($CDCl_3$, 75.47 MHz) δ: 127.7 (C-1), 113.8 (C-2), 163.2 (C-3), 101.6 (C-4), 157.3 (C-4a), 117.9 (C-5), 135.2 (C-6), 124.4 (C-7), 125.9 (C-8), 121.2 (C-8a), 174.9 (C-9), 115.6 (C-9a), 155.6 (C-10a), 65.0 (C-1'), 168.6 (C-2'), 52.0 (O$\underline{C}H_3$-2').

4.2.1.5. Hydrolysis of the methyl ester of methyl 2-((9-oxo-9*H*-xanthen-3-yl)oxy)acetate (113)

To a solution of 2-((9-oxo-9*H*-xanthen-3-yl)oxy)acetate (**119**) (6.41 mmol, 1.82 g) in dichloromethane:methanol (1:1 *v/v*, 155 mL), NaOH 5N (12 mL) was added. The reaction was stirred at room temperature for 5 h. The solvents were evaporated under reduced pressure and water (100mL) was added. The crude product was washed with dichloromethane (3 x 100mL). The aqueous layer was acidified with a HCl 5N resulting in the formation of a precipitate that was collected by filtration under reduced pressure and dissolved in saturated $NaHCO_3$ solution. The solution was washed with dichloromethane (3 x 100 mL) and the aqueous layer was acidified with HCl 5N. The precipitate was collected by filtration under reduced pressure and washed with cooled water, to afford the 2-((9-oxo-9H-xanthen-3-yl)oxy)acetic acid (XD-2) (**113**) as a white solid. Yield: 90 %; m.p. 211-213 ºC; IR ν_{max} (cm^{-1}) (KBr): 3442, 1714, 1645, 1464, 1447, 1420, 1233; ^{1}H NMR ($CDCl_3$, 300MHz) δ: 12.74 (1H, s, 2'-O$\underline{H}$), 8.17 (1H, *dd, J*= 1.7 and 8.4 Hz, 8-H), 8.11 (1H, *d, J*=8.8 Hz, 1-H), 7.85 (1H, *ddd, J*= 1.5, 6.8 and 8.4 Hz, 6-H), 7.62 (1H, *dd, J*=8.4 and 3.3 Hz, 5-H), 7.47 (1H, *ddd, J*= 3.3, 6.4 and 8.4, 7-H), 7.19 (1H, *d, J*=2.4, 4-H), 7.08 (1H, *dd, J*=2.4 and 8.8, 2-H), 4.91 (2H, s, 1'-C$\underline{H}_2$); ^{13}C NMR ($CDCl_3$, 75.47 MHz) δ: 127.7 (C-1), 113.8 (C-2), 163.4

(C-3), 101.5 (C-4), 157.3 (C-4a), 117.9 (C-5), 135.1 (C-6), 124.4 (C-7), 125.9 (C-8), 121.2 (C-8a), 174.9 (C-9), 115.3 (C-9a), 155.6 (C-10a), 65.0 (C-1'), 169.5 (C-2').

4.2.2. Attempt reaction of XD-2 (113) with cellulose through coupling reaction with TBTU

A mixture of XD-2 (**113**) (50 mg, 185.90 μmol) and TBTU (15 mg, 61.7 μmol) were dissolved in dry pyridine (5 mL) and stirred at 80ºC for 30 min. Cellulose (**109**) (12 mg, 61.70 μmol), previously suspended in pyridine (6 mL) was added. The mixture was stirred at 80ºC for 24 h. The crude product was filtrated under reduced pressure and washed with methanol.

4.2.3. Attempt reaction of XD-2 (113) with chitosan through coupling reaction with TBTU

A mixture of XD-2 (**113**) (250 mg, 925.10 μmol) and TBTU (169 mg, 528.60 μmol) were dissolved in dry pyridine (10 mL) and stirred at 80ºC for 30 min. Chitosan (**112**) (48 mg, 264.30 μmol), previously suspended in pyridine (10 mL) with LiCl (66 mg, 1.57 mmol) was added. The mixture was stirred at 80ºC for 24 h. The crude product was filtrated under reduced pressure and washed with methanol.

4.2.4. Attempt reaction of XD-2 (113) with chitosan through coupling reaction with DCC/NHS

A mixture of XD-2 (**113**) (50 mg, 185.90 μmol), DCC (76 mg, 368.30 μmol) and NHS (21.5 mg, 186.40 μmol) was dissolved in DMF (5 mL) and stirred for 30 min at room temperature. Chitosan (**112**) (12 mg, 61.70 μmol), previously dissolved in acetic acid (5 mL, 10% *v/v*) and stirred at room temperature for 24 h was added. The mixture was stirred at 35ºC for 24 h. The crude product was poured over ethanol and the solid was filtrated under reduced pressure.

4.2.5. Synthesis of chitosan *N*-2-((9-oxo-9*H*-xanthen-3-yl)oxy)acetamide (121)

To a solution of 2-((9-oxo-9*H*-xanthen-3-yl)oxy)acetic acid (XD-2) (**113**) (1 g, 3.70 mmol) in dry toluene (20 mL), $SOCl_2$ (0.7 mL, 9.65 mmol) was added. The mixture was stirred under reflux for 2 h. Then, toluene and $SOCl_2$ were evaporated under a distillation

apparatus and chitosan (**112**) (620.7 mg, 3.46 mmol), previously suspended in pyridine (15 mL) was added. The mixture was stirred at 90ºC for 72 h. The crude product was poured over methanol and the solid was filtrated under reduced pressure, to afford the chitosan *N*-2-((9-oxo-9*H*-xanthen-3-yl)oxy)acetamide (**121**). Yield: 74 %; IR ν_{max} (cm^{-1}) (KBr): 3442, 1714, 1645, 1464, 1447, 1420, 1233;

4.2.6. Synthesis of chitosan 3,6-*bis*(3,5-dimethylphenylcarbamate)-2-((9-oxo-9*H*-xanthen-3-yl)oxy)acetamide) (122) (3,5-DMPC-XD2-Chitosan)

Chitosan *N*-2-((9-oxo-9*H*-xanthen-3-yl)oxy)acetamide (**121**) (1 g, 2.32 mmol) was suspended in dry DMA (16 mL, 197.70 mmol) and LiCl (197 mg, 4.64 mmol) and 3,5-dimethylisocyanate (**107**) (853 mg, 5.80 mmol) was added. The mixture was stirred under reflux for 72 h. Then, the mixture was concentrated and poured over methanol. The solid was filtered under reduced pressure and washed abundantly with methanol, to afford the chitosan 3,6-*bis*(3,5-dimethylphenylcarbamate)-2-((9-oxo-9*H*-xanthen-3-yl)oxy)acetamide) (**122**) as a brown solid. Yield: 81 %; IR ν_{max} (cm^{-1}) (KBr): 3442, 1714, 1645, 1464, 1447, 1420, 1233; Elemental analysis (C, 65.19%; H, 6.55%; N, 9.03%).

4.2.7. Silica coating and column packing of CSP-4

Aminopropylsilica (2.70 g, 100 Å, 5 μm) was suspended in DMF (30 mL) and refluxed for 30 min. Chitosan 3,6-*bis*(3,5-dimethylphenylcarbamate)-2-((9-oxo-9*H*-xanthen-3-yl)oxy)acetamide) (**122**) (0.675 g, 0.93 mmol) was dissolved in DMF and added to the suspended aminopropylsilica. Then, the solvent was slowly evaporated under reduced pressure. The coated phase was dried in a desiccator under vacuum for 24 h, yielded 3.5 g of CSP-4 (**95**). Elemental analysis (C, 19.70%; H, 3.90%; N, 6.14%).

CSP-4 (2.3 g) was mixed with *n*-hexane/isopropanol (50:50 v/v) (50 mL), and then was sonicated for 3 min. The suspension was poured into the chamber of a column packer and was packed into empty HPLC column (150 x 4.6 mm i.d.) with *n*-hexane/isopropanol/paraffin oil (80:20:0.01 *v/v/v*) as packing solvent, under the pressure of 6000 psi.

B. EVALUATION OF ENANTIORESOLUTION BY LIQUID CHROMATOGRAPHY

1. Instrumentation and chromatographic conditions

Analytical LC analyses were performed on a JASCO LC-NetII/ADC equipped with an 880-PU pump, an 880-30 solvent mixing module, an injector and an UV detector, 875-UV.

The solvents were HPLC grade and purchased from Sigma-Aldrich Co (St. Louis, Missouri, USA).

HPLC analysis were performed at room temperature with four different mobile phases, specifically *n*-hexane/2-propanol (9:1 *v/v*), *n*-hexane/ethanol (9:1 and 8:2 *v/v*) and methanol (100%). The mobile phases were degassed in a sonicator bath for 15 to 30 min before use.

The dead-time (t_0) was considered to be equal to the peak of the solvent front and was taken from each run. The working flow rate was 0.5 mL/min and the chromatograms were monitored by UV detection at a wavelength of 254 nm.

Working solutions of analytes in racemic form were prepared from stock solutions (1 mg/mL in ethanol) and further diluted in ethanol to a concentration of 50 μg/mL Working solutions of analytes in enantiomeric mixture were prepared by mixing equal aliquots of each enantiomer to obtain a concentration of 50 μg/mL

Sample injections (10 μL) were carried out in duplicate.

2. Chromatographic parameters

The chromatographic parameters determined in LC analysis of all the prepared CSPs were: the retention factor (***k***), the separation factor (***α***), the number of theoretical plates (***N***), and the resolution (***Rs***). These parameters are calculated through chromatogram interpretation. In **Figure 19** it is represented a general chromatogram of an enantiomeric separation.

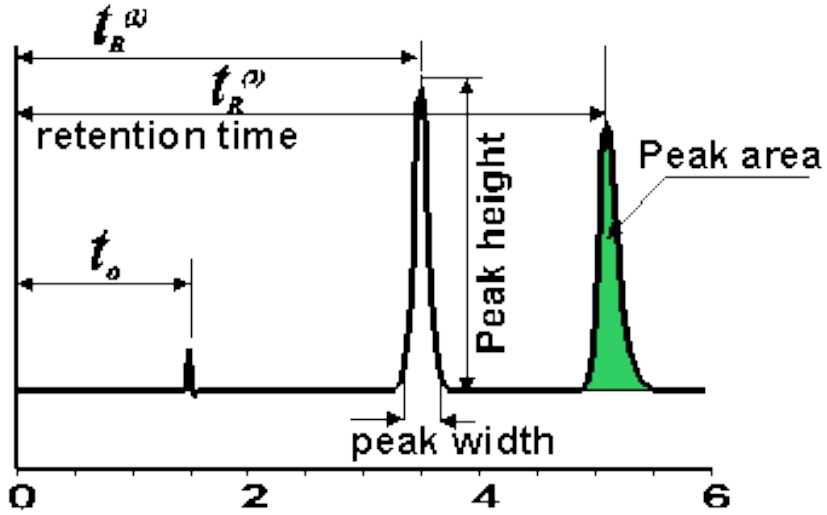

***Figure 19**. Example of a chromatogram of a enantioseparation with the measurements related to chromatographic parameters [150].*

The retention factor (***k***) is the ratio of the retention time of the analyte in the column (t_R) and the dead time (t_o) to give the retention of a certain component on the chromatographic column. The retention factor is calculated by the following equation:

$$k=\frac{(t_R-t_0)}{t_0} \quad \textbf{Equation 2}$$

The separation factor (***α***) measures the ability of the chromatographic system to separate the enantiomers in a sample and it is calculated by the following equation:

$$\alpha=\frac{k_2}{k_1} \quad \textbf{Equation 3}$$

The number of theoretical plates (***N***) measures the efficiency of the chromatographic conditions. This parameter is also used to evaluate the performance of the column. This number is calculated by using the following equation:

$$N=16\left(\frac{t_R}{w_b}\right)^2 \langle=\rangle N=5.54\left(\frac{t_R}{w_{\frac{1}{2}}}\right)^2 \quad \textbf{Equation 4}$$

where w_b is the width of the base of the peak and $w_{1/2}$ is the width of the band mid-height,

The resolution (***Rs***) measures the quality of a separation and it is calculated by the following equation:

$$R_S=\frac{t_{R2}-t_{R1}}{0.5\ (W_1+W_2)} \quad \textbf{Equation 5}$$

where, *W* is the width of the band at its base.

V. Conclusions

In this dissertation, four chiral stationary phases (CSPs) were successfully prepared: **CSP-1** with a small molecule as chiral selector, **CSP-2** and **CSP-3** (polysaccharide-based) and **CSP-4** with a xanthone-polysaccharide derivative as chiral selector.

The total synthesis of two xanthone derivatives (XDs), XD-1 and XD-2, was successfully achieved by two distinct multi-step synthetic pathways, *via* diaryl-ether and *via* benzophenone, respectively.

Several binding attempts of the XDs to the polysaccharides amylose, cellulose, chitin and chitosan, were carried out, however, being unsuccessful.

CSP-1, prepared with XD-1 demonstrated good enantiorecognition abilities for several commercially available racemates, as well as for several chiral derivatives of xanthones (CDXs) synthesized "in house". Moreover, the obtained results show that the CSP was efficient and well packed.

CSPs-2 and **-3** were prepared by reaction of 3,5-dimethylphenylcarbamate with amylose and cellulose, respectively. The enantioresolution performance of these CSPs was evaluated. They showed similar enantiorecognition abilities to those from the literature. The results demonstrated that the coating of the amylose and cellulose derivatives in aminopropylsilica (APS) as well as the column packing were successfully achieved.

CSPs-4 was prepared by reaction of XD-2 with thionyl chloride to give the correspondent acyl chloride that was further reacted with chitosan. The obtained product was then reacted with 3,5-dimethylisocyanate to give the chiral selector that was coated to APS to afford the **CSP-4**. This CSP demonstrated excellent enantiorecognition to the CDX A24 with an $\boldsymbol{\alpha}$ value of 6.18 and a $\boldsymbol{Rs}$ value of 2.81.

This preliminary result is very promising, however, the evaluation of this CSP with more racemates and mobile phases is necessary, as well as the preparation of other xanthone-polysaccharide based CSPs that may provide better results for the enantiorecognition of several racemates.

VI. References

The bibliographic research was made using the following databases:

http://www.scopus.com/
http://www.sciencedirect.com/
http://www.webofknowledge.com/
http://www.mdpi.com/
http://scholar.google.com/

1. K. Peter C. Vollhardt, N. E. S., *Organic Chemistry: Structure and Function*. 7th edition ed.; W. H. Freeman: 2014; p 1223.
2. Morrison, R. T.; Boyd, R. N., *Organic chemistry*. 6th ed ed.; Prentice-Hall International: London, 1992; p xxvi, 1279, 35 p.
3. Tiritan, M. E.; Ribeiro, A. R.; Fernandes, C.; Pinto, M. M. M., Chiral Pharmaceuticals. In *Kirk-Othmer Encyclopedia of Chemical Technology*, John Wiley & Sons, Inc.: 2016.
4. Okamoto, Y.; Ikai, T., Chiral HPLC for efficient resolution of enantiomers. *Chemical Society Reviews* **2008,** *37* (12), 2593-2608.
5. Mannschreck, A.; Kiesswetter, R.; von Angerer, E., Unequal Activities of Enantiomers via Biological Receptors: Examples of Chiral Drug, Pesticide, and Fragrance Molecules. *Journal of Chemical Education* **2007,** *84* (12), 2012.
6. Brocks, D. R., Drug disposition in three dimensions: an update on stereoselectivity in pharmacokinetics. *Biopharmaceutics & Drug Disposition* **2006,** *27* (8), 387-406.
7. Rentsch, K. M., The importance of stereoselective determination of drugs in the clinical laboratory. *Journal of Biochemical and Biophysical Methods* **2002,** *54* (1–3), 1-9.
8. Cordato, D. J.; Mather, L. E.; Herkes, G. K., Stereochemistry in clinical medicine: a neurological perspective. *Journal of Clinical Neuroscience* **2003,** *10* (6), 649-654.
9. Smith, S. W., Chiral Toxicology: It's the Same Thing...Only Different. *Toxicological Sciences* **2009,** *110* (1), 4-30.
10. Francotte, E. R., Enantioselective chromatography as a powerful alternative for the preparation of drug enantiomers. *J. Chromatogr. A* **2001,** *906* (1-2), 379-397.
11. Zhang, Y.; Wu, D.-R.; Wang-Iverson, D. B.; Tymiak, A. A., Enantioselective chromatography in drug discovery. *Drug Discovery Today* **2005,** *10* (8), 571-577.
12. Ward, T. J.; Ward, K. D., Chiral separations: fundamental review 2010. *Anal Chem* **2010,** *82* (12), 4712-22.
13. Lämmerhofer, M., Chiral recognition by enantioselective liquid chromatography: Mechanisms and modern chiral stationary phases. *J. Chromatogr. A* **2010,** *1217* (6), 814-856.
14. Scriba, G. K. E., Chiral recognition mechanisms in analytical separation sciences. *Chromatographia* **2012,** *75* (15-16), 815-838.
15. Carla, F.; Madalena, P.; Maria, E. T., Enantioresolution of Chiral Derivatives of Xanthones on Different Types of Liquid Chromatography Stationary Phases: A Comparative Study. *Current Chromatography* **2014,** *1* (2), 139-150.
16. Chen, X.; Yamamoto, C.; Okamoto, Y., Polysaccharide derivatives as useful chiral stationary phases in high-performance liquid chromatography. *Pure Appl. Chem.* **2007,** *79* (9), 1561-1573.
17. Pirkle, W. H.; House, D. W., Chiral high-performance liquid chromatographic stationary phases. 1. Separation of the enantiomers of sulfoxides, amines, amino acids, alcohols, hydroxy acids, lactones, and mercaptans. *The Journal of Organic Chemistry* **1979,** *44* (12), 1957-1960.
18. Welch, C. J., Evolution of chiral stationary phase design in the Pirkle laboratories. *J. Chromatogr. A* **1994,** *666* (1), 3-26.
19. Ikai, T.; Okamoto, Y., Structure control of polysaccharide derivatives for efficient separation of enantiomers by chromatography. *Chemical Reviews* **2009,** *109* (11), 6077-6101.

20. Okamoto, Y.; Kawashima, M.; Hatada, K., Chromatographic resolution : XI. Controlled chiral recognition of cellulose triphenylcarbamate derivatives supported on silica gel. *J. Chromatogr. A* **1986,** *363* (2), 173-186.
21. Cass, Q. B.; Degani, A. L. G.; Cassiano, N. M., Effects on enantioselectivity by the use of polysaccharide-based columns by multimodal elution. *Journal of Liquid Chromatography and Related Technologies* **2003,** *26* (13), 2083-2101.
22. Cass, Q. B.; Bassi, A. L.; Calafatti, S. A.; Matlin, S. A.; Tiritan, M. E.; de Campos, L. M. M., Carbohydrate carbamate coated onto microporous silica: Application to chiral analysis of commercial pharmaceutical drugs. *Chirality* **1996,** *8* (1), 143-146.
23. Cass, Q. B.; Degani, A. L. G.; Tiritan, M. E.; Matlin, S. A.; Curran, D. P.; Balog, A., Enantiomeric resolution by HPLC of axial chiral amides using amylose tris[(S)-1-phenylethylcarbamate]. *Chirality* **1997,** *9* (2), 109-112.
24. Tiritan, M. E.; Cass, Q. B.; Del Alamo, A.; Matlin, S. A.; Grieb, S. J., Preparative enantioseparation on polysaccharide phase using microporous silica as a support. *Chirality* **1998,** *10* (7), 573-577.
25. Armstrong, D. W.; DeMond, W., Cyclodextrin Bonded Phases For the Liquid Chromatographic Separation of Optical, Geometrical, and Structural Isomers. *Journal of Chromatographic Science* **1984,** *22* (9), 411-415.
26. Armstrong, D. W.; Tang, Y.; Chen, S.; Zhou, Y.; Bagwill, C.; Chen, J. R., Macrocyclic antibiotics as a new class of chiral selectors for liquid chromatography. *ANAL. CHEM.* **1994,** *66* (9), 1473-1484.
27. Jacek, B.; Hassan, Y. A.-E.; Ashraf, G., Whats New in Chromatographic Enantioseparations. *Current Analytical Chemistry* **2005,** *1* (1), 59-77.
28. Ribeiro, A. R.; Maia, A. S.; Cass, Q. B.; Tiritan, M. E., Enantioseparation of chiral pharmaceuticals in biomedical and environmental analyses by liquid chromatography: An overview. *Journal of Chromatography B: Analytical Technologies in the Biomedical and Life Sciences* **2014,** *968*, 8-21.
29. Yashima, E., Polysaccharide-based chiral stationary phases for high-performance liquid chromatographic enantioseparation. *J Chromatogr A* **2001,** *906* (1-2), 105-25.
30. Cavazzini, A.; Pasti, L.; Massi, A.; Marchetti, N.; Dondi, F., Recent applications in chiral high performance liquid chromatography: A review. *Analytica Chimica Acta* **2011,** *706* (2), 205-222.
31. Ward, T. J.; Ward, K. D., Chiral separations: a review of current topics and trends. *Anal Chem* **2012,** *84* (2), 626-35.
32. Felix, G.; Berthod, A., Commercial chiral stationary phases for the separations of clinical racemic drugs. *Separation and Purification Reviews* **2007,** *36* (4), 285-481.
33. Asnin, L.; Gritti, F.; Kaczmarski, K.; Guiochon, G., Features of the adsorption of Naproxen on the chiral stationary phase (S,S)-Whelk-O1 under reversed-phase conditions. *J Chromatogr A* **2010,** *1217* (3), 264-75.
34. Asnin, L. D.; Guiochon, G., Retention of Naproxen enantiomers on the chiral stationary phase Whelk-O1 under reversed-phase conditions. A reconsideration of the adsorption mechanism in the light of new experimental data. *J Chromatogr A* **2010,** *1217* (10), 1709-11.
35. Fernandes, C.; Tiritan, M. E.; Pinto, M., Small molecules as chromatographic tools for HPLC enantiomeric resolution: Pirkle-type chiral stationary phases evolution. *Chromatographia* **2013,** *76* (15-16), 871-897.
36. Gasparrini, F.; Misiti, D.; Villani, C., High-performance liquid chromatography chiral stationary phases based on low-molecular-mass selectors. *J. Chromatogr. A* **2001,** *906* (1), 35-50.
37. Fernandes, C.; Phyo, Y.; Silva, A. S.; Tiritan, M. E.; Kijjoa, A.; Pinto, M. M. M., Chiral stationary phases based on small molecules: an update of the last seventeen years. *Sep. Purif. Rev.* **2017**, DOI: 10.1080/15422119.2017.1326939.
38. Hesse, G.; Hagel, R., A complete separation of a racemic mixture by elution chromatography on cellulose triacetate. *Chromatographia* **1973,** *6* (6), 277-280.
39. Okamoto, Y.; Kawashima, M.; Hatada, K., Useful chiral packing materials for high-performance liquid chromatographic resolution of enantiomers: Phenylcarbamates of

polysaccharides coated on silica gel. *Journal of the American Chemical Society* **1984,** *106* (18), 5357-5359.
40. Witte, D. T.; Bruggeman, F. J.; Franke, J. P.; Copinga, S.; Jansen, J. M.; De Zeeuw, R. A., Comparison between cellulose and amylose tris(3,5- dimethylphenylcarbamate) chiral stationary phases for enantiomeric separation of 17 amidotetralins. *Chirality* **1993,** *5* (7), 545-553.
41. Matlin, S. A.; Tiritan, M. E.; Crawford, A. J.; Cass, Q. B.; Boyd, D. R., HPLC with carbohydrate carbamate chiral phases: Influence of chiral phase structure on enantioselectivity. *Chirality* **1994,** *6* (2), 135-140.
42. Chankvetadze, B.; Yashima, E.; Okamoto, Y., Dimethyl-, dichloro- and chloromethylphenylcarbamates of amylose as chiral stationary phases for high-performance liquid chromatography. *J. Chromatogr. A* **1995,** *694* (1), 101-109.
43. Park, J. H.; Whang, Y. C.; Jung, Y. J.; Okamoto, Y.; Yamamoto, C.; Carr, P. W.; McNeff, C. V., Separation of racemic compounds on amylose and cellulose dimethylphenylcarbamate-coated zirconia in HPLC. *Journal of Separation Science* **2003,** *26* (15-16), 1331-1336.
44. Shen, J.; Zhao, Y.; Inagaki, S.; Yamamoto, C.; Shen, Y.; Liu, S.; Okamoto, Y., Enantioseparation using ortho- or meta-substituted phenylcarbamates of amylose as chiral stationary phases for high-performance liquid chromatography. *J. Chromatogr. A* **2013,** *1286*, 41-46.
45. Chankvetadze, B.; Yashima, E.; Okamoto, Y., Chloromethylphenylcarbamate derivatives of cellulose as chiral stationary phases for high-performance liquid chromatography. *J. Chromatogr. A* **1994,** *670* (1–2), 39-49.
46. Kaida, Y.; Okamoto, Y., Optical resolution by high-performance liquid chromatography on benzylcarbamates of cellulose and amylose. *J. Chromatogr. A* **1993,** *641* (2), 267-278.
47. Cass, Q. B.; Tiritan, M. E.; Calafatti, S. A.; Matlin, S. A., Enantioseparation on amylose triso,5-dimethoxyphenyl carbamate): Application to commercial pharmaceutical chiral drugs. *Journal of Liquid Chromatography and Related Technologies* **1999,** *22* (20), 3091-3099.
48. Ichida, A.; Shibata, T.; Okamoto, I.; Yuki, Y.; Namikoshi, H.; Toga, Y., Resolution of enantiomers by HPLC on cellulose derivatives. *Chromatographia* **1984,** *19* (1), 280-284.
49. Castells, C. B.; Carr, P. W., Cellulose tris(3,5-dimethylphenylcarbamate)-coated zirconia as a chiral stationary phase for HPLC. *ANAL. CHEM.* **1999,** *71* (15), 3013-3021.
50. Castells, C. B.; Carr, P. W., Fast enantioseparations of basic analytes by high-performance liquid chromatography using cellulose tris(3,5-dimethylphenylcarbamate)-coated zirconia stationary phases. *J. Chromatogr. A* **2000,** *904* (1), 17-33.
51. Kasuya, N.; Kusaka, Y.; Habu, N.; Ohnishi, A., Development of chiral stationary phases consisting of low-molecular-weight cellulose derivatives covalently bonded to silica gel. *Cellulose* **2002,** *9* (3-4), 263-269.
52. Chen, X.; Zou, H.; Ni, J.; Feng, S., Synthesis and characteristics of composite chiral stationary phases based on cellulose derivatives. *Journal of Separation Science* **2003,** *26* (1-2), 29-36.
53. Liu, Y.; Zou, H., High-performance liquid chromatographic evaluation of a coated cellulose tris(3,5-dimethylphenylcarbamate) chiral stationary phase having a small-pore silica support. *J. Chromatogr. A* **2008,** *1178* (1-2), 118-125.
54. Matlin, S. A.; Tiritan, M. E.; Cass, Q. B.; Boyd, D. R., Enantiomeric resolution of chiral sulfoxides on polysaccharide phases by HPLC. *Chirality* **1996,** *8* (1), 147-152.
55. Ali, I.; Aboul-Enein, H. Y., Immobilized polysaccharide CSPs: An advancement in enantiomeric separations. *Current Pharmaceutical Analysis* **2007,** *3* (1), 71-82.
56. Al-Othman, Z. A.; Ali, I.; Asim, M.; Khan, T. A., Recent trends in chiral separations on immobilized polysaccharides CSPs. *Comb. Chem. High Throughput Screen.* **2012,** *15* (4), 339-346.
57. Chankvetadze, B., Recent developments on polysaccharide-based chiral stationary phases for liquid-phase separation of enantiomers. *J. Chromatogr. A* **2012,** *1269*, 26-51.

58. Ali, I.; Saleem, K.; Hussain, I.; Gaitonde, V. D.; Aboul-Enein, H. Y., Polysaccharides chiral stationary phases in liquid chromatography. *Separation and Purification Reviews* **2009,** *38* (2), 97-147.
59. Maier, N. M.; Franco, P.; Lindner, W., Separation of enantiomers: needs, challenges, perspectives. *J. Chromatogr. A* **2001,** *906* (1–2), 3-33.
60. Ikai, T.; Yamamoto, C.; Kamigaito, M.; Okamoto, Y., Immobilized-type chiral packing materials for HPLC based on polysaccharide derivatives. *J. Chromatogr. B Anal. Technol. Biomed. Life Sci.* **2008,** *875* (1), 2-11.
61. Shen, J.; Okamoto, Y., Efficient Separation of Enantiomers Using Stereoregular Chiral Polymers. *Chemical Reviews* **2016,** *116* (3), 1094-1138.
62. Fanali, C.; Fanali, S.; Chankvetadze, B., HPLC Separation of Enantiomers of Some Flavanone Derivatives Using Polysaccharide-Based Chiral Selectors Covalently Immobilized on Silica. *Chromatographia* **2016,** *79* (3-4), 119-124.
63. Belboukhari, N.; Lahmar, N.; Sekkoum, K.; Cheriti, A.; Aboul-Enein, H. Y., Chiral Separation of Several Flavanones by Liquid Chromatography. *Current Pharmaceutical Analysis* **2015,** *11* (3), 201-209.
64. López-Ram-de-Víu, P.; Gálvez, J. A.; Díaz-de-Villegas, M. D., High-performance liquid chromatographic enantioseparation of unusual amino acid derivatives with axial chirality on polysaccharide-based chiral stationary phases. *J. Chromatogr. A* **2015,** *1390*, 78-85.
65. Albals, D.; Heyden, Y. V.; Schmid, M. G.; Chankvetadze, B.; Mangelings, D., Chiral separations of cathinone and amphetamine-derivatives: Comparative study between capillary electrochromatography, supercritical fluid chromatography and three liquid chromatographic modes. *Journal of Pharmaceutical and Biomedical Analysis* **2016,** *121*, 232-243.
66. Ghanem, A.; Hoenen, H.; Müller, P.; Aboul-Enein, H. Y., Enantiomeric separation of cyclopropane derivatives on a polysaccharide-based chiral stationary phase. *Analytica Chimica Acta* **2005,** *538* (1-2), 15-24.
67. Lipka, E.; Yous, S.; Furman, C.; Carato, P.; Deghaye, C.; Bonte, J. P.; Vaccher, C., Analytical and preparative chiral separation of β-carboline derivatives, LDL oxidation inhibitors, using HPLC and CE methodologies: Determination of enantiomeric purity. *Chromatographia* **2012,** *75* (7-8), 337-345.
68. Gallinella, B.; Ferretti, R.; Zanitti, L.; Sestili, I.; Mosca, A.; Cirilli, R., Comparison of reversed-phase enantioselective HPLC methods for determining the enantiomeric purity of (S)-omeprazole in the presence of its related substances. *J. Pharmaceut.Analy.* **2016,** *6* (2), 132-136.
69. Okamoto, Y.; Aburatani, R.; Miura, S. I.; Hatada, K., Chiral stationary phases for HPLC: Cellulose tris(3,5-dimethylphenyl-carbamate) and tris(3,5-dichlorophenylcarbamate) chemically bonded to silica gel. *J. Liq. Chromatogr.* **1987,** *10* (8-9), 1613-1628.
70. Franco, P.; Senso, A.; Minguillón, C.; Oliveros, L., 3,5-dimethylphenylcarbamates of amylose, chitosan and cellulose bonded on silica gel comparison of their chiral recognition abilities as high- performance liquid chromatography chiral stationary phases. *J. Chromatogr. A* **1998,** *796* (2), 265-272.
71. Francotte, E.; Huynh, D., Immobilized halogenophenylcarbamate derivatives of cellulose as novel stationary phases for enantioselective drug analysis. *Journal of Pharmaceutical and Biomedical Analysis* **2002,** *27* (3-4), 421-429.
72. Cass, Q. B.; Batigalhia, F., Enantiomeric resolution of a series of chiral sulfoxides by high-performance liquid chromatography on polysaccharide-based columns with multimodal elution. *J. Chromatogr. A* **2003,** *987* (1–2), 445-452.
73. Cass, Q. B.; Watanabe, C.; amp; x; lia, S. F.; Rabi, J. A.; Bottari, P.; amp; x; cia, Q.; Costa, M. R.; Nascimento, R. M.; Cruz, J. E. D.; Ronald, R. C., Polysaccharide-based chiral phase under polar organic mode of elution in the determination of the enantiomeric purity of emtricitabine an anti-HIV analogue nucleoside. *Journal of Pharmaceutical and Biomedical Analysis* **2003,** *33* (4), 581-587.

74. Lourenço, T. C.; Armstrong, D. W.; Cass, Q. B., Enantiomeric Resolution of a Chiral Sulfoxide Series by LC on Synthetic Polymeric Columns with Multimodal Elution. *Chromatographia* **2010,** *71* (5), 361-372.
75. Dossou, K. S. S.; Chiap, P.; Servais, A. C.; Fillet, M.; Crommen, J., Development and validation of a LC method for the enantiomeric purity determination of S-ropivacaine in a pharmaceutical formulation using a recently commercialized cellulose-based chiral stationary phase and polar non-aqueous mobile phase. *Journal of Pharmaceutical and Biomedical Analysis* **2011,** *54* (4), 687-693.
76. Li, J.; Dong, F.; Cheng, Y.; Liu, X.; Xu, J.; Li, Y.; Chen, X.; Kong, Z.; Zheng, Y., Simultaneous enantioselective determination of triazole fungicide difenoconazole and its main chiral metabolite in vegetables and soil by normal-phase high-performance liquid chromatography. *Anal. Bioanal. Chem.* **2012,** *404* (6-7), 2017-2031.
77. Jie, Z.; Qiuzheng, D.; Suzhen, Z.; Fang, S.; Xinyu, L.; Zhenzhong, Z., Enantioseparation of Three Important Intermediates of Tanikolide with Immobilized Cellulose Chiral Stationary Phase. *Journal of Chromatographic Science* **2015,** *53* (6), 959-962.
78. Zacharis, C. K.; Vastardi, E., A Validated LC Method for the Determination of Enantiomeric Purity of Clopidogrel Intermediate Using Amylose-Based Stationary Phase. *Chromatographia* **2015,** *78* (11-12), 819-824.
79. Ramisetti, N. R.; Arnipalli, M. S.; Nimmu, N. V.; Bondigalla, R., UHPLC Determination of Besifloxacin Enantiomers on Immobilized Amylose Tris(3,5-dichlorophenylcarbamate) Chiral Stationary Phase. *Chromatographia* **2017**.
80. Lourenço, T. C.; Batista Jr, J. M.; Furlan, M.; He, Y.; Nafie, L. A.; Santana, C. C.; Cass, Q. B., Albendazole sulfoxide enantiomers: Preparative chiral separation and absolute stereochemistry. *J. Chromatogr. A* **2012,** *1230*, 61-65.
81. Belaz, K. R. A.; Coimbra, M.; Barreiro, J. C.; Montanari, C. A.; Cass, Q. B., Multimilligram enantioresolution of sulfoxide proton pump inhibitors by liquid chromatography on polysaccharide-based chiral stationary phase. *Journal of Pharmaceutical and Biomedical Analysis* **2008,** *47* (1), 81-87.
82. Cass, Q. B.; Oliveira, R. V., SEPARATION OF MULTI-MILLIGRAM QUANTITIES OF GOSSYPOL ENANTIOMERS ON POLYSACCHARIDE-BASED STATIONARY PHASES. *Journal of Liquid Chromatography & Related Technologies* **2002,** *25* (5), 819-829.
83. Heydari, R.; Shamsipur, M., Enantiomeric separation and quantitation of tenofovir disoproxil fumarate using amylose-based chiral stationary phases by high-performance liquid chromatography. *Acta Chromatogr.* **2015,** *27* (4), 583-595.
84. Lal, M.; Bhushan, R., Analytical and semi-preparative enantioresolution of (RS)-ketorolac from pharmaceutical formulation and in human plasma by HPLC. *Biomed. Chromatogr.* **2016,** *30* (10), 1526-1534.
85. Sadutto, D.; Ferretti, R.; Zanitti, L.; Casulli, A.; Cirilli, R., Analytical and semipreparative high performance liquid chromatography enantioseparation of bicalutamide and its chiral impurities on an immobilized polysaccharide-based chiral stationary phase. *J. Chromatogr. A* **2016,** *1445*, 166-171.
86. Fernandes, C.; Brandão, P.; Santos, A.; Tiritan, M. E.; Afonso, C.; Cass, Q. B.; Pinto, M. M., Resolution and determination of enantiomeric purity of new chiral derivatives of xanthones using polysaccharide-based stationary phases. *J. Chromatogr. A* **2012,** *1269*, 143-153.
87. Sousa, E. P.; Tiritan, M. E.; Oliveira, R. V.; Afonso, C. M. M.; Cass, Q. B.; Pinto, M. M. M., Enantiomeric Resolution of Kielcorin Derivatives by HPLC on Polysaccharide Stationary Phases Using Multimodal Elution. *Chirality* **2004,** *16* (5), 279-285.
88. Sousa, M. E.; Tiritan, M. E.; Belaz, K. R. A.; Pedro, M.; Nascimento, M. S. J.; Cass, Q. B.; Pinto, M. M. M., Multimilligram enantioresolution of low-solubility xanthonolignoids on polysaccharide chiral stationary phases using a solid-phase injection system. *J. Chromatogr. A* **2006,** *1120* (1-2), 75-81.
89. Fernandes, C.; Palmeira, A.; Santos, A.; Tiritan, M. E.; Afonso, C.; Pinto, M. M., Enantioresolution of chiral derivatives of xanthones on (S,S)-Whelk-O1 and l -

phenylglycine stationary phases and chiral recognition mechanism by docking approach for (S,S)-Whelk-O1. *Chirality* **2013,** *25* (2), 89-100.
90. Fernandes, C.; Tiritan, M. E.; Cass, Q.; Kairys, V.; Fernandes, M. X.; Pinto, M., Enantioseparation and chiral recognition mechanism of new chiral derivatives of xanthones on macrocyclic antibiotic stationary phases. *J. Chromatogr. A* **2012,** *1241*, 60-68.
91. Fernandes, C.; Pinto, M.; Tiritan, M. E., Enantioresolution of Chiral Derivatives of Xanthones on Different Types of Liquid Chromatography Stationary Phases: A Comparative Study. *Current Chromatography* **2014,** *1* (2), 139-150.
92. Silva, B.; Fernandes, C.; Tiritan, M. E.; Pinto, M. M. M.; Valente, M. J.; Carvalho, M.; de Pinho, P. G.; Remião, F., Chiral enantioresolution of cathinone derivatives present in "legal highs", and enantioselectivity evaluation on cytotoxicity of 3,4-methylenedioxypyrovalerone (MDPV). *Forensic Toxicol.* **2016**, 1-14.
93. Jeuniaux C. In: Domard A, J. C., Muzzarelli RAA, Roberts G, A brief survey of the early contribution of European scientists to chitin
knowledge. In *Advances in Chitin Sciences*, Jacques André Publishers,: Lyon, France, 1996; pp 1-9.
94. Khor, E., Chapter 1 - The Relevance of Chitin. In *Chitin*, Elsevier Science Ltd: Oxford, 2001; pp 1-8.
95. Rinaudo, M., Chitin and chitosan: Properties and applications. *Progress in Polymer Science* **2006,** *31* (7), 603-632.
96. Hou, J.; Yu, X.; Shen, Y.; Shi, Y.; Su, C.; Zhao, L., Triphenyl Phosphine-Functionalized Chitosan Nanoparticles Enhanced Antitumor Efficiency Through Targeted Delivery of Doxorubicin to Mitochondria. *Nanoscale Research Letters* **2017,** *12* (1), 158.
97. Kato, Y.; Onishi, H.; Machida, Y., Application of chitin and chitosan derivatives in the pharmaceutical field. *Current pharmaceutical biotechnology* **2003,** *4* (5), 303-9.
98. Venkatesan, J.; Vinodhini, P. A.; Sudha, P. N.; Kim, S. K., Chitin and chitosan composites for bone tissue regeneration. *Advances in food and nutrition research* **2014,** *73*, 59-81.
99. Krajewska, B., Application of chitin- and chitosan-based materials for enzyme immobilizations: a review. *Enzyme and Microbial Technology* **2004,** *35* (2), 126-139.
100. Cass, Q. B.; Bassi, A. L.; Matlin, S. A., Chiral discrimination by HPLC on aryl carbamate derivatives of chitin coated onto microporous aminopropyl silica. *Chirality* **1996,** *8* (1), 131-135.
101. Yamamoto, C.; Hayashi, T.; Okamoto, Y.; Kobayashi, S., Enantioseparation by using chitin phenylcarbamates as chiral stationary phases for high-performance liquid chromatography. *Chemistry Letters* **2000,** (1), 12-13.
102. Yamamoto, C.; Hayashi, T.; Okamoto, Y., High-performance liquid chromatographic enantioseparation using chitin carbamate derivatives as chiral stationary phases. *J. Chromatogr. A* **2003,** *1021* (1-2), 83-91.
103. Zhang, J.; Wang, Z. Q.; Wang, X. C.; Zhang, J. J.; Bai, Z. W.; Chen, W., Enantioseparation characteristics of tadalafil and its intermediate on chitin derived chiral stationary phases. *Analyst* **2015,** *140* (16), 5593-5600.
104. Zhang, J.; Wang, Z. Q.; Chen, W.; Bai, Z. W., Preparation and enantioseparation of biselector chiral stationary phases based on amylose and chitin derivatives. *Anal. Sci.* **2015,** *31* (10), 1091-1097.
105. Wang, X. C.; Zhang, J.; Xu, X. Q.; Chen, W.; Yang, Y. G.; Bai, Z. W., Enantioseparation characteristics of chiral stationary phases based on the derivatives of cellulose and chitin. *Analytical Methods* **2015,** *7* (6), 2786-2793.
106. Okamoto, Y.; Noguchi, J.; Yashima, E., Enantioseparation on 3,5-dichloro- and 3,5-dimethylphenylcarbamates of polysaccharides as chiral stationary phases for high-performance liquid chromatography. *Reactive and Functional Polymers* **1998,** *37* (1-3), 183-188.
107. Senso, A.; Oliveros, L.; Minguillón, C., Chitosan derivatives as chiral selectors bonded on allyl silica gel: preparation, characterisation and study of the resulting high-performance liquid chromatography chiral stationary phases. *J. Chromatogr. A* **1999,** *839* (1-2), 15-21.

108. Yamamoto, C.; Fujisawa, M.; Kamigaito, M.; Okamoto, Y., Enantioseparation using urea- and imide-bearing chitosan phenylcarbamate derivatives as chiral stationary phases for high-performance liquid chromatography. *Chirality* **2008,** *20* (3-4), 288-294.
109. Han, X.; An, L.; Cui, H.; Li, H.; Liu, W., Enantioseparation using chitosan tris(3-chlorophenylcarbamate) as a chiral stationary phase for HPLC. *Chromatographia* **2011,** *73* (11-12), 1043-1047.
110. Zhang, L.; Shen, J.; Zuo, W.; Okamoto, Y., Synthesis of chitosan 3,6-diphenylcarbamate-2-urea derivatives and their applications as chiral stationary phases for high-performance liquid chromatography. *J. Chromatogr. A* **2014,** *1365*, 86-93.
111. Guntari, S. N.; Nam, E.; Pranata, N. N.; Chia, K.; Wong, E. H. H.; Blencowe, A.; Goh, T. K.; Caruso, F.; Qiao, G. G., Fabrication of chiral stationary phases via continuous assembly of polymers for resolution of enantiomers by liquid chromatography. *Macromolecular Materials and Engineering* **2014,** *299* (11), 1285-1291.
112. Son, S. H.; Jegal, J., Synthesis and characterization of the chiral stationary phase based on Chitosan. *Journal of Applied Polymer Science* **2007,** *106* (5), 2989-2996.
113. Tang, S.; Bin, Q.; Chen, W.; Bai, Z. W.; Huang, S. H., Chiral stationary phases based on chitosan bis(methylphenylcarbamate)-(isobutyrylamide) for high-performance liquid chromatography. *J. Chromatogr. A* **2016,** *1440*, 112-122.
114. Tang, S.; Bin, Q.; Feng, Z.-W.; Chen, W.; Huang, S.-H.; Bai, Z.-W., Chitosan bis(halophenylcarbamate)-(isobutyrylamide) based chiral stationary phases for enantiomeric separation. *New Journal of Chemistry* **2016,** *40* (11), 9657-9665.
115. Tang, S.; Liu, J. D.; Bin, Q.; Fu, K. Q.; Wang, X. C.; Luo, Y. B.; Huang, S. H.; Bai, Z. W., N-Acylated chitosan bis(arylcarbamate)s: A class of promising chiral separation materials with powerful enantioseparation capability and high eluents tolerability. *J. Chromatogr. A* **2016,** *1476*, 53-62.
116. Feng, Z. W.; Chen, W.; Bai, Z. W., Chiral stationary phases based on chitosan bis(4-methylphenylcarbamate)-(alkoxyformamide). *Journal of Separation Science* **2016,** *39* (19), 3728-3735.
117. Zhang, J.; Wang, X.-C.; Chen, W.; Bai, Z.-W., Synthesis of substituted phenylcarbamates of N-cyclobutylformylated chitosan and their application as chiral selectors in enantioseparation. *Analyst* **2016,** *141* (14), 4470-4480.
118. Feng, Z. W.; Qiu, G. S.; Mei, X. M.; Liang, S.; Yang, F.; Huang, S. H.; Chen, W.; Bai, Z. W., Structural dependence on the property of chiral stationary phases derived from chitosan bis(arylcarbamate)-(amide)s. *Carbohydr Polym* **2017,** *168*, 301-309.
119. Wang, J.; Huang, S. H.; Chen, W.; Bai, Z. W., Eluent Tolerance and Enantioseparation Recovery of Chiral Packing Materials Based on Chitosan Bis(Phenylcarbamate)-(n-Octyl Urea)s for High Performance Liquid Chromatography. *Molecules* **2016,** *21* (11).
120. Wang, J.; Xi, J.-B.; Chen, W.; Huang, S.-H.; Bai, Z.-W., High performance chiral separation materials based on chitosan bis(3,5-dimethylphenylcarbamate)-(alkyl urea)s. *Carbohydr Polym* **2017,** *156*, 481-489.
121. Liang, S.; Huang, S.-H.; Chen, W.; Bai, Z.-W., High-performance chiral stationary phases based on chitosan derivatives with a branched-chain alkyl urea. *Analytica Chimica Acta* **2017**.
122. Liu, Y.; Zou, H.; Haginaka, J., Preparation and evaluation of a novel chiral stationary phase based on covalently bonded chitosan for ligand-exchange chromatography. *Journal of Separation Science* **2006,** *29* (10), 1440-1446.
123. Pinto, M. M.; Sousa, M. E.; Nascimento, M. S., Xanthone derivatives: new insights in biological activities. *Curr Med Chem* **2005,** *12* (21), 2517-38.
124. Marona, H.; Pękala, E.; Antkiewicz-Michaluk, L.; Walczak, M.; Szneler, E., Anticonvulsant activity of some xanthone derivatives. *Bioorganic & Medicinal Chemistry* **2008,** *16* (15), 7234-7244.
125. Paiva, A. M.; Sousa, M. E.; Camões, A.; Nascimento, M. S. J.; Pinto, M. M. M., Prenylated xanthones: antiproliferative effects and enhancement of the growth inhibitory action of 4-hydroxytamoxifen in estrogen receptor-positive breast cancer cell line. *Medicinal Chemistry Research* **2011,** *21* (5), 552-558.

126. Fernandes, C.; Masawang, K.; Tiritan, M. E.; Sousa, E.; De Lima, V.; Afonso, C.; Bousbaa, H.; Sudprasert, W.; Pedro, M.; Pinto, M. M., New chiral derivatives of xanthones: Synthesis and investigation of enantioselectivity as inhibitors of growth of human tumor cell lines. *Bioorg. Med. Chem.* **2014,** *22* (3), 1049-1062.
127. Castanheiro, R.; Silva, A.; Campos, N.; Nascimento, M.; Pinto, M., Antitumor Activity of Some Prenylated Xanthones. *Pharmaceuticals* **2009,** *2* (2), 33.
128. Correia-da-Silva, M.; Sousa, E.; Duarte, B.; Marques, F.; Carvalho, F.; Cunha-Ribeiro, L. M.; Pinto, M. M., Polysulfated xanthones: multipathway development of a new generation of dual anticoagulant/antiplatelet agents. *J Med Chem* **2011,** *54* (15), 5373-84.
129. Pinto, E.; Afonso, C.; Duarte, S.; Vale-Silva, L.; Costa, E.; Sousa, E.; Pinto, M., Antifungal activity of xanthones: evaluation of their effect on ergosterol biosynthesis by high-performance liquid chromatography. *Chem Biol Drug Des* **2011,** *77* (3), 212-22.
130. Masters, K. S.; Brase, S., Xanthones from fungi, lichens, and bacteria: the natural products and their synthesis. *Chem Rev* **2012,** *112* (7), 3717-76.
131. Shagufta; Ahmad, I., Recent insight into the biological activities of synthetic xanthone derivatives. *European Journal of Medicinal Chemistry* **2016,** *116*, 267-280.
132. Horton, D. A.; Bourne, G. T.; Smythe, M. L., The combinatorial synthesis of bicyclic privileged structures or privileged substructures. *Chem Rev* **2003,** *103* (3), 893-930.
133. Muthukrishnan, M.; Basavanag, U. M. V.; Puranik, V. G., The first ionic liquid-promoted Kabbe condensation reaction for an expeditious synthesis of privileged bis-spirochromanone scaffolds. *Tetrahedron Letters* **2009,** *50* (22), 2643-2648.
134. Sousa, M. E.; Pinto, M. M. M., Synthesis of xanthones: An overview. *Current Medicinal Chemistry* **2005,** *12* (21), 2447-2479.
135. Vieira, L. M. M.; Kijjoa, A., Naturally-Occurring Xanthones: Recent Developments. *Current Medicinal Chemistry* **2005,** *12* (21), 2413-2446.
136. Pinto, M. M. M.; Castanheiro, R. A. P.; Kijjoa, A., Xanthones from Marine-Derived Microorganisms: Isolation, Structure Elucidation and Biological Activities. In *Encyclopedia of Analytical Chemistry*, John Wiley & Sons, Ltd: 2006.
137. Fernandes, C.; Oliveira, L.; Tiritan, M. E.; Leitao, L.; Pozzi, A.; Noronha-Matos, J. B.; Correia-de-Sá, P.; Pinto, M. M., Synthesis of new chiral xanthone derivatives acting as nerve conduction blockers in the rat sciatic nerve. *European Journal of Medicinal Chemistry* **2012,** *55*, 1-11.
138. Azevedo, C. M. G.; Afonso, C. M. M.; Pinto, M. M. M., Routes to xanthones: An update on the synthetic approaches. *Curr. Org. Chem.* **2012,** *16* (23), 2818-2867.
139. Maiti, D.; Buchwald, S. L., Cu-Catalyzed Arylation of Phenols: Synthesis of Sterically Hindered and Heteroaryl Diaryl Ethers. *The Journal of Organic Chemistry* **2010,** *75* (5), 1791-1794.
140. Carraro, M. L. Chiral derivatives of xanthones: synthesis, enantiomeric purity and effect on human tumor cell lines. University of Porto, 2016.
141. M. Pinto, M. E. T., C. Fernandes, Q. Cass Fases Estacionárias Quirais baseadas em Derivados Xantónicos. Portuguese Patent nº104679, In Boletim da Propriedade Industrial Nº15/2011, 21-01-2011, 2011.
142. Fernandes, C.; Tiritan, M. E.; Cravo, S.; Phyo, Y. Z.; Kijjoa, A.; Silva, A. M. S.; Cass, Q. B.; Pinto, M. M. M., New chiral stationary phases based on xanthone derivatives for liquid chromatography. *Chirality* **2017,** *29* (8), 430-442.
143. Valeur, E.; Bradley, M., Amide bond formation: beyond the myth of coupling reagents. *Chemical Society Reviews* **2009,** *38* (2), 606-631.
144. Maria, E. T. Resolução de sulfóxidos quirais por CLAE, em carbamatos de polissacarídeos. Universidade Federal de São Carlos, São Carlos-SP, 1996.
145. Maria, E. T. Resolução de sulfóxidos quirais por CLAE, em carbamatos de polissacarídeos. Universidade Federal de São Carlos, 1996.
146. Unger, K., Silica gel and bonded phases: Their production; properties and use in LC. By R. P. W. Scott; John Wiley & sons; Chichester; 1993; 261 pp. *AIChE Journal* **1995,** *41* (12), 2666-2666.
147. Berthod, A., Silica: backbone material of liquid chromatographic column packings. *J. Chromatogr. A* **1991,** *549* (C), 1-28.

148. Wiens, M.; Elkhooly, T. A.; Schröder, H.-C.; Mohamed, T. H. A.; Müller, W. E. G., Characterization and osteogenic activity of a silicatein/biosilica-coated chitosan-graft-polycaprolactone. *Acta Biomaterialia* **2014,** *10* (10), 4456-4464.
149. Fernandes, C.; Masawang, K.; Tiritan, M. E.; Sousa, E.; de Lima, V.; Afonso, C.; Bousbaa, H.; Sudprasert, W.; Pedro, M.; Pinto, M. M., New chiral derivatives of xanthones: Synthesis and investigation of enantioselectivity as inhibitors of growth of human tumor cell lines. *Bioorganic & Medicinal Chemistry* **2014,** *22* (3), 1049-1062.
150. http://hplc.chem.shu.edu/NEW/HPLC_Book/Theory/th_selrs.html (accessed 10th september, 2017).

VII. Appendixes

Appendix A.

Abstract and poster of Escola de Inverno de Farmácia, 2nd ed, 19-27 January 2017.

Abstract

INSTITUTO DE DESENVOLVIMENTO HUMANO INTEGRAL APLICADO (ideHia)
ESCOLA DE INVERNO DE FARMÁCIA

P.15 (DESENVOLVIMENTO DE NOVOS MEDICAMENTOS)

Carboxyxanthone derivatives: synthesis and structure elucidation

João Ribeiro[1], Y.Z. Phyo[2], Catarina Leite[1],Carla Fernandes[1,3*], Maria Elizabeth Tiritan[1,3,4], Anake Kijjoa[2,3],Madalena M.M. Pinto[1,3]

[1]Laboratório de Química Orgânica e Farmacêutica, Departamento de Ciências Químicas, Faculdade de Farmácia, Universidade do Porto, Portugal

[2]Instituto de Ciências Abel Salazar, Universidade do Porto, Portugal

[3]Centro Interdisciplinar de Investigação Marinha e Ambiental (CIIMAR), Universidade do Porto, Portugal

[4]CESPU, Instituto de Investigação e Formação Avançada em Ciências e Tecnologias da Saúde, Gandra, Portugal

*cfernandes@ff.up.pt

Xanthones are oxygenated heterocyclic compounds with a dibenzo-γ-pirone scaffold, well known for their role in Medicinal Chemistry. In fact, this class of compounds proved to have several biological and pharmacological activities, mainly due to the substituents linked to their scaffold[1].

In the last few years, carboxyxanthone derivatives have been studied as interesting building blocks for chiral derivative of xanthones[2] and as potential antitumor agents[3].

Therefore, the synthesis of new carboxyxanthone derivatives remains one of the research areas of our group due to their wide range of possible applications. Herein, the total synthesis of different carboxyxanthonederivativesis described. The structure elucidation of the synthesized carboxyxanthones and its intermediates was established by spectroscopic methods (^{1}H and ^{13}C NMR and IR).

Poster

Carboxyxanthone derivatives: synthesis and structure elucidation

João Ribeiro[1], Y.Z. Phyo[2], Catarina Leite[1], Carla Fernandes[1,3]*, Maria Elizabeth Tiritan[1,3,4], Anake Kijjoa[2,3], Madalena M.M. Pinto[1,3]

[1] Laboratório de Química Orgânica e Farmacêutica, Departamento de Ciências Químicas, Faculdade de Farmácia, Universidade do Porto, Porto, Portugal.
[3] Instituto de Ciências Abel Salazar, Universidade do Porto, Portugal
[3] Centro Interdisciplinar de Investigação Marinha e Ambiental (CIIMAR/CIMAR), Universidade do Porto, Porto, Portugal
[4] CESPU, Instituto de Investigação e Formação Avançada em Ciências e Tecnologias da Saúde, Gandra, Portugal
*cfernandes@ff.up.pt

1. INTRODUCTION

Xanthones are oxygenated heterocyclic compounds with a dibenzo-γ-pirone scaffold, well known for their role in Medicinal Chemistry. In fact, this class of compounds proved to have several biological and pharmacological activities, mainly due to the substituents linked to their scaffold[1]. In the last few years, carboxyxanthone derivatives (XCar) (Fig. 1) have been studied as interesting building blocks for chiral derivative of xanthones[2] and as potential antitumor agents[3]. Therefore, the synthesis of new XCar remains one of the research areas of our group due to their wide range of possible applications. Herein, the total synthesis of different XCar is described. The structure elucidation of the synthesized XCar and its intermediates was established by spectroscopic methods (^{1}H and ^{13}C NMR and IR).

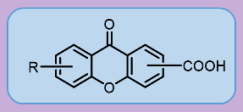

Fig.1 General structure of a XCar.

2. RESULTS

Synthesis and Structure Elucidation:

XCar-1:

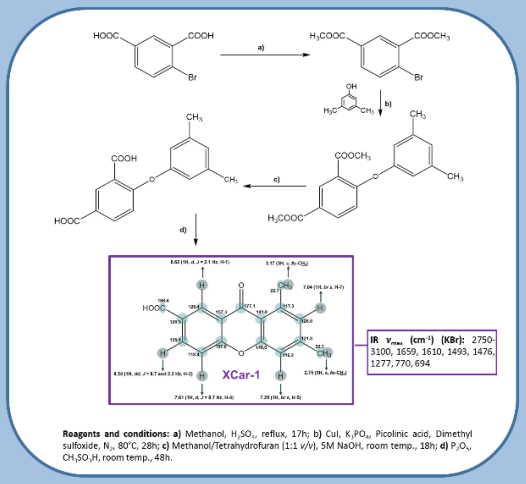

IR γ_{max} (cm^{-1}) (KBr): 2750-3100, 1659, 1610, 1493, 1476, 1277, 770, 694

Reagents and conditions: a) Methanol, H_2SO_4, reflux, 17h; **b)** CuI, K_3PO_4, Picolinic acid, Dimethyl sulfoxide, N_2, 80°C, 28h; **c)** Methanol/Tetrahydrofuran (1:1 *v/v*), 5M NaOH, room temp., 18h; **d)** P_2O_5, CH_3SO_3H, room temp., 48h.

XCar-2:

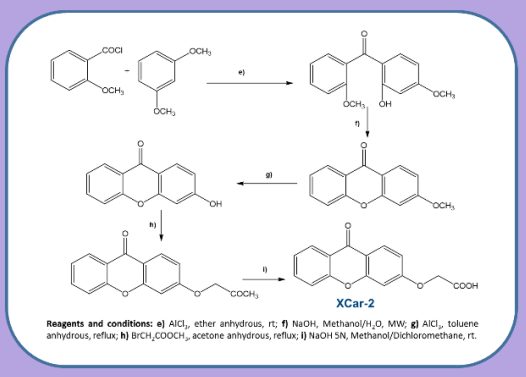

Reagents and conditions: e) $AlCl_3$, ether anhydrous, rt; **f)** NaOH, Methanol/H_2O, MW; **g)** $AlCl_3$, toluene anhydrous, reflux; **h)** $BrCH_2COOCH_3$, acetone anhydrous, reflux; **i)** NaOH 5N, Methanol/Dichloromethane, rt.

XCar-3 and XCar-4:

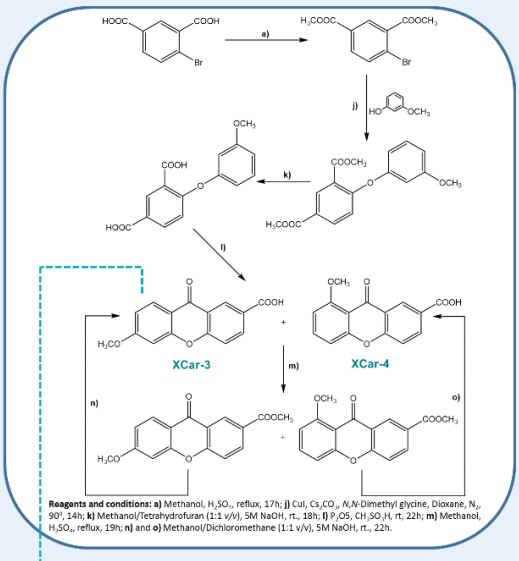

Reagents and conditions: a) Methanol, H_2SO_4, reflux, 17h; **j)** CuI, Cs_2CO_3, *N,N*-Dimethyl glycine, Dioxane, N_2, 90°, 14h; **k)** Methanol/Tetrahydrofuran (1:1 *v/v*), 5M NaOH, rt., 18h; **l)** P_2O_5, CH_3SO_3H, rt, 22h; **m)** Methanol, H_2SO_4, reflux, 19h; **n)** and **o)** Methanol/Dichloromethane (1:1 v/v), 5M NaOH, rt., 22h.

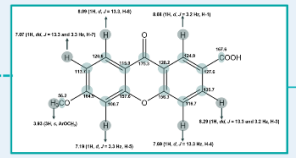

IR γ_{max} (cm^{-1}) (KBr): 3411, 2901, 1687, 1610, 1575, 1500, 1433, 1271, 766

3. CONCLUSIONS

In this study four carboxyxanthone derivatives were successfully obtained by total synthesis *via* Ullmann reaction, with formation of a diaryl ether intermediate (**XCar-1**, **XCar-3** and **XCar-4**) or *via* benzophenone intermediate (**XCar-2**).

The XCar will be evaluated for growth inhibitory activity on human tumor cell lines and for anti-inflammatory activity by inhibition of enzymes involved in the inflammatory cascade. Additionally, it will be used as suitable functionalized chemical substrate to obtain new chiral derivatives of xanthones.

References

[1] Pinto, M. M. M.; Sousa, M. E.; Nascimento, M. S. J.*Curr. Med. Chem.* **2005,** *12* (21), 2517-2538.
[2] Fernandes, C.; Masawang, K.; Tiritan, M. E.; Sousa, E.; De Lima, V.; Afonso, C.; Bousbaa, H.; Sudprasert, W.; Pedro, M.; Pinto, M. M.*Bioorg. Med. Chem.* **2014,** *22* (3), 1049-1062.
[3] Azevedo, C. M. G.; Afonso, C. M. M.; Pinto, M. M. M.*Curr. Org. Chem.* **2012,** *16* (23), 2818-2867.

Acknowledgements

This work was supported through national funds from Foundation for Science and Technology (FCT) and European Regional Development Fund (ERDF) and COMPETE under the projects PEst-C/MAR/LA0015/2013, PTDC/MAR-BIO/4694/2014 (POCI-01-0145-FEDER-016790), QOPNA (FCT UID/QUI/00062/2013), and INNOVMAR (Innovation and Sustainability in the Management and Exploitation of Marine Resources) - NORTE-01-0145-FEDER-000035, Research Line NOVELMAR and COXANT –CESPU- 2016.

Appendix B.

Abstract and poster of 10th Meeting of Young Researchers of University of Porto (IJUP17), Porto, Portugal, 8-10 February 2017, P. 26.

Abstract

- **12519 | Synthesis and structure elucidation of carboxyxanthone derivative**

Ribeiro, João, Faculdade de Farmácia, Portugal
Fernandes, Carla, Faculdade de Farmácia, Portugal
Tiritan, Maria Elizabeth, Faculdade de Farmácia, Portugal
Pinto, Madalena M. M., Faculdade de Farmácia, Portugal

Xanthones are oxygenated heterocyclic compounds with a dibenzo-γ-pirone scaffold (Fig.1), well known for their role in Medicinal Chemistry. In fact, this class of compounds proved to have several biological and pharmacological activities, mainly due to the substituents linked to their scaffold1.
In the last few years, carboxyxanthone derivatives have been studied as interesting building blocks for chiral derivative of xanthones2 and as potential antitumor agents3.
Therefore, the synthesis of new carboxyxanthone derivatives remains one of the research areas of our group due to their wide range of possible applications. Herein, the total synthesis of a carboxyxanthone derivative via diaryl-ether route (Ullman reaction) was described. The structure elucidation of the synthesized carboxyxanthone and its intermediates was established by spectroscopic methods (1H and 13C NMR and IR).

This work was supported through national funds from Foundation for Science and Technology (FCT) and European Regional Development Fund (ERDF) and COMPETE under the projects PEst-C/MAR/LA0015/2013, PTDC/MAR-BIO/4694/2014 (POCI-01-0145-FEDER-016790), QOPNA (FCT UID/QUI/00062/2013), and INNOVMAR (Innovation and Sustainability in the Management and Exploitation of Marine Resources) - NORTE-01-0145-FEDER-000035, Research Line NOVELMAR and COXANT –CESPU- 2016.

1. Pinto, M. M. M.; Sousa, M. E.; Nascimento, M. S. J. Curr. Med. Chem. 2005, 12 (21), 2517-2538.
2. Fernandes, C.; Masawang, K.; Tiritan, M. E.; Sousa, E.; De Lima, V.; Afonso, C.; Bousbaa, H.; Sudprasert, W.; Pedro, M.; Pinto, M. M. Bioorg. Med. Chem. 2014, 22 (3), 1049-1062.
3. Azevedo, C. M. G.; Afonso, C. M. M.; Pinto, M. M. M. Curr. Org. Chem. 2012, 16 (23), 2818-2867.

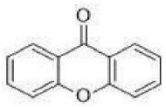

Chemical structure of xanthone

Poster

Synthesis and structure elucidation of one carboxyxanthone derivative

João Ribeiro[1], Carla Fernandes[1,2*], Maria Elizabeth Tiritan[1,2,3], Madalena M.M. Pinto[1,2]
[1]Laboratório de Química Orgânica e Farmacêutica, Departamento de Ciências Químicas, Faculdade de Farmácia, Universidade do Porto, Portugal.
[2]Centro Interdisciplinar de Investigação Marinha e Ambiental (CIIMAR/CIMAR), Universidade do Porto, Portugal.
[3]CESPU, Instituto de Investigação e Formação Avançada em Ciências e Tecnologias da Saúde, Gandra, Portugal
*cfernandes@ff.up.pt

Introduction

Xanthones are oxygenated heterocyclic compounds with a dibenzo-γ-pirone scaffold, well known for their role in Medicinal Chemistry. In fact, this class of compounds proved to have several biological and pharmacological activities, mainly due to the substituents linked to their scaffold[1]. In the last few years, carboxyxanthone derivatives (XCar) (**Fig. 1**) have been studied as interesting building blocks for chiral derivative of xanthones[2] and as potential antitumor agents[3]. Therefore, the synthesis of new XCar remains one of the research areas of our group due to their wide range of possible applications. Herein, the total synthesis of one carboxyxanthone derivative *via* diaryl-ether route (Ullman Reaction) is described. The structure elucidation of the synthesized compound and its intermediates was established by spectroscopic methods (^{1}H and ^{13}C NMR and IR).

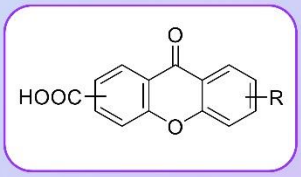

Fig. 1 – General structure for carboxyxanthone derivatives (XCar)

Results

Synthesis and structure elucidation:

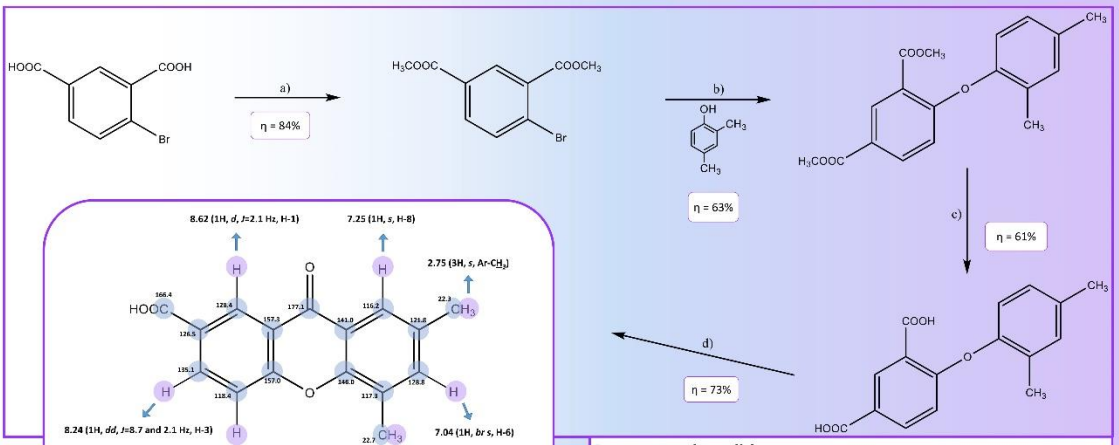

IR ν_{max} (cm^{-1}) (KBr): 2750-3100, 1659, 1610, 1493, 1476, 1277, 770, 694.

Reagents and conditions:
a) Methanol, H_2SO_4, reflux, 17h;
b) CuI, K_3PO_4, Picolinic acid, Dimethyl Sulfoxide, N_2, 80^{0}C, 28h;
c) Methanol/Tetrahydrofuran (1:1 *v/v*), 5M NaOH, room temp., 18h;
d) P_2O_5, CH_3SO_3H, room temp., 48h.

Conclusion and Future Work

In this study, one carboxyxanthone derivative was successfully obtained by total synthesis *via* Ullmann reaction, with the formation of a diaryl ether intermediate.

The obtained compound will be evaluated for growth inhibitory activity on human tumour cell lines and for anti-inflammatory activity by inhibition of enzymes involved in the inflammatory cascade. Additionally, it will be used as suitable functionalized chemical substrate to obtain new chiral derivatives of xanthones.

REFERENCES

1. A.J. Shaguftu, Eur J Med Chem 2016, 116, 267 280.
2. Fernandes, C.; Masawang, K.; Tiritan, M. E.; Sousa, E.; De Lima, V.; Afonso, C.; Bousbaa, H.; Sudoraserl, W.; Pedro, M.; Pinto, M. M. Bioorg. Med. Chem. 2014, 22 (3), 1049-1062.
3. Pinto, M. M. M.; Sousa, M. E.; Nascimento, M. S. J. Curr. Med. Chem. 2005, 12 (21), 2517-2538.

ACKNOWLEDGEMENTS

This work was supported through national funds from Foundation for Science and Technology (FCT) and European Regional Development Fund (ERDF) and COMPETE under the projects PEst-C/MAR/LA0015/2013, PTDC/MAR-BIO/4694/2014 (POCI-01-0145-FEDER-016790), QOPNA (FCT UID/QUI/00062/2013), and INNOVMAR (Innovation and Sustainability in the Management and Exploitation of Marine Resources) - NORTE-01-0145-FEDER-000035, Research Line NOVELMAR and COXANT –CESPU- 2016.

Appendix C.

Table 1. Chitin-based CSPs.

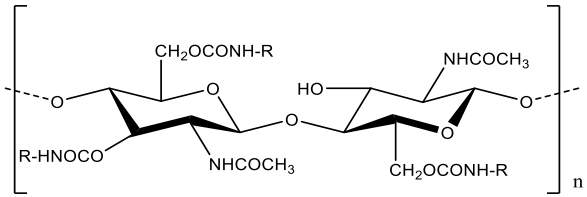

R	Separated Analytes ($\alpha > 1.00$)	Mobile Phase/Flow rate	REF.
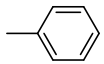 **1**	(E)-1-Chloro-1,2-diphenylethene oxide, flavanone, *N*-(3,5-dinitrobenzoyl)leucine, 1-(9-anthry1)-2,2,2-trifluoroethanol, 2,2′-dihydroxy-6,6′-dimethylbiphenyl, benzoin, cobalt(III) *tris* (acetylacetonate), 2-arylpropionic acids	Hex/2-PrOH (90:10 *v*/*v*); Hex/2-PrOH/CF_3COOH (95:5:1 *v*/*v*/*v*) 0.5 or 1.0 mL/min	100-102
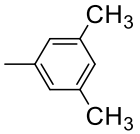 **2**	(E)-1-Chloro-1,2-diphenylethene oxide, atropine, flavanone, *N*-(3,5-dinitrobenzoyl)leucine, 3-bromo-2-cumarenone, 2,2′-dihydroxy-6,6′-dimethylbiphenyl, benzoin, Tröger base, 1-(9-anthry1)-2,2,2-trifluoroethanol, cobalt(III) *tris* (acetylacetonate), 1,2,2,2-tetraphenylethanol, *trans*-cyclopropanedicarboxylic acid dianilide, 2-arylpropionic acids, *trans*-stilbene oxide, 2-phenylcyclohexanone, 4-(dimethylamino)-1-(4-fluorophenyl-1-(hydroxymethyl)phenyl)butan-1-ol, 4-phenyl-oxalidin-2-one, *N*-(1-phenylethyl)-benzamide, methyl phenyl sulfoxide, omeprazole sodium, citalopram, voriconazole, aminoglutethimide, glutethimide	Hex/2-PrOH (90:10 *v*/*v*); Hex/2-PrOH/CF_3COOH (95:5:1 *v*/*v*/*v*); Hex/$CHCl_3$/2-PrOH (90:10:1 *v*/*v*/*v*); Hex/$CHCl_3$ (90:10 *v*/*v*); Hex/AcOEt/2-PrOH (90:10:1 *v*/*v*/*v*); MeOH/H_2O (75:25 *v*/*v*); Hex/EtOH (90:10 *v*/*v*) 0.5 or 1.0 mL/min	100-102, 105

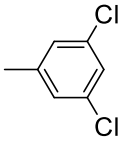 **3**	2-Arylpropionic acids, 2,2′-dihydroxy-6,6′-dimethylbiphenyl, benzoin, 2-phenylcyclohexanone, cobalt(III) *tris* (acetylacetonate), flavanone, *trans*-stilbene oxide, Tröger base, *trans*-cyclopropanedicarboxylic acid dianilide, 1-(9-anthry1)-2,2,2-trifluoroethanol, 1,2,2,2-tetraphenylethanol	Hex/2-PrOH/CF_3COOH (95:5:1 *v*/*v*/*v*) or (90:10:1 *v*/*v*/*v*); Hex/2-PrOH (90:10 *v*/*v*); Hex/$CHCl_3$/2-PrOH (90:10:1 *v*/*v*/*v*); Hex/AcOEt/2-PrOH (90:10:1 *v*/*v*/*v*); MeOH/H_2O (75:25 *v*/*v*) 0.5 or 1.0 mL/min	101-102
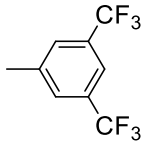 **4**	2,2′-Dihydroxy-6,6′-dimethylbiphenyl, benzoin, flavanone, 2-phenylcyclohexanone, 1-(9-anthry1)-2,2,2-trifluoroethanol, *trans*-cyclopropanedicarboxylic acid dianilide	Hex/2-PrOH (90:10 *v*/*v*) 0.5 mL/min	102
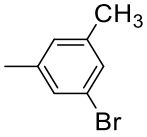 **5**	2,2′-Dihydroxy-6,6′-dimethylbiphenyl, benzoin, flavanone, 2-phenylcyclohexanone, cobalt(III) *tris* (acetylacetonate), 1-(9-anthry1)-2,2,2-trifluoroethanol, 1,2,2,2-tetraphenylethanol	Hex/2-PrOH (90:10 *v*/*v*) 0.5 mL/min	102
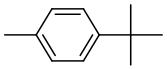 **6**	2,2′-Dihydroxy-6,6′-dimethylbiphenyl, 2-phenylcyclohexanone, flavanone, *trans*-cyclopropanedicarboxylic acid dianilide	Hex/2-PrOH (90:10 *v*/*v*) 0.5 mL/min	102
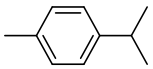 **7**	2,2′-Dihydroxy-6,6′-dimethylbiphenyl, benzoin, flavanone, 2-phenylcyclohexanone, *trans*-cyclopropanedicarboxylic acid dianilide	Hex/2-PrOH (90:10 *v*/*v*) 0.5 mL/min	102

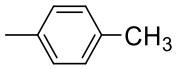 **8**	2,2′-Dihydroxy-6,6′-dimethylbiphenyl, benzoin, 1-(9-anthry1)-2,2,2-trifluoroethanol, cobalt(III) t*ris* (acetylacetonate), 1,2,2,2-tetraphenylethanol, flavanone	Hex/2-PrOH (90:10 *v*/*v*) 0.5 mL/min	[102]
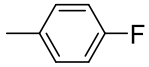 **9**	2,2′-Dihydroxy-6,6′-dimethylbiphenyl, benzoin, 1-(9-anthry1)-2,2,2-trifluoroethanol, cobalt(III) *tris* (acetylacetonate), 1,2,2,2-tetraphenylethanol, flavanone	Hex/2-PrOH (90:10 *v*/*v*) 0.5 mL/min	[102]
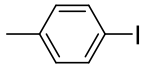 **10**	2,2′-Dihydroxy-6,6′-dimethylbiphenyl, flavanone	Hex/2-PrOH (90:10 *v*/*v*) 0.5 mL/min	[102]
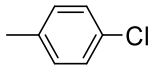 **11**	2,2′-Dihydroxy-6,6′-dimethylbiphenyl, benzoin, *trans*-stilbene oxide, 2-phenylcyclohexanone, cobalt(III) *tris* (acetylacetonate), flavanone, Tröger base, *trans*-cyclopropanedicarboxylic acid dianilide, 1,2,2,2-tetraphenylethanol	Hex/2-PrOH (90:10 *v*/*v*) 0.5 mL/min	[102]
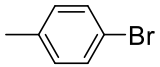 **12**	No separation	Hex/2-PrOH (90:10 *v*/*v*) 0.5 mL/min	[102]
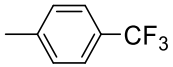 **13**	Benzoin, 2-phenylcyclohexanone, cobalt(III) *tris* (acetylacetonate), flavanone, *trans*-stilbene oxide, Tröger base, *trans*-cyclopropanedicarboxylic acid dianilide, 1,2,2,2-tetraphenylethanol	Hex/2-PrOH (90:10 *v*/*v*) 0.5 mL/min	[102]

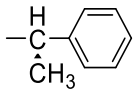 **14 (*S*)**	Benzoin, 2-phenylcyclohexanone, 1-(9-anthry1)-2,2,2-trifluoroethanol	Hex/2-PrOH (90:10 *v*/*v*) 0.5 mL/min	102
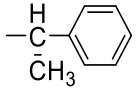 **14 (*R*)**	2,2′-Dihydroxy-6,6′-dimethylbiphenyl, 1,2,2,2-tetraphenylethanol, *trans*-cyclopropanedicarboxylic acid dianilide	Hex/2-PrOH (90:10 *v*/*v*) 0.5 mL/min	102
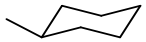 **15**	2,2′-Dihydroxy-6,6′-dimethylbiphenyl, 2-phenylcyclohexanone	Hex/2-PrOH (90:10 *v*/*v*) 0.5 mL/min	102
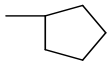 **16**	2,2′-Dihydroxy-6,6′-dimethylbiphenyl, 2-phenylcyclohexanone	Hex/2-PrOH (90:10 *v*/*v*) 0.5 mL/min	102
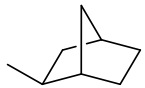 **17**	No separation	Hex/2-PrOH (90:10 *v*/*v*) 0.5 mL/min	102
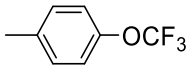 **18**	Tadalafil and its intermediates	Hex/EtOH (80:20 and 90:10 *v*/*v*) 1.0 mL/min	103

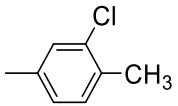 **19**	Tadalafil and its intermediates, Tröger base, benzoin, flavanone, methyl phenyl sulfoxide, *trans*-stilbene oxide, *N*-(1-phenylethyl)-benzamide, 3,5-dimethoxy-*N*-(1-phenylethyl)-benzamide, 1,1′-binaphthyl-2,2′-diol, 2-(5-chloro-2-(((4-methoxybenzyl)-amino)phenyl)-4-cyclopropyl-1,1,1-trifluorobut-3-yn-2-ol, 1-(2,4-dichlorophenyl)-2-(1*H*-imidazol-1-yl)ethanol, 1-(naphthalene-1-yl)-3-(1-phenylethyl)urea, (1-(1-(4-methoxyphenyl)-ethyl)-3-urea), 1-(1-phenylethyl)-3-(*p*-tolyl)urea, 4-methyl-*N*-(1-phenylethyl)-benzamide, *N*-(1-phenylethyl)-propionamide, ethyl-3-(1-phenylethyl)urea, mephobarbital, 3,5-dinitro-*N*-(1-phenylethyl)-benzamide, omeprazole sodium	Hex/EtOH (90:10 *v*/*v*); Hex/2-PrOH (95:5, 90:10, 70:30 *v*/*v*); Hex/AcOEt/2-PrOH (90:5:5, 90:2.5:2.5 *v*/*v*/*v*) 1.0 mL/min	103-104
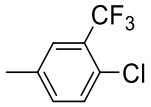 **20**	Tadalafil and its intermediates	Hex/EtOH (90:10 *v*/*v*) 1.0 mL/min	103

Hex – n-Hexane; 2-PrOH – 2-Propanol; EtOH – Ethanol; MeOH – Methanol; AcOEt - Ethyl acetate.

Appendix D.

Table 2. Chitosan *tris*-carbamate CSPs.

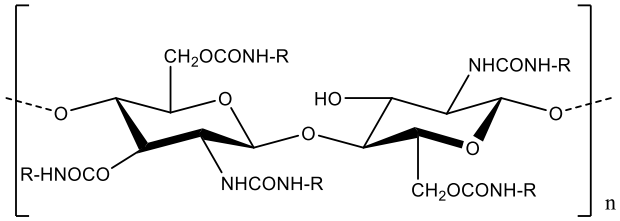

R	Separated Analytes (α > 1.00)	Mobile Phase/Flow rate	REF.
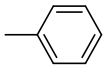 21	1-(9-anthry1)-2,2,2-trifluoroethanol, *trans*-2,3-diphenyloxirane, *trans*-stilbene oxide, benzoin, flavanone, 1-phenyl-2-propyn-1-ol, 2,2'-dimethyl-6,6'-dinitro-1,1'-biphenyl	Hex/2-PrOH (90:10 *v*/*v*) 0.1 and 0.5 mL/min	39, 110
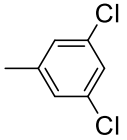 22	Tröger base, 2-phenylcyclohexanone, cobalt(III) *tris* (acetylacetonate, benzoin, 1-(9-anthry1)-2,2,2-trifluoroethanol, *trans*-stilbene oxide, 1,2,2,2-tetraphenylethanol, flavanone, *trans*-cyclopropanedicarboxylic acid dianilide, 1-phenyl-2-propyn-1-ol, 2,2'-dimethyl-6,6'-dinitro-1,1'-biphenyl, 1,1′-binaphthyl-2,2′-diol	Hex/2-PrOH (90:10 *v*/*v*) 0.1 and 0.5 mL/min	106-108, 110
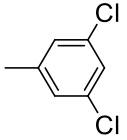 22i	Benzoin, lorazepam, lormetazepam, oxazepam, temazepam, warfarin, *trans*-stilbene oxide, (E)-1-chloro-1,2-diphenylethene oxide, 1,1′-binaphthyl-2,2′-diol, methyl (3,5-dimethylbenzoyl)alaninate, *N*-(1-(naphthalen-2-yl)ethyl)-3,5-dinitrobenzamide, 3,5-dinitro-*N*-(1-phenylethyl)-benzamide, ethyl 2-([1,1'-biphenyl]-4-yloxy)propanoate, methyl 2-(3,5-dinitro benzamido)-3,3-methylbutanoate	Hep/2-PrOH (90:10 and 80:20 *v*/*v*); Hep/$CHCl_3$ (75:25 *v*/*v*) 1.0 mL/min	107

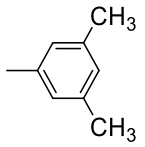 23	Flavanone, 2-phenylcyclohexanone, benzoin, *trans*-cyclopropanedicarboxylic acid dianilide, 2,2′-dihydroxy-6,6′-dimethylbiphenyl, 1-(9-anthry1)-2,2,2-trifluoroethanol, 1,2,2,2-tetraphenylethanol, Tröger base, *trans*-stilbene oxide, cobalt(III) *tris* (acetylacetonate), 1,1′-binaphthyl-2,2′-diol, 1-phenyl-2-propyn-1-ol	Hex/2-PrOH (95:05 and 90:10 *v*/*v*); Hex/$CHCl_3$/2-PrOH (90:10:1 *v*/*v*/*v*); Hex/EtOAc/2-PrOH (90:10 *v*/*v*) 0.1 and 0.5 mL/min	106, 108, 110
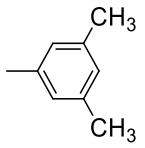 23i	Lorazepam, lormetazepam, oxazepam, temazepam, warfarin, 1-(9-anthry1)-2,2,2-trifluoroethanol, *trans*-stilbene oxide, (E)-1-chloro-1,2-diphenylethene oxide, benzoin, 1,1′-binaphthyl-2,2′-diol, 3,5-dinitro-*N*-(1-phenylethyl)-benzamide, methyl 2-(3,5-dinitro benzamido)-3,3-methylbutanoate, methyl (3,5-dinitrobenzoyl)phenylalaninate, *N*-(1-(naphthalen-2-yl)ethyl)-3,5-dinitrobenzamide, methyl (3,5-dimethylbenzoyl)alaninate, 1-(naphthalen-2-yl)ethyl 3,5-dinitrobenzoate, 2,2'-dimethyl-1,1'-binaphthalene, ethyl 2-([1,1'-biphenyl]-4-yloxy)propanoate, 5-phenyl-5-(4-tolyl)hydantoin, Tröger base	100% Hex; Hep/2-PrOH (90:10 and 80:20 *v*/*v*); Hep/$CHCl_3$ (50:50, 75:25, 90:10 and 95:5 *v*/*v*) 1.0 mL/min	70, 111
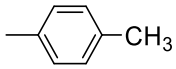 24	Benzoin, 1-(9-anthry1)-2,2,2-trifluoroethanol, flavanone, 1-phenyl-2-propyn-1-ol, 2,2'-dimethyl-6,6'-dinitro-1,1'-biphenyl	Hex/2-PrOH (90:10 *v*/*v*) 0.1 mL/min	110
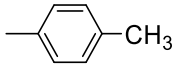 24i	Benzoin, lorazepam, lormetazepam, oxazepam, temazepam, warfarin, *trans*-stilbene oxide, (E)-1-chloro-1,2-diphenylethene oxide, 1,1′-binaphthyl-2,2′-diol, methyl (3,5-dimethylbenzoyl)alaninate, *N*-(1-(naphthalen-2-yl)ethyl)-3,5-dinitrobenzamide, 3,5-dinitro-*N*-(1-phenylethyl)-benzamide, ethyl 2-([1,1'-biphenyl]-4-yloxy)propanoate, methyl 2-(3,5-dinitro benzamido)-3,3-methylbutanoate	Hep/2-PrOH (90:10 and 80:20 *v*/*v*); Hep/$CHCl_3$ (75:25 *v*/*v*) 1.0 mL/min	107
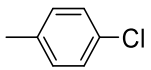 25	2-Phenylcyclohexanone, cobalt(III) *tris* (acetylacetonate), benzoin,1-(9-anthry1)-2,2,2-trifluoroethanol, *trans*-stilbene oxide, 1,2,2,2-tetraphenylethanol, flavanone, *trans*-cyclopropanedicarboxylic acid dianilide, Tröger base, 1,1′-binaphthyl-2,2′-diol, 1-phenyl-2-propyn-1-ol, 2,2'-dimethyl-6,6'-dinitro-1,1'-biphenyl	Hex/2-PrOH (90:10 *v*/*v*) 0.1 and 0.5 mL/min	107, 110

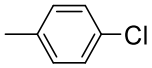 25i	Benzoin, lorazepam, lormetazepam, oxazepam, temazepam, warfarin, *trans*-stilbene oxide, (E)-1-chloro-1,2-diphenylethene oxide, 1,1′-binaphthyl-2,2′-diol, methyl (3,5-dimethylbenzoyl)alaninate, *N*-(1-(naphthalen-2-yl)ethyl)-3,5-dinitrobenzamide, 3,5-dinitro-*N*-(1-phenylethyl)-benzamide, ethyl 2-([1,1'-biphenyl]-4-yloxy)propanoate, methyl 2-(3,5-dinitro benzamido)-3,3-methylbutanoate	Hep/2-PrOH (90:10 and 80:20 *v*/*v*); Hep/$CHCl_3$ (75:25 *v*/*v*) 1.0 mL/min	[107]
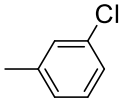 26	Tröger base, 2-phenylcyclohexanone, cobalt(III) *tris* (acetylacetonate), 2,2′-dihydroxy-6,6′-dimethylbiphenyl, 1-(9-anthry1)-2,2,2-trifluoroethanol, *trans*-stilbene oxide, 1,2,2,2-tetraphenylethanol, flavanone, benzoin, diclofop-methyl, triadimefon, penconazole, tebuconazole, hexaconazole, tetrahedrane metal cluster ($(C_9H_8)(\mu_3\text{-}S)WFeMo(CO)_7(\eta^5\text{-}C_5H_4COMe)$), 1-phenyl-2-propyn-1-ol, 2,2'-dimethyl-6,6'-dinitro-1,1'-biphenyl	Hex/2-PrOH (95:05, 90:10, 80:20 and 70:30 *v*/*v*) 0.1 and 0.5 mL/min	[108-110]
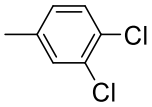 27	Tröger base, 2-phenylcyclohexanone, cobalt(III) *tris* (acetylacetonate), benzoin, 1-(9-anthry1)-2,2,2-trifluoroethanol, *trans*-stilbene oxide, 1,2,2,2-tetraphenylethanol, flavanone, *trans*-cyclopropanedicarboxylic acid dianilide	Hex/2-PrOH (90:10 *v*/*v*), Hex/$CHCl_3$/2-PrOH (90:10:1 and 50:50:1 *v*/*v*/*v*) 0.5 mL/min	[108]
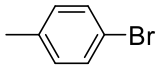 28	Tröger base, 2-phenylcyclohexanone, cobalt(III) *tris* (acetylacetonate), benzoin, 1-(9-anthry1)-2,2,2-trifluoroethanol, *trans*-stilbene oxide, 1,2,2,2-tetraphenylethanol, flavanone, 1,1′-binaphthyl-2,2′-diol, 1-phenyl-2-propyn-1-ol, 2,2'-dimethyl-6,6'-dinitro-1,1'-biphenyl	Hex/2-PrOH (90:10 *v*/*v*) 0.1 and 0.5 mL/min	[108, 110]
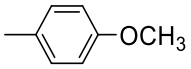 29*	No separation	Hex/2-PrOH (90:10 *v*/*v*) 0.1 mL/min	[110]
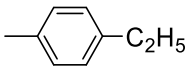 30	Tröger base, benzoin, 1-(9-anthry1)-2,2,2-trifluoroethanol, cobalt(III) *tris* (acetylacetonate), flavanone	Hex/2-PrOH (90:10 *v*/*v*) 0.1 mL/min	[110]

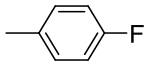 31	Tröger base, *trans*-stilbene oxide, benzoin, cobalt(III) *tris* (acetylacetonate), flavanone, 1-phenyl-2-propyn-1-ol, 2,2'-dimethyl-6,6'-dinitro-1,1'-biphenyl	Hex/2-PrOH (90:10 *v*/*v*) 0.1 mL/min	[110]
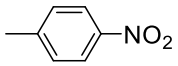 32*	Benzoin, 2-phenylcyclohexanone	Hex/2-PrOH (90:10 *v*/*v*) 0.1 mL/min	[110]
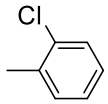 33	*trans*-Stilbene oxide	Hex/2-PrOH (90:10 *v*/*v*) 0.1 mL/min	[110]
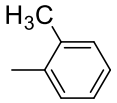 34	No separation	Hex/2-PrOH (90:10 *v*/*v*) 0.1 mL/min	[110]
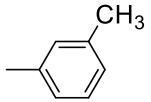 35	*trans*-Stilbene oxide, benzoin, 1-(9-anthry1)-2,2,2-trifluoroethanol, flavanone, 1-phenyl-2-propyn-1-ol, 2,2'-dimethyl-6,6'-dinitro-1,1'-biphenyl	Hex/2-PrOH (90:10 *v*/*v*) 0.1 mL/min	[110]

All chitosan *tris*-carbamate derivatives were coated with THF on APS, except * (coated with DMSO), and **22i-25i** (immobilized on allyl silica gel).
APS – Aminopropyl silica; THF – Tetrahydrofuran; DMSO – Dimethylsulfoxide; Hex – *n*-Hexane; Hep – Heptane; 2-PrOH – 2-Propanol; EtOH – Ethanol; EtOAc – Ethyl Acetate.

Appendix E.

Table 3. Chitosan *bis*-carbamate CSP with the amine group of the chitosan modified by *N*-nicotinoyl-L-phenylalanine.

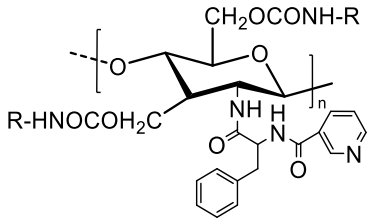

Structure	Separated analytes ($\alpha > 1.00$)	Mobile Phase/ Flow rate	REF.
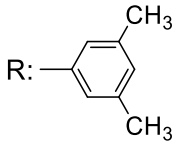 **36**	*trans*-Stilbene oxide, 2,2',6,6'-tetramethyl-1,1'-biphenyl, 1,2,2,2-tetraphenylethanol, benzoin, cobalt(III) *tris* (acetylacetonate), Tröger base, flavanone, *trans*-cyclopropanedicarboxylic acid dianilide, warfarin, pindolol	Hex/2-PrOH (95:5, 80:20, 75:25, 60:40 *v*/*v*); Hex/2-PrOH/TFA (60:40:0.2 *v*/*v*/*v*); Hex/$CHCl_3$ (50:50, 25:75 *v*/*v*); 1.0 mL/min	[112]

Coated with THF on APS.

APS – Aminopropyl silica; THF – Tetrahydrofuran; DMSO – Dimethylsulfoxide; Hex – *n*-Hexane; 2-PrOH – 2-Propanol; TFA – Trifluoracetic acid.

Appendix F.

Table 4. Chitosan bis-carbamate CSPs with the amine group of the chitosan replaced by an imide moiety.

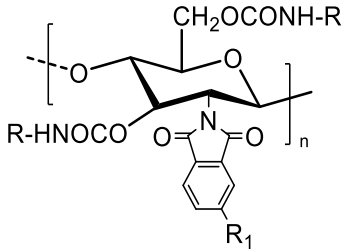

Structure	Separated analytes ($\alpha > 1.00$)	REF.
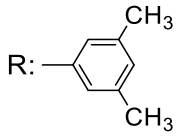 **R_1 = H** **37**	Tröger base, 1,2,2,2-tetraphenylethanol, 2,2′-dihydroxy-6,6′-dimethylbiphenyl, flavanone, cobalt(III) *tris* (acetylacetonate), 1-(9-anthry1)-2,2,2-trifluoroethanol	108, 113
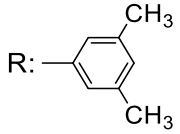 **R_1 = CH_3** **38**	2-Phenylcyclohexanone, 2,2′-dihydroxy-6,6′-dimethylbiphenyl, flavanone	108
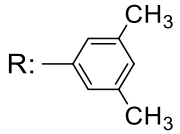 **R_1 = Cl** **39**	Tröger base, 1,2,2,2-tetraphenylethanol, 2,2′-dihydroxy-6,6′-dimethylbiphenyl, benzoin, flavanone, cobalt(III) *tris* (acetylacetonate)	108

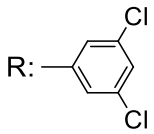 **R_1 = H** **40***	Tröger base, 2-phenylcyclohexanone, flavanone, cobalt(III) *tris* (acetylacetonate), *trans*-cyclopropanedicarboxylic acid dianilide	108
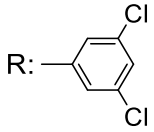 **R_1 = CH_3** **41***	Flavanone, 2-phenylcyclohexanone, benzoin, *trans*-cyclopropanedicarboxylic acid dianilide, 1-(9-anthry1)-2,2,2-trifluoroethanol, 1,2,2,2-tetraphenylethanol, Tröger base, *trans*-stilbene oxide, cobalt(III) *tris* (acetylacetonate)	108
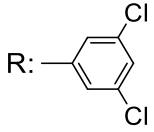 **R_1 = Cl** **42***	Tröger base, *trans*-stilbene oxide, 1,2,2,2-tetraphenylethanol, 2,2′-dihydroxy-6,6′-dimethylbiphenyl, flavanone, benzoin, cobalt(III) *tris* (acetylacetonate), *trans*-cyclopropanedicarboxylic acid dianilide	108
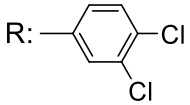 **R_1 = H** **43**	Tröger base, *trans*-stilbene oxide, 2,2′-dihydroxy-6,6′-dimethylbiphenyl, flavanone, benzoin, cobalt(III) *tris* (acetylacetonate), *trans*-cyclopropanedicarboxylic acid dianilide	108
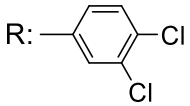 **R_1 = CH_3** **44****	Tröger base, *trans*-stilbene oxide, 2,2′-dihydroxy-6,6′-dimethylbiphenyl, flavanone, benzoin, cobalt(III) *tris* (acetylacetonate), *trans*-cyclopropanedicarboxylic acid dianilide	108

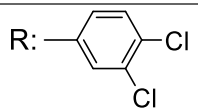 **R_1 = Cl** **45****	Tröger base, 2,2′-dihydroxy-6,6′-dimethylbiphenyl, flavanone, benzoin, cobalt(III) *tris* (acetylacetonate), *trans*-cyclopropanedicarboxylic acid dianilide	108

Coated with THF on APS, except * (DMSO), and ** (DMF). Hex/2-PrOH (90:10 *v/v*), 0.5 mL/min.

APS – Aminopropyl silica; THF – Tetrahydrofuran; DMSO – Dimethylsulfoxide; DMF – Dimethylformamide; Hex – *n*-Hexane; 2-PrOH – 2-Propanol.

Appendix G.

Table 5. Chitosan *bis*-carbamate CSPs with the amine moiety of chitosan modified by an alkylamide moiety.

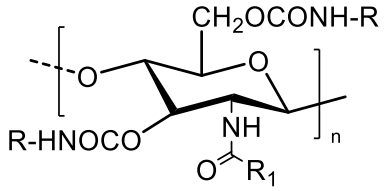

Structure	Separated analytes ($\alpha > 1.00$)	REF.
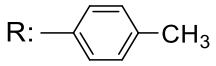 $R_1 = CH(CH_3)_2$ **46**	Tröger base, 2-phenylchroman-4-one, 1-(2-naphthyl)-ethanol, methyl phenyl sulfoxide, 1-phenylethanol, 4-phenyloxazolidin-2-one, 1-(1-phenylethyl)-3-(*p*-tolyl)urea, 1-(2,4-dichlorophenyl)-2-(1*H*-imidazol-1-yl)ethanol, 4-methyl-*N*-(phenylethyl)benzamide, benzoin, 1-(1-(4-methoxyphenyl)ethyl)-3-phenylurea, aminoglutethimide, glutethimide, citalopram hydrobromide, efavirenz, *N*-(1-(4-methoxyphenyl)ethyl)-3,5-dinitrobenzamide, omeprazole sodium, voriconazole, flavanone, *N*-(1-phenylethyl)benzamide, 4-phenyloxazolidin-2-one, methyl 4-(1-(1-(2-phenoxyethyl)piperidine-2-carboxamido)ethyl)benzoate	113, 116
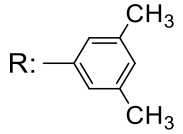 $R_1 = CH(CH_3)_2$ **47**	Tröger base, 2-phenylchroman-4-one, 1-(2-naphthyl)-ethanol, methyl phenyl sulfoxide, 1-phenylethanol, 4-phenyloxazolidin-2-one, 1-(1-phenylethyl)-3-(*p*-tolyl)urea, 1-(2,4-dichlorophenyl)-2-(1*H*-imidazol-1-yl)ethanol, 4-methyl-*N*-(phenylethyl)benzamide, benzoin, 1-(1-(4-methoxyphenyl)ethyl)-3-phenylurea, aminoglutethimide, glutethimide, citalopram hydrobromide, efavirenz, *N*-(1-(4-methoxyphenyl)ethyl)-3,5-dinitrobenzamide, omeprazole sodium, 4-(4-(dimethylamino)-1-(4-fluorophenyl)-1-hydroxybutyl)-3-(hydroxymethyl)benzonitrile, voriconazole	113

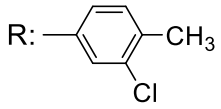 $R_1 = CH(CH_3)_2$ **48**	Tröger base, 2-phenylchroman-4-one, 1-(2-naphthyl)-ethanol, methyl phenyl sulfoxide, 1-phenylethanol, 4-phenyloxazolidin-2-one, 1-(1-phenylethyl)-3-(*p*-tolyl)urea, 1-(2,4-dichlorophenyl)-2-(1*H*-imidazol-1-yl)ethanol, 4-methyl-*N*-(phenylethyl)benzamide, benzoin, 1-(1-(4-methoxyphenyl)ethyl)-3-phenylurea, aminoglutethimide, glutethimide, citalopram hydrobromide, efavirenz, *N*-(1-(4-methoxyphenyl)ethyl)-3,5-dinitrobenzamide, omeprazole sodium, 4-(4-(dimethylamino)-1-(4-fluorophenyl)-1-hydroxybutyl)-3-(hydroxymethyl)benzonitrile, voriconazole	113
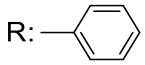 $R_1 = CH(CH_3)_2$ **49**	Tröger base, 2-phenylchroman-4-one, 1-(2-naphthyl)-ethanol, methyl phenyl sulfoxide, 1-phenylethanol, 1-(1-phenylethyl)-3-(*p*-tolyl)urea, 1-(2,4-dichlorophenyl)-2-(1*H*-imidazol-1-yl)ethanol, 4-methyl-*N*-(phenylethyl)benzamide, benzoin, 1-(1-(4-methoxyphenyl)ethyl)-3-phenylurea, aminoglutethimide, glutethimide, efavirenz, *N*-(1-(4-methoxyphenyl)ethyl)-3,5-dinitrobenzamide, omeprazole sodium, voriconazole	113
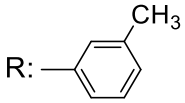 $R_1 = CH(CH_3)_2$ **50**	Tröger base, 2-phenylchroman-4-one, 1-(2-naphthyl)-ethanol, methyl phenyl sulfoxide, 1-phenylethanol, 4-phenyloxazolidin-2-one, 1-(1-phenylethyl)-3-(*p*-tolyl)urea, 1-(2,4-dichlorophenyl)-2-(1*H*-imidazol-1-yl)ethanol, 4-methyl-*N*-(phenylethyl)benzamide, benzoin, 1-(1-(4-methoxyphenyl)ethyl)-3-phenylurea, aminoglutethimide, glutethimide, citalopram hydrobromide, efavirenz, *N*-(1-(4-methoxyphenyl)ethyl)-3,5-dinitrobenzamide, omeprazole sodium, 4-(4-(dimethylamino)-1-(4-fluorophenyl)-1-hydroxybutyl)-3-(hydroxymethyl)benzonitrile, voriconazole	113, 115
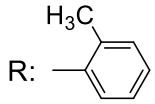 $R_1 = CH(CH_3)_2$ **51**	Tröger base, 2-phenylchroman-4-one, 1-phenylethanol, 4-phenyloxazolidin-2-onebenzoin, efavirenz, *N*-(1-(4-methoxyphenyl)ethyl)-3,5-dinitrobenzamide, omeprazole sodium, voriconazole	113

R: 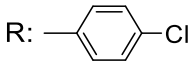 $R_1 = CH(CH_3)_2$ **52**	Tröger base, 2-phenylchroman-4-one, 1-(2-naphthyl)-ethanol, methyl phenyl sulfoxide, 1-phenylethanol, 4-phenyloxazolidin-2-one, 1-(1-phenylethyl)-3-(*p*-tolyl)urea, 1-(2,4-dichlorophenyl)-2-(1*H*-imidazol-1-yl)ethanol, 4-methyl-*N*-(phenylethyl)benzamide, benzoin, 1-(1-(4-methoxyphenyl)ethyl)-3-phenylurea, aminoglutethimide, glutethimide, citalopram hydrobromide, efavirenz, *N*-(1-(4-methoxyphenyl)ethyl)-3,5-dinitrobenzamide, omeprazole sodium, 4-(4-(dimethylamino)-1-(4-fluorophenyl)-1-hydroxybutyl)-3-(hydroxymethyl)benzonitrile, voriconazole	114
R: 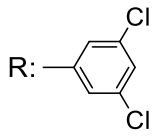 $R_1 = CH(CH_3)_2$ **53**	Tröger base, 2-phenylchroman-4-one, methyl phenyl sulfoxide, 4-phenyloxazolidin-2-one, 1-(1-phenylethyl)-3-(*p*-tolyl)urea, 1-(2,4-dichlorophenyl)-2-(1*H*-imidazol-1-yl)ethanol, 4-methyl-*N*-(phenylethyl)benzamide, benzoin, 1-(1-(4-methoxyphenyl)ethyl)-3-phenylurea, efavirenz, omeprazole sodium, 4-(4-(dimethylamino)-1-(4-fluorophenyl)-1-hydroxybutyl)-3-(hydroxymethyl)benzonitrile, voriconazole	114
R: 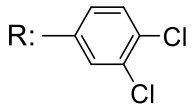 $R_1 = CH(CH_3)_2$ **54**	Tröger base, 2-phenylchroman-4-one, 1-(2-naphthyl)-ethanol, methyl phenyl sulfoxide, 1-phenylethanol, 4-phenyloxazolidin-2-one, 1-(1-phenylethyl)-3-(*p*-tolyl)urea, 1-(2,4-dichlorophenyl)-2-(1*H*-imidazol-1-yl)ethanol, 4-methyl-*N*-(phenylethyl)benzamide, benzoin, 1-(1-(4-methoxyphenyl)ethyl)-3-phenylurea, aminoglutethimide, glutethimide, citalopram hydrobromide, omeprazole sodium, 4-(4-(dimethylamino)-1-(4-fluorophenyl)-1-hydroxybutyl)-3-(hydroxymethyl)benzonitrile, voriconazole	114
R: 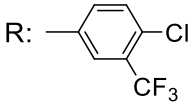 $R_1 = CH(CH_3)_2$ **55**	Tröger base, 2-phenylchroman-4-one, methyl phenyl sulfoxide, 4-phenyloxazolidin-2-one, 1-(1-phenylethyl)-3-(*p*-tolyl)urea, 1-(2,4-dichlorophenyl)-2-(1*H*-imidazol-1-yl)ethanol, 4-methyl-*N*-(phenylethyl)benzamide, benzoin, 1-(1-(4-methoxyphenyl)ethyl)-3-phenylurea, aminoglutethimide, glutethimide, omeprazole sodium, 4-(4-(dimethylamino)-1-(4-fluorophenyl)-1-hydroxybutyl)-3-(hydroxymethyl)benzonitrile, voriconazole	114

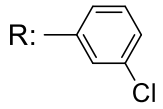 $R_1 = CH(CH_3)_2$ **56**	Tröger base, 2-phenylchroman-4-one, methyl phenyl sulfoxide, 4-phenyloxazolidin-2-one, 1-(1-phenylethyl)-3-(*p*-tolyl)urea, 1-(2,4-dichlorophenyl)-2-(1*H*-imidazol-1-yl)ethanol, 4-methyl-*N*-(phenylethyl)benzamide, benzoin, 1-(1-(4-methoxyphenyl)ethyl)-3-phenylurea, aminoglutethimide, glutethimide, omeprazole sodium, voriconazole	114
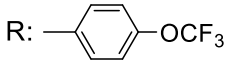 $R_1 = CH(CH_3)_2$ **57**	Tröger base, 2-phenylchroman-4-one, methyl phenyl sulfoxide, 4-phenyloxazolidin-2-one, 1-(1-phenylethyl)-3-(*p*-tolyl)urea, 1-(2,4-dichlorophenyl)-2-(1*H*-imidazol-1-yl)ethanol, 4-methyl-*N*-(phenylethyl)benzamide, benzoin, 1-(1-(4-methoxyphenyl)ethyl)-3-phenylurea, aminoglutethimide, glutethimide, efavirenz, *N*-(1-(4-methoxyphenyl)ethyl)-3,5-dinitrobenzamide, omeprazole sodium, 4-(4-(dimethylamino)-1-(4-fluorophenyl)-1-hydroxybutyl)-3-(hydroxymethyl)benzonitrile, voriconazole	114
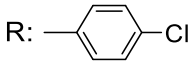 $R_1 = C_3H_5$ **58**	Tröger base, 2-phenylchroman-4-one, 1-(2-naphtyl)-ethanol, methyl phenyl sulfoxide, 1-phenylethanol, mephobarbital, 4-phenyloxazolidin-2-one, 1-(1-phenylethyl)-3-(*p*-tolyl)urea, 1-(2,4-dichlorophenyl)-2-(1*H*-imidazol-1-yl)ethanol, 4-methyl-N-(phenylethyl)benzamide, benzoin, 1-(1-(4-methoxyphenyl)ethyl)-3-phenylurea, glutethimide, citalopram hydrobromide, efavirenz, *N*-(1-(4-methoxyphenyl)ethyl)-3,5-dinitrobenzamide, omeprazole sodium, 4-(4-(dimethylamino)-1-(4-fluorophenyl)-1-hydroxybutyl)-3-(hydroxymethyl)benzonitrile, voriconazole	115
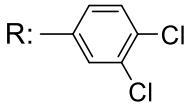 $R_1 = C_5H_9$ **59**	Tröger base, 2-phenylchroman-4-one, 1-(2-naphtyl)-ethanol, methyl phenyl sulfoxide, mephobarbital, 4-phenyloxazolidin-2-one, 1-(1-phenylethyl)-3-(*p*-tolyl)urea, 1-(2,4-dichlorophenyl)-2-(1*H*-imidazol-1-yl)ethanol, 4-methyl-N-(phenylethyl)benzamide, benzoin, 1-(1-(4-methoxyphenyl)ethyl)-3-phenylurea, glutethimide, citalopram hydrobromide, efavirenz, *N*-(1-(4-methoxyphenyl)ethyl)-3,5-dinitrobenzamide, omeprazole sodium, 4-(4-(dimethylamino)-1-(4-fluorophenyl)-1-hydroxybutyl)-3-(hydroxymethyl)benzonitrile, voriconazole	115

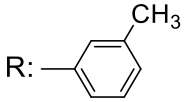 $R_1 = (CH_2)_2CH_3$ **60**	Tröger base, 2-phenylchroman-4-one, methyl phenyl sulfoxide, mephobarbital, 4-phenyloxazolidin-2-one, 1-(1-phenylethyl)-3-(*p*-tolyl)urea, 1-(2,4-dichlorophenyl)-2-(1*H*-imidazol-1-yl)ethanol, 4-methyl-N-(phenylethyl)benzamide, benzoin, 1-(1-(4-methoxyphenyl)ethyl)-3-phenylurea, glutethimide, citalopram hydrobromide, efavirenz, *N*-(1-(4-methoxyphenyl)ethyl)-3,5-dinitrobenzamide, omeprazole sodium, voriconazole	115
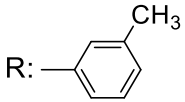 $R_1 = (CH_2)_4CH_3$ **61**	Tröger base, 2-phenylchroman-4-one, methyl phenyl sulfoxide, mephobarbital, 4-phenyloxazolidin-2-one, 1-(1-phenylethyl)-3-(*p*-tolyl)urea, 1-(2,4-dichlorophenyl)-2-(1*H*-imidazol-1-yl)ethanol, 4-methyl-N-(phenylethyl)benzamide, benzoin, 1-(1-(4-methoxyphenyl)ethyl)-3-phenylurea, citalopram hydrobromide, efavirenz, *N*-(1-(4-methoxyphenyl)ethyl)-3,5-dinitrobenzamide, omeprazole sodium, 4-(4-(dimethylamino)-1-(4-fluorophenyl)-1-hydroxybutyl)-3-(hydroxymethyl)benzonitrile, voriconazole	115
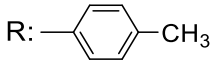 $R_1 = CH_2CH_3$ **62**	Tröger base, flavanone, methyl phenyl sulfoxide, efavirenz, 1-(2,4-dichlorophenyl)-2-(1*H*-imidazol-1-yl)ethanol, benzoin, *N*-(1-phenylethyl)benzamide, 3-(dimethylamino)-1-thiophen-2-yl)propan-1-ol, 1,1′-binaphthyl-2,2′-diol, 1-(1-(4-methoxyphenyl)ethyl)-3-phenylurea, voriconazole, omeprazole sodium, methyl 4-(1-(1-(2-phenoxyethyl)piperidine-2-carboxamido)ethyl)benzoate, 4-phenyloxazolidin-2-one	116
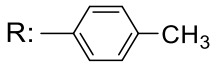 $R_1 = CH_2(CH_2)_3CH_3$ **63**	Flavanone, methyl phenyl sulfoxide, efavirenz, 1-(2,4-dichlorophenyl)-2-(1*H*-imidazol-1-yl)ethanol, 4-methyl-*N*-(phenylethyl)benzamide, 1,1′-binaphthyl-2,2′-diol, 1-(1-(4-methoxyphenyl)ethyl)-3-phenylurea, 1-(1-phenylethyl)-3-(*p*-tolyl)urea, voriconazole, methyl 4-(1-(1-(2-phenoxyethyl)piperidine-2-carboxamido)ethyl)benzoate	116
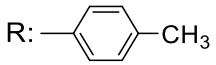 $R_1 = CH_2C_6H_5$ **64**	Flavanone, methyl phenyl sulfoxide, 1-(2,4-dichlorophenyl)-2-(1*H*-imidazol-1-yl)ethanol, 4-methyl-*N*-(phenylethyl)benzamide, benzoin, *N*-(1-phenylethyl)benzamide, 1-(1-(4-methoxyphenyl)ethyl)-3-phenylurea, 1-(1-phenylethyl)-3-(*p*-tolyl)urea, voriconazole, omeprazole sodium, methyl 4-(1-(1-(2-phenoxyethyl)piperidine-2-carboxamido)ethyl)benzoate, 4-phenyloxazolidin-2-one	116

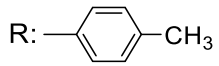 $R_1 = C_4H_7$ **65**	Tröger base, 2-phenylchroman-4-one, 1-(2-naphthyl)-ethanol, methyl phenyl sulfoxide, mephobarbital, 4-phenyloxazolidin-2-one, 1-(1-phenylethyl)-3-(*p*-tolyl)urea, 1-(2,4-dichlorophenyl)-2-(1*H*-imidazol-1-yl)ethanol, 4-methyl-*N*-(phenylethyl)benzamide, benzoin, 1-(1-(4-methoxyphenyl)ethyl)-3-phenylurea, aminoglutethimide, efavirenz, *N*-(1-(4-methoxyphenyl)ethyl)-3,5-dinitrobenzamide, omeprazole sodium, voriconazole	117
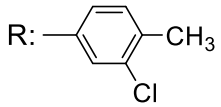 $R_1 = C_4H_7$ **66**	Tröger base, 2-phenylchroman-4-one, 1-(2-naphthyl)-ethanol, methyl phenyl sulfoxide, mephobarbital, 4-phenyloxazolidin-2-one, 1-(1-phenylethyl)-3-(*p*-tolyl)urea, 1-(2,4-dichlorophenyl)-2-(1*H*-imidazol-1-yl)ethanol, 4-methyl-*N*-(phenylethyl)benzamide, benzoin, 1-(1-(4-methoxyphenyl)ethyl)-3-phenylurea, aminoglutethimide, citalopram hydrobromide, efavirenz, *N*-(1-(4-methoxyphenyl)ethyl)-3,5-dinitrobenzamide, omeprazole sodium, 4-(4-(dimethylamino)-1-(4-fluorophenyl)-1-hydroxybutyl)-3-(hydroxymethyl)benzonitrile, voriconazole	117
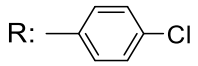 $R_1 = C_4H_7$ **67**	Tröger base, 2-phenylchroman-4-one, 1-(2-naphthyl)-ethanol, methyl phenyl sulfoxide, mephobarbital, 4-phenyloxazolidin-2-one, 1-(1-phenylethyl)-3-(*p*-tolyl)urea, 1-(2,4-dichlorophenyl)-2-(1*H*-imidazol-1-yl)ethanol, 4-methyl-*N*-(phenylethyl)benzamide, benzoin, 1-(1-(4-methoxyphenyl)ethyl)-3-phenylurea, aminoglutethimide, efavirenz, *N*-(1-(4-methoxyphenyl)ethyl)-3,5-dinitrobenzamide, omeprazole sodium, 4-(4-(dimethylamino)-1-(4-fluorophenyl)-1-hydroxybutyl)-3-(hydroxymethyl)benzonitrile, voriconazole	117
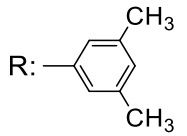 $R_1 = C_4H_7$ **68**	2-Phenylchroman-4-one, methyl phenyl sulfoxide, mephobarbital, 4-phenyloxazolidin-2-one, 1-(1-phenylethyl)-3-(*p*-tolyl)urea, 1-(2,4-dichlorophenyl)-2-(1*H*-imidazol-1-yl)ethanol, benzoin, 1-(1-(4-methoxyphenyl)ethyl)-3-phenylurea, aminoglutethimide, citalopram hydrobromide, efavirenz, *N*-(1-(4-methoxyphenyl)ethyl)-3,5-dinitrobenzamide, omeprazole sodium, 4-(4-(dimethylamino)-1-(4-fluorophenyl)-1-hydroxybutyl)-3-(hydroxymethyl)benzonitrile, voriconazole	117

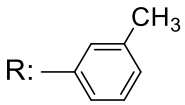 $R_1 = C_4H_7$ **69**	Tröger base, 2-phenylchroman-4-one, methyl phenyl sulfoxide, mephobarbital, 4-phenyloxazolidin-2-one, 1-(1-phenylethyl)-3-(*p*-tolyl)urea, 1-(2,4-dichlorophenyl)-2-(1*H*-imidazol-1-yl)ethanol, 4-methyl-*N*-(phenylethyl)benzamide, benzoin, 1-(1-(4-methoxyphenyl)ethyl)-3-phenylurea, aminoglutethimide, citalopram hydrobromide, efavirenz, *N*-(1-(4-methoxyphenyl)ethyl)-3,5-dinitrobenzamide, omeprazole sodium, 4-(4-(dimethylamino)-1-(4-fluorophenyl)-1-hydroxybutyl)-3-(hydroxymethyl)benzonitrile, voriconazole	117
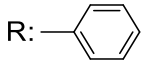 $R_1 = C_4H_7$ **70**	Tröger base, 2-phenylchroman-4-one, methyl phenyl sulfoxide, mephobarbital, 4-phenyloxazolidin-2-one, 1-(1-phenylethyl)-3-(*p*-tolyl)urea, 1-(2,4-dichlorophenyl)-2-(1*H*-imidazol-1-yl)ethanol, 4-methyl-*N*-(phenylethyl)benzamide, 1-(1-(4-methoxyphenyl)ethyl)-3-phenylurea, aminoglutethimide, *N*-(1-(4-methoxyphenyl)ethyl)-3,5-dinitrobenzamide, omeprazole sodium, 4-(4-(dimethylamino)-1-(4-fluorophenyl)-1-hydroxybutyl)-3-(hydroxymethyl)benzonitrile, voriconazole	117
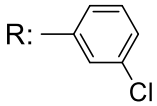 $R_1 = C_4H_7$ **71**	Tröger base, 2-phenylchroman-4-one, methyl phenyl sulfoxide, mephobarbital, 4-phenyloxazolidin-2-one, 1-(1-phenylethyl)-3-(*p*-tolyl)urea, 1-(2,4-dichlorophenyl)-2-(1*H*-imidazol-1-yl)ethanol, 1-(1-(4-methoxyphenyl)ethyl)-3-phenylurea, citalopram hydrobromide, *N*-(1-(4-methoxyphenyl)ethyl)-3,5-dinitrobenzamide, omeprazole sodium, 4-(4-(dimethylamino)-1-(4-fluorophenyl)-1-hydroxybutyl)-3-(hydroxymethyl)benzonitrile, voriconazole	117
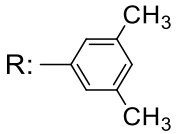 $R_1 = (CH_2)_3CH_3$ **72**	Tröger base, flavanone, methyl phenyl sulfoxide, efavirenz, 1-(2-naphtyl)-ethanol, 1-(2,4-dichlorophenyl)-2-(1*H*-imidazol-1-yl)ethanol, 4-methyl-N-(phenylethyl)benzamide, benzoin, *N*-(1-phenylethyl)benzamide, 1,1′-binaphthyl-2,2′-diol, 1-(1-(4-methoxyphenyl)ethyl)-3-phenylurea, 1-(1-phenylethyl)-3-(*p*-tolyl)urea, voriconazole, omeprazole sodium, methyl 4-(1-(1-(2-phenoxyethyl)piperidine-2-carboxamido)ethyl)benzoate, 4-phenyloxazolidin-2-one, citalopram hydrobromide	118

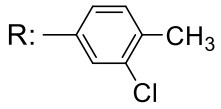 $R_1 = (CH_2)_3CH_3$ **73**	Tröger base, flavanone, methyl phenyl sulfoxide, efavirenz, 1-(2,4-dichlorophenyl)-2-(1*H*-imidazol-1-yl)ethanol, 4-methyl-N-(phenylethyl)benzamide, benzoin, *N*-(1-phenylethyl)benzamide, 1,1′-binaphthyl-2,2′-diol, 1-(1-(4-methoxyphenyl)ethyl)-3-phenylurea, 1-(1-phenylethyl)-3-(*p*-tolyl)urea, voriconazole, omeprazole sodium, methyl 4-(1-(1-(2-phenoxyethyl)piperidine-2-carboxamido)ethyl)benzoate, 4-phenyloxazolidin-2-one, citalopram hydrobromide	[118]
 $R_1 = (CH_2)_3CH_3$ **74**	Tröger base, flavanone, methyl phenyl sulfoxide, efavirenz, 1-(2,4-dichlorophenyl)-2-(1*H*-imidazol-1-yl)ethanol, 4-methyl-N-(phenylethyl)benzamide, benzoin, *N*-(1-phenylethyl)benzamide, 1,1′-binaphthyl-2,2′-diol, 1-(1-(4-methoxyphenyl)ethyl)-3-phenylurea, 1-(1-phenylethyl)-3-(*p*-tolyl)urea, voriconazole, omeprazole sodium, methyl 4-(1-(1-(2-phenoxyethyl)piperidine-2-carboxamido)ethyl)benzoate, 4-phenyloxazolidin-2-one, citalopram hydrobromide, 1-phenylethanol	[118]
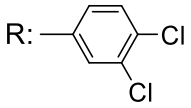 $R_1 = (CH_2)_3CH_3$ **75**	Tröger base, flavanone, methyl phenyl sulfoxide, efavirenz, 1-(2,4-dichlorophenyl)-2-(1*H*-imidazol-1-yl)ethanol, 4-methyl-N-(phenylethyl)benzamide, benzoin, *N*-(1-phenylethyl)benzamide, 1,1′-binaphthyl-2,2′-diol, 1-(1-(4-methoxyphenyl)ethyl)-3-phenylurea, 1-(1-phenylethyl)-3-(*p*-tolyl)urea, voriconazole, omeprazole sodium, methyl 4-(1-(1-(2-phenoxyethyl)piperidine-2-carboxamido)ethyl)benzoate, 4-phenyloxazolidin-2-one, citalopram hydrobromide	[118]
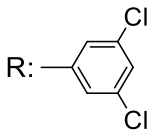 $R_1 = (CH_2)_3CH_3$ **76a**	Tröger base, flavanone, methyl phenyl sulfoxide, efavirenz, 1-(2,4-dichlorophenyl)-2-(1*H*-imidazol-1-yl)ethanol, 4-methyl-N-(phenylethyl)benzamide, benzoin, *N*-(1-phenylethyl)benzamide, 3-(dimethylamino)-1-thiophen-2-yl)propan-1-ol, 1,1′-binaphthyl-2,2′-diol, 1-(1-(4-methoxyphenyl)ethyl)-3-phenylurea, 1-(1-phenylethyl)-3-(*p*-tolyl)urea, voriconazole, omeprazole sodium, methyl 4-(1-(1-(2-phenoxyethyl)piperidine-2-carboxamido)ethyl)benzoate, 4-phenyloxazolidin-2-one, citalopram hydrobromide	[118]

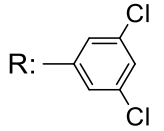 $R_1 = (CH_2)_3CH_3$ **76b**	Tröger base, flavanone, methyl phenyl sulfoxide, efavirenz, 1-(2,4-dichlorophenyl)-2-(1*H*-imidazol-1-yl)ethanol, 4-methyl-N-(phenylethyl)benzamide, benzoin, 1,1′-binaphthyl-2,2′-diol, 1-(1-(4-methoxyphenyl)ethyl)-3-phenylurea, 1-(1-phenylethyl)-3-(*p*-tolyl)urea, voriconazole, omeprazole sodium, methyl 4-(1-(1-(2-phenoxyethyl)piperidine-2-carboxamido)ethyl)benzoate, 4-phenyloxazolidin-2-one, citalopram hydrobromide, 1-phenylethanol, 1-phenyl-1,2-ethenodiolphenylethyleneglycol	[118]

Coated with DMF on APS. Hex/2-PrOH (90:10 *v/v*), Hex/EtOH (90:10 *v/v*) or Hex/2-EtOH/MeOH (90:5:5 *v/v/v*), 1.0 mL/min.
APS – Aminopropyl silica; DMF – Dimethylformamide; Hex – *n*-Hexane; 2-PrOH – 2-Propanol; EtOH – Ethanol; MeOH – Methanol; a – CSPs prepared with higher molecular weight chitosan ; b - CSPs prepared with lower molecular weight chitosan.

Appendix H.

Table 6. Chitosan *bis*-carbamate CSPs with the amine moiety of chitosan modified by an *N*-alkyl urea.

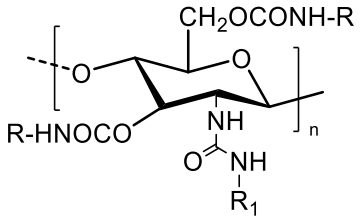

Structure	Separated analytes (α > 1.00)	REF.
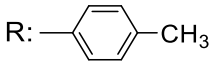 $R_1 = (CH_2)_7CH_3$ **77**	Tröger base, benzoin, flavanone, methyl phenyl sulfoxide, 1-phenylethane-1,2-diol, citalopram hydrobromide, *N*-(1-phenylethyl)benzamide, methyl 4-(1-(1-(2-phenoxyethyl)piperidine-2-carboxamido)ethyl)benzoate, 1,1'-binaphthyl-2,2'-diol, efavirenz, 1-(2,4-dichlorophenyl)-2-(1*H*-imidazol-1-yl)ethanol, 1-(1-(4-methoxyphenyl)ethyl)-3-phenylurea, 1-(1-phenylethyl)-3-(*p*-tolyl)urea, 4-methyl-N-(phenylethyl)benzamide, 4-phenyloxazolidin-2-one, omeprazole sodium, voriconazole	[119]
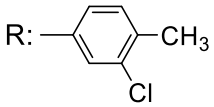 $R_1 = (CH_2)_7CH_3$ **78**	Tröger base, benzoin, flavanone, methyl phenyl sulfoxide, 1-phenylethane-1,2-diol, citalopram hydrobromide, 3-(dimethylamino)-1-(thiophen-2-yl)propan-1-ol,*N*-(1-phenylethyl)benzamide, methyl 4-(1-(1-(2-phenoxyethyl)piperidine-2-carboxamido)ethyl)benzoate, 1,1'-binaphthyl-2,2'-diol, efavirenz, 1-(2,4-dichlorophenyl)-2-(1*H*-imidazol-1-yl)ethanol, 1-(1-(4-methoxyphenyl)ethyl)-3-phenylurea, 1-(1-phenylethyl)-3-(*p*-tolyl)urea, 4-methyl-N-(phenylethyl)benzamide, 4-phenyloxazolidin-2-one, omeprazole sodium, voriconazole	[119]

R: 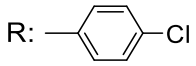 $R_1 = (CH_2)_7CH_3$ **79**	Tröger base, benzoin, flavanone, methyl phenyl sulfoxide, 1-phenylethane-1,2-diol, citalopram hydrobromide, 3-(dimethylamino)-1-(thiophen-2-yl)propan-1-ol,*N*-(1-phenylethyl)benzamide, methyl 4-(1-(1-(2-phenoxyethyl)piperidine-2-carboxamido)ethyl)benzoate, 1,1′-binaphthyl-2,2′-diol, efavirenz, 1-(2,4-dichlorophenyl)-2-(1*H*-imidazol-1-yl)ethanol, 1-(1-(4-methoxyphenyl)ethyl)-3-phenylurea, 1-(1-phenylethyl)-3-(*p*-tolyl)urea, 4-methyl-N-(phenylethyl)benzamide, 4-phenyloxazolidin-2-one, omeprazole sodium, voriconazole	119
R: 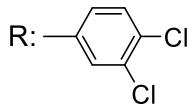 $R_1 = (CH_2)_7CH_3$ **80**	Tröger base, benzoin, flavanone, methyl phenyl sulfoxide, 1-phenylethane-1,2-diol, citalopram hydrobromide, 3-(dimethylamino)-1-(thiophen-2-yl)propan-1-ol,*N*-(1-phenylethyl)benzamide, methyl 4-(1-(1-(2-phenoxyethyl)piperidine-2-carboxamido)ethyl)benzoate, 1,1′-binaphthyl-2,2′-diol, efavirenz, 1-(2,4-dichlorophenyl)-2-(1*H*-imidazol-1-yl)ethanol, 1-(1-(4-methoxyphenyl)ethyl)-3-phenylurea, 1-(1-phenylethyl)-3-(*p*-tolyl)urea, 4-methyl-N-(phenylethyl)benzamide, 4-phenyloxazolidin-2-one, omeprazole sodium, voriconazole	119
R: 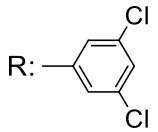 $R_1 = (CH_2)_7CH_3$ **81**	Tröger base, benzoin, flavanone, methyl phenyl sulfoxide, 1-phenylethane-1,2-diol, citalopram hydrobromide, 3-(dimethylamino)-1-(thiophen-2-yl)propan-1-ol,*N*-(1-phenylethyl)benzamide, methyl 4-(1-(1-(2-phenoxyethyl)piperidine-2-carboxamido)ethyl)benzoate, 1,1′-binaphthyl-2,2′-diol, efavirenz, 1-(2,4-dichlorophenyl)-2-(1*H*-imidazol-1-yl)ethanol, 1-(1-(4-methoxyphenyl)ethyl)-3-phenylurea, 1-(1-phenylethyl)-3-(*p*-tolyl)urea, 4-methyl-N-(phenylethyl)benzamide, 4-phenyloxazolidin-2-one, omeprazole sodium, voriconazole	119
R: 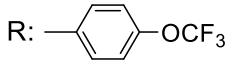 $R_1 = (CH_2)_7CH_3$ **82**	Tröger base, benzoin, flavanone, methyl phenyl sulfoxide, 1-phenylethane-1,2-diol, citalopram hydrobromide, 3-(dimethylamino)-1-(thiophen-2-yl)propan-1-ol,*N*-(1-phenylethyl)benzamide, methyl 4-(1-(1-(2-phenoxyethyl)piperidine-2-carboxamido)ethyl)benzoate, 1,1′-binaphthyl-2,2′-diol, efavirenz, 1-(2,4-dichlorophenyl)-2-(1*H*-imidazol-1-yl)ethanol, 1-(1-(4-methoxyphenyl)ethyl)-3-phenylurea, 1-(1-phenylethyl)-3-(*p*-tolyl)urea, 4-methyl-N-(phenylethyl)benzamide, 4-phenyloxazolidin-2-one, omeprazole sodium, voriconazole	119

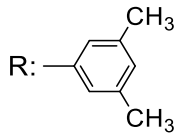 $R_1 = (CH_2)_7CH_3$ **83**	Tröger base, 1-(2-naphtyl-ethanol), benzoin, flavanone, methyl phenyl sulfoxide, citalopram hydrobromide, efavirenz, 1-(2,4-dichlorophenyl)-2-(1*H*-imidazol-1-yl)ethanol, 1-(1-(4-methoxyphenyl)ethyl)-3-phenylurea, 1-(1-phenylethyl)-3-(*p*-tolyl)urea, 4-methyl-N-(phenylethyl)benzamide, 4-(4-(dimethylamino)-1-(4-fluorophenyl)-1-hydroxybutyl)-3-(hydroxymethyl)benzonitrile, 4-phenyloxazolidin-2-one, omeprazole sodium, voriconazole, *N*-(1-(4-methoxyphenyl)ethyl)-3,5-dinitrobenzamide, glutethimide	[120]
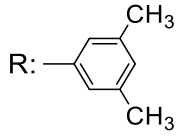 $R_1 = CH_2C_6H_5$ **84**	Tröger base, benzoin, flavanone, methyl phenyl sulfoxide, citalopram hydrobromide, efavirenz, 1-(2,4-dichlorophenyl)-2-(1*H*-imidazol-1-yl)ethanol, 1-(1-(4-methoxyphenyl)ethyl)-3-phenylurea, 1-(1-phenylethyl)-3-(*p*-tolyl)urea, 4-methyl-N-(phenylethyl)benzamide, 4-(4-(dimethylamino)-1-(4-fluorophenyl)-1-hydroxybutyl)-3-(hydroxymethyl)benzonitrile, 4-phenyloxazolidin-2-one, omeprazole sodium, voriconazole, *N*-(1-(4-methoxyphenyl)ethyl)-3,5-dinitrobenzamide, glutethimide	[120]
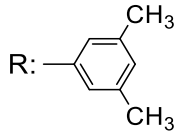 $R_1 = (CH_2)_3CH_3$ **85**	Tröger base, benzoin, flavanone, methyl phenyl sulfoxide, citalopram hydrobromide, efavirenz, 1-(2,4-dichlorophenyl)-2-(1*H*-imidazol-1-yl)ethanol, 1-(1-(4-methoxyphenyl)ethyl)-3-phenylurea, 1-(1-phenylethyl)-3-(*p*-tolyl)urea, 4-methyl-N-(phenylethyl)benzamide, 4-(4-(dimethylamino)-1-(4-fluorophenyl)-1-hydroxybutyl)-3-(hydroxymethyl)benzonitrile, 4-phenyloxazolidin-2-one, omeprazole sodium, voriconazole, *N*-(1-(4-methoxyphenyl)ethyl)-3,5-dinitrobenzamide, glutethimide	[120]
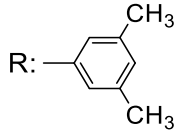 $R_1 = (CH_2)_{11}CH_3$ **86**	Tröger base, benzoin, flavanone, 1-phenylethanol, citalopram hydrobromide, efavirenz, 1-(2,4-dichlorophenyl)-2-(1*H*-imidazol-1-yl)ethanol, 1-(1-(4-methoxyphenyl)ethyl)-3-phenylurea, 1-(1-phenylethyl)-3-(*p*-tolyl)urea, 4-(4-(dimethylamino)-1-(4-fluorophenyl)-1-hydroxybutyl)-3-(hydroxymethyl)benzonitrile, 4-phenyloxazolidin-2-one, omeprazole sodium, voriconazole, *N*-(1-(4-methoxyphenyl)ethyl)-3,5-dinitrobenzamide, glutethimide	[120]

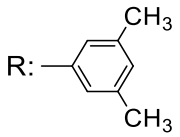 $R_1 = C_6H_{11}$ **87**	Tröger base, 1-(2-naphtyl-ethanol), benzoin, flavanone, methyl phenyl sulfoxide, 1-phenylethanol, citalopram hydrobromide, efavirenz, 1-(2,4-dichlorophenyl)-2-(1*H*-imidazol-1-yl)ethanol, 1-(1-(4-methoxyphenyl)ethyl)-3-phenylurea, 1-(1-phenylethyl)-3-(*p*-tolyl)urea, 4-methyl-N-(phenylethyl)benzamide, 4-(4-(dimethylamino)-1-(4-fluorophenyl)-1-hydroxybutyl)-3-(hydroxymethyl)benzonitrile, 4-phenyloxazolidin-2-one, omeprazole sodium, voriconazole, *N*-(1-(4-methoxyphenyl)ethyl)-3,5-dinitrobenzamide, glutethimide	120
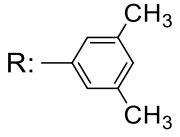 $R_1 = CH_2CH(CH_3)_2$ **88a**	Tröger base, flavanone, methyl phenyl sulfoxide, 4-phenyloxazolidin-2-one, 1-(1-phenylethyl)-3-(*p*-tolyl)urea, 1-(2,4-dichlorophenyl)-2-(1*H*-imidazol-1-yl)ethanol, benzoin, 1-(1-(4-methoxyphenyl)ethyl)-3-phenylurea, citalopram hydrobromide, efavirenz, omeprazole sodium, voriconazole, methyl 4-(1-(1-(2-phenoxyethyl)piperidine-2-carboxamido)ethyl)benzoate, 1,1′-binaphthyl-2,2′-diol, 1-phenylethane-1,2-diol	121
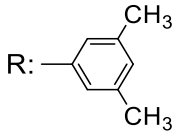 $R_1 = CH_2CH(CH_3)_2$ **88b**	Tröger base, flavanone, 1-(2-naphtyl-ethanol), methyl phenyl sulfoxide, 4-phenyloxazolidin-2-one, 1-(1-phenylethyl)-3-(*p*-tolyl)urea, 1-(2,4-dichlorophenyl)-2-(1*H*-imidazol-1-yl)ethanol, 4-methyl-N-(phenylethyl)benzamide, benzoin, 1-(1-(4-methoxyphenyl)ethyl)-3-phenylurea, citalopram hydrobromide, efavirenz, omeprazole sodium, voriconazole, 3-dimethylamino)1-1-(thiophen-2-yl)propan-1-ol, 1,1′-binaphthyl-2,2′-diol, 1-phenylethane-1,2-diol, *N*-(1-phenylethyl)benzamide	121
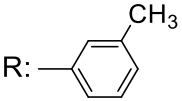 $R_1 = CH_2CH(CH_3)_2$ **89a**	Tröger base, flavanone, methyl phenyl sulfoxide, 4-phenyloxazolidin-2-one, 1-(1-phenylethyl)-3-(*p*-tolyl)urea, 1-(2,4-dichlorophenyl)-2-(1*H*-imidazol-1-yl)ethanol, benzoin, 1-(1-(4-methoxyphenyl)ethyl)-3-phenylurea, citalopram hydrobromide, efavirenz, omeprazole sodium, voriconazole, 1,1′-binaphthyl-2,2′-diol, 1-phenylethane-1,2-diol, *N*-(1-phenylethyl)benzamide	121

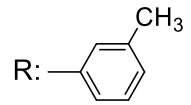 $R_1 = CH_2CH(CH_3)_2$ **89b**	Tröger base, flavanone, 1-(2-naphtyl-ethanol), methyl phenyl sulfoxide, 4-phenyloxazolidin-2-one, 1-(1-phenylethyl)-3-(*p*-tolyl)urea, 1-(2,4-dichlorophenyl)-2-(1*H*-imidazol-1-yl)ethanol, 4-methyl-N-(phenylethyl)benzamide, benzoin, 1-(1-(4-methoxyphenyl)ethyl)-3-phenylurea, citalopram hydrobromide, efavirenz, omeprazole sodium, voriconazole, methyl 4-(1-(1-(2-phenoxyethyl)piperidine-2-carboxamido)ethyl)benzoate, 1,1′-binaphthyl-2,2′-diol, 1-phenylethane-1,2-diol, *N*-(1-phenylethyl)benzamide	[121]
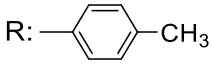 $R_1 = CH_2CH(CH_3)_2$ **90a**	Tröger base, flavanone, 1-(2-naphtyl-ethanol), methyl phenyl sulfoxide, 1-phenylethanol, 4-phenyloxazolidin-2-one, 1-(1-phenylethyl)-3-(*p*-tolyl)urea, 1-(2,4-dichlorophenyl)-2-(1*H*-imidazol-1-yl)ethanol, 4-methyl-N-(phenylethyl)benzamide, benzoin, 1-(1-(4-methoxyphenyl)ethyl)-3-phenylurea, citalopram hydrobromide, efavirenz, omeprazole sodium, voriconazole, 3-dimethylamino)1-1-(thiophen-2-yl)propan-1-ol, 1,1′-binaphthyl-2,2′-diol, 1-phenylethane-1,2-diol, *N*-(1-phenylethyl)benzamide	[121]
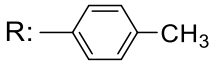 $R_1 = CH_2CH(CH_3)_2$ **90b**	Tröger base, flavanone, 1-(2-naphtyl-ethanol), methyl phenyl sulfoxide, 1-phenylethanol, 4-phenyloxazolidin-2-one, 1-(1-phenylethyl)-3-(*p*-tolyl)urea, 1-(2,4-dichlorophenyl)-2-(1*H*-imidazol-1-yl)ethanol, 4-methyl-N-(phenylethyl)benzamide, benzoin, 1-(1-(4-methoxyphenyl)ethyl)-3-phenylurea, citalopram hydrobromide, efavirenz, omeprazole sodium, voriconazole, 1,1′-binaphthyl-2,2′-diol, 1-phenylethane-1,2-diol, *N*-(1-phenylethyl)benzamide	[121]
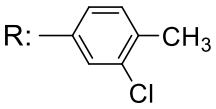 $R_1 = CH_2CH(CH_3)_2$ **91a**	Tröger base, flavanone, methyl phenyl sulfoxide, 1-phenylethanol, 4-phenyloxazolidin-2-one, 1-(1-phenylethyl)-3-(*p*-tolyl)urea, 1-(2,4-dichlorophenyl)-2-(1*H*-imidazol-1-yl)ethanol, 4-methyl-N-(phenylethyl)benzamide, benzoin, 1-(1-(4-methoxyphenyl)ethyl)-3-phenylurea, citalopram hydrobromide, efavirenz, omeprazole sodium, voriconazole, methyl 4-(1-(1-(2-phenoxyethyl)piperidine-2-carboxamido)ethyl)benzoate, 1,1′-binaphthyl-2,2′-diol, 1-phenylethane-1,2-diol, *N*-(1-phenylethyl)benzamide	[121]

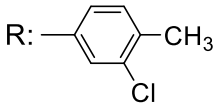 $R_1 = CH_2CH(CH_3)_2$ **91b**	Tröger base, flavanone, 1-(2-naphtyl-ethanol), methyl phenyl sulfoxide, 1-phenylethanol, 4-phenyloxazolidin-2-one, 1-(1-phenylethyl)-3-(*p*-tolyl)urea, 1-(2,4-dichlorophenyl)-2-(1*H*-imidazol-1-yl)ethanol, 4-methyl-N-(phenylethyl)benzamide, benzoin, 1-(1-(4-methoxyphenyl)ethyl)-3-phenylurea, citalopram hydrobromide, efavirenz, omeprazole sodium, voriconazole, 3-dimethylamino)1-1-(thiophen-2-yl)propan-1-ol, methyl 4-(1-(1-(2-phenoxyethyl)piperidine-2-carboxamido)ethyl)benzoate, 1,1′-binaphthyl-2,2′-diol, 1-phenylethane-1,2-diol, *N*-(1-phenylethyl)benzamide	[121]

Coated with DMF on APS. Hex/2-PrOH (90:10 *v/v*), Hex/EtOH (90:10 *v/v*) or Hex/2-EtOH/MeOH (90:5:5 *v/v/v*), 1.0 mL/min.

APS – Aminopropyl silica; DMF – Dimethylformamide; Hex – *n*-Hexane; 2-PrOH – 2-Propanol; EtOH – Ethanol; MeOH – Methanol; a – CSPs developed with higher molecular weight chitosan ; b - CSPs developed with lower molecular weight chitosan.